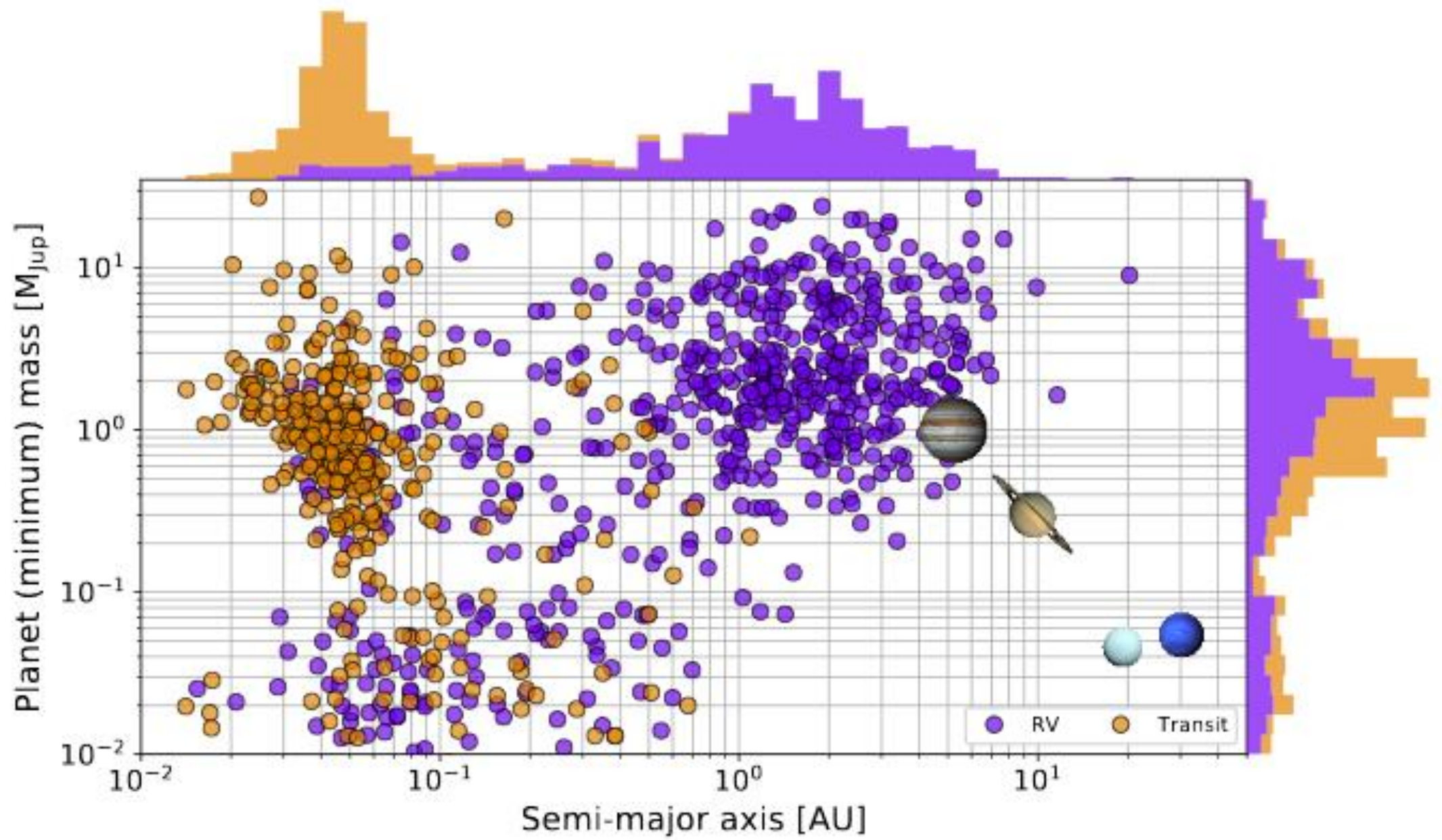
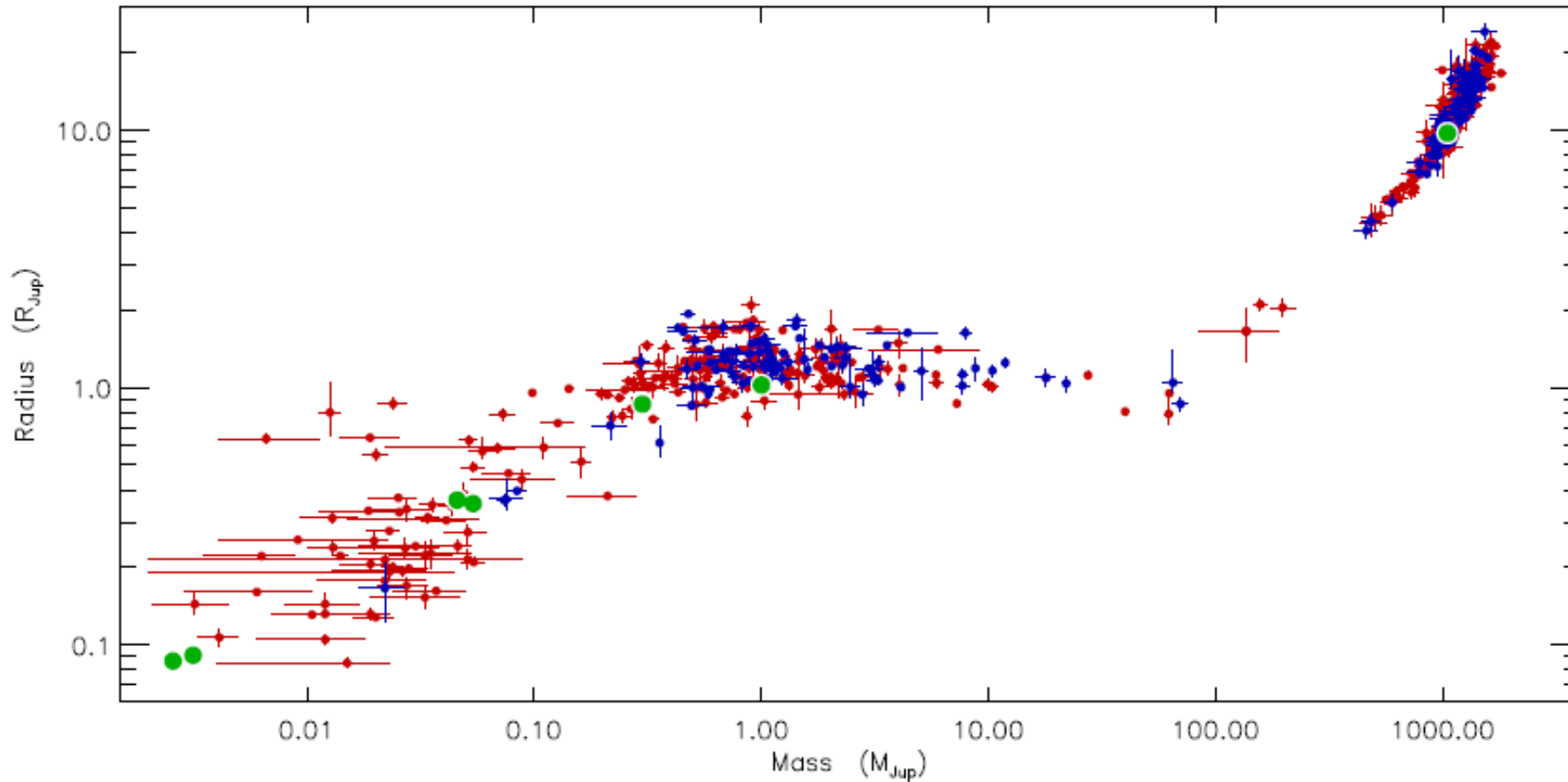


Planet detection methods

SERGEI POPOV

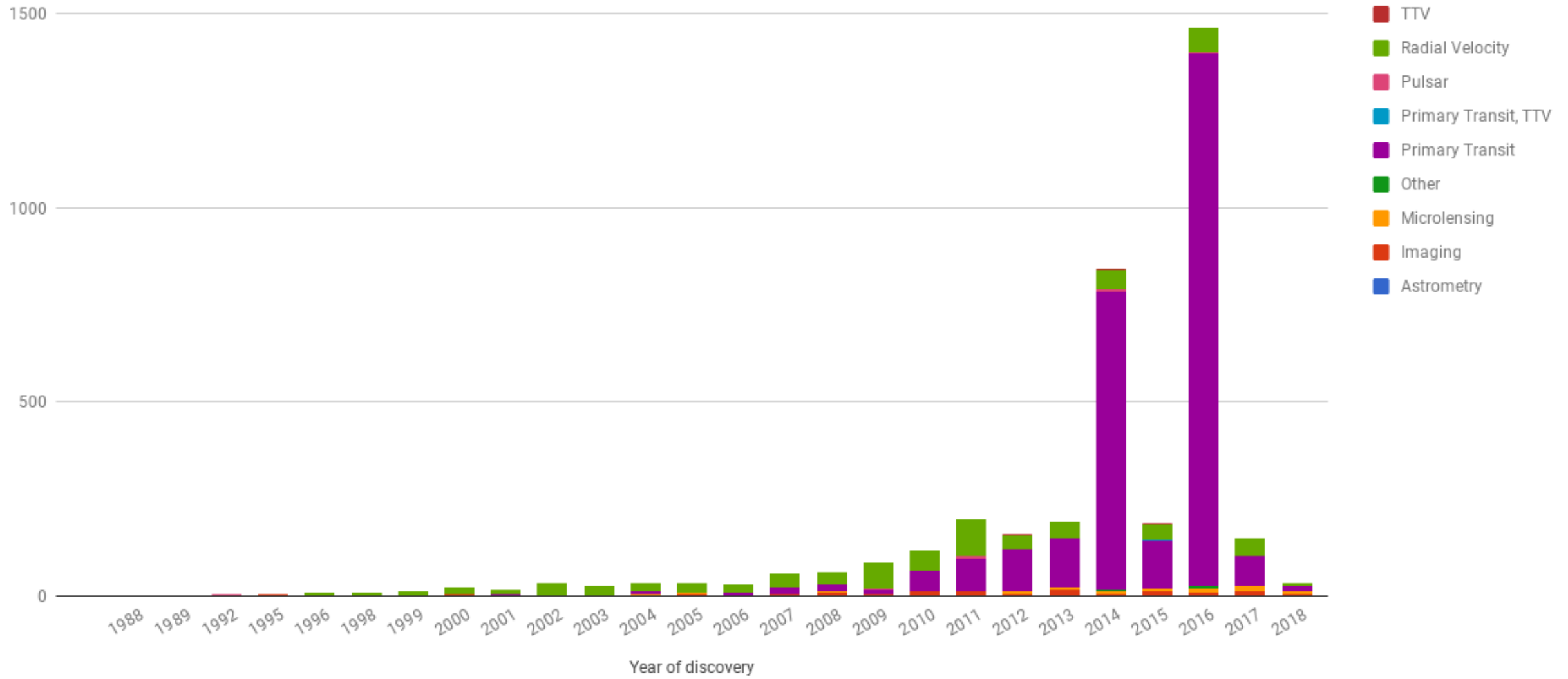


Planets, brown dwarfs stars



Brown dwarfs:
(12-13)<M<(75-80)
Jupiter masses

Rate of exoplanet discovery



Exoplanet catalogues

| Catalog | Mass criteria | Confidence criteria | Number of planets [†] |
|-------------------------|------------------------------------|----------------------------------|--------------------------------|
| Exoplanet Encyclopaedia | $M_p - 1\sigma < 60M_{\text{Jup}}$ | Submitted paper, conference talk | 3741 |
| NASA Exoplanet Archive | $M_p < 30M_{\text{Jup}}$ | Accepted, refereed paper | 3704 |
| Open Exoplanet Catalog | None listed | Open-source | 3504 |

[†]: as of February 27th, 2018.

<http://exoplanets.org/>

<http://exoplanet.eu/catalog>

<http://exoplanetarchive.ipac.caltech.edu/index.html>

<http://www.openexoplanetcatalogue.com>

exoplanets.org

Exoplanets Data Explorer | Methodology and FAQ | Exoplanets Links | California Planet Survey

Table 2925 Planets with good orbits listed in the Exoplanet Orbit Database.

Plots 25 Other Planets including microlensing and imaged planets.

Search 2950 Total Confirmed Planets

2337 Unconfirmed Kepler Candidates

5287 Total Planets (confirmed planets + Kepler Candidates)

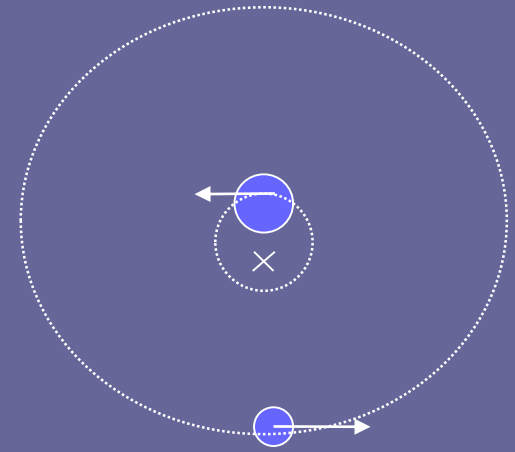
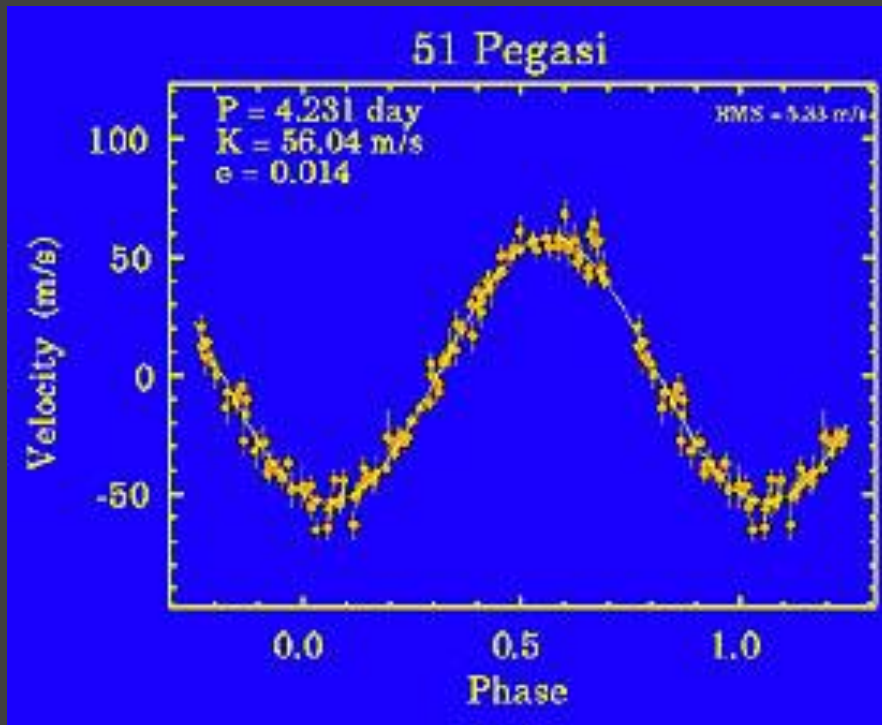
The Exoplanet Data Explorer is an interactive table and plotter for exploring and displaying data from the Exoplanet Orbit Database. The Exoplanet Orbit Database is a carefully constructed compilation of quality, spectroscopic orbital parameters of exoplanets orbiting normal stars from the peer reviewed literature, and updates the Catalog of nearby exoplanets.

A detailed description of the Exoplanet Orbit Database and Explorers is published [here](#) and is available on [astro.ph](#).

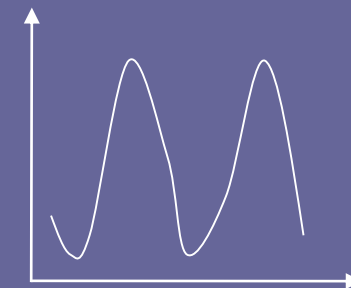
In addition to the Exoplanet Data Explorer, we have also provided the entire Exoplanet Orbit Database in CSV format for a quick and convenient download [here](#). A list of all archived CSVs is available [here](#).

Radial velocities

Michel Mayor and Didier Queloz 1995

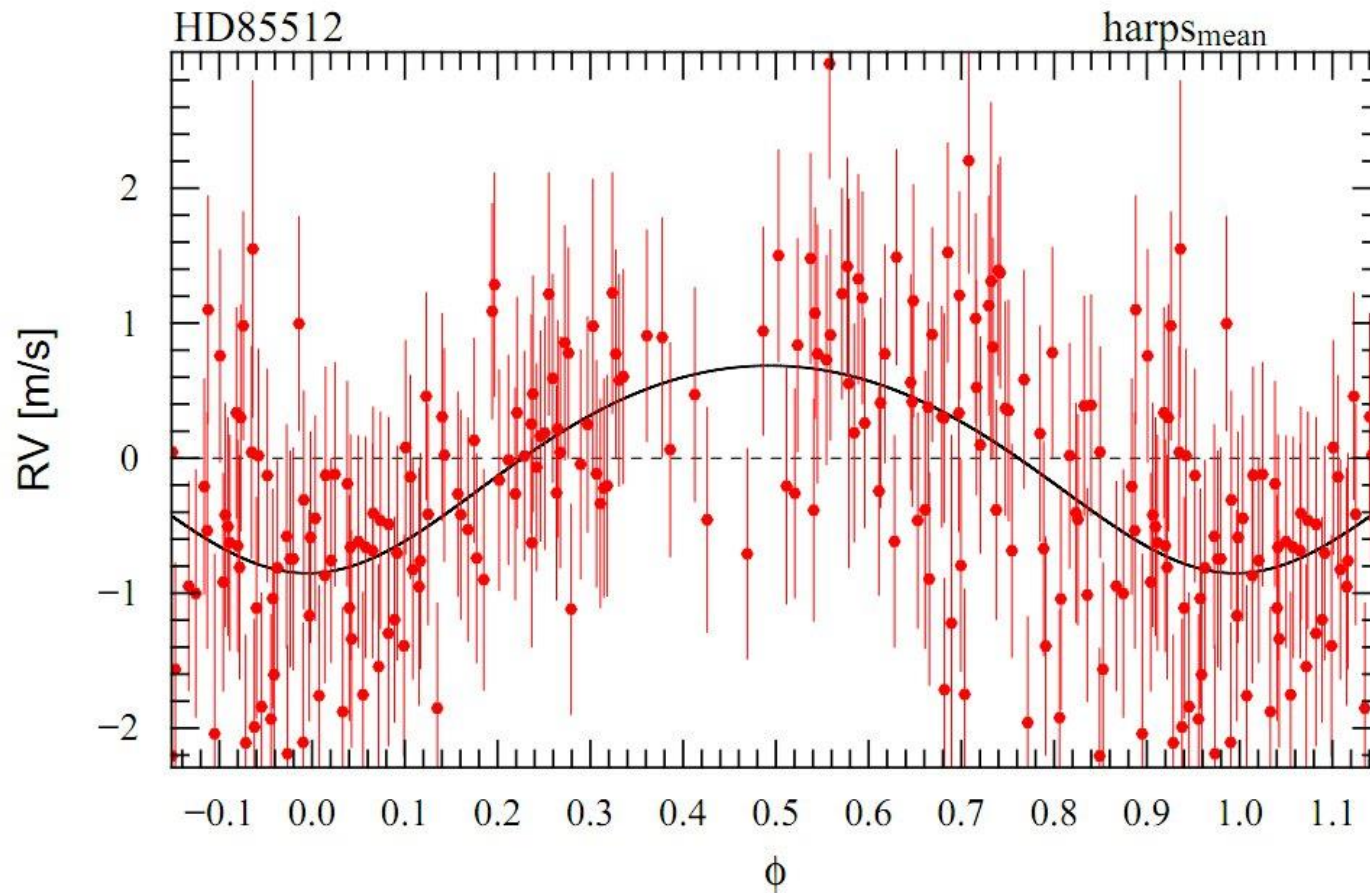


We see just the bright star.
We measure that its radial velocity
periodically changes.



Measure:
- Period
- Mass

First light planets

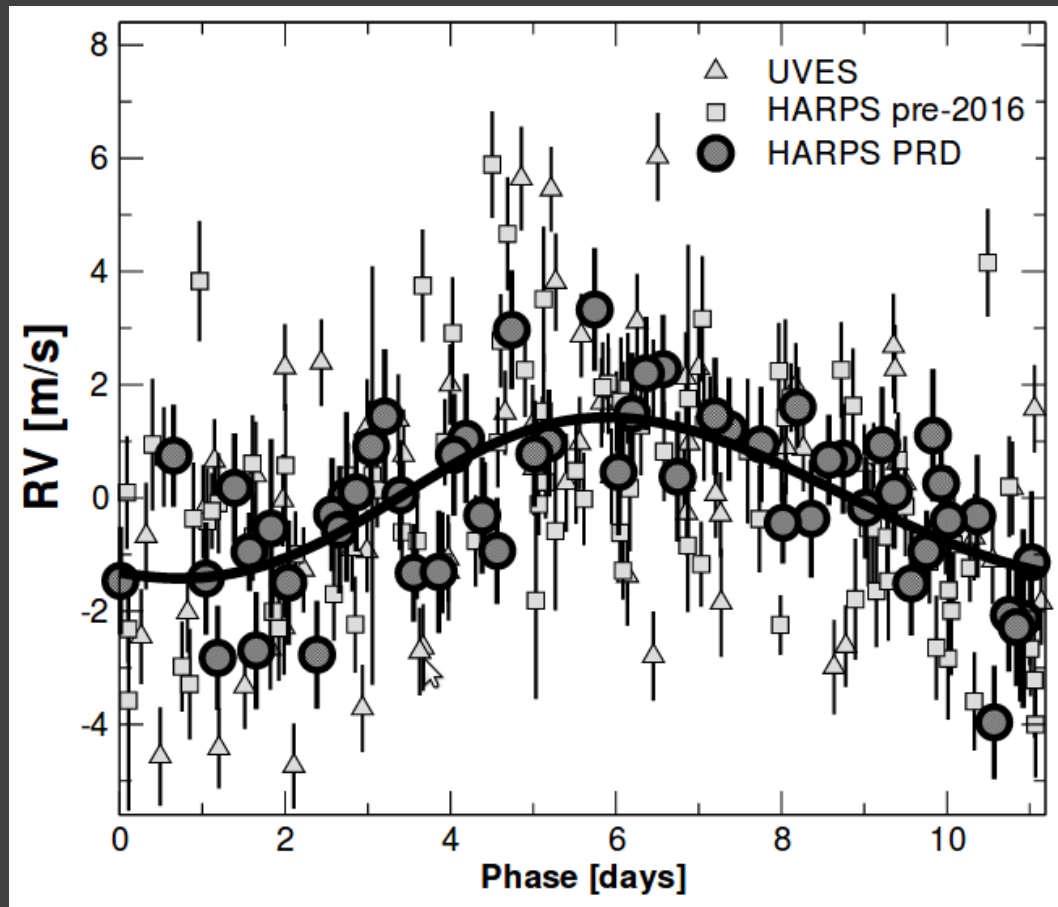


The problem is to measure small velocity variations for relatively long time.

Quality and stability of the spectrograph is more important than the telescope size.

This planet discovered by HARPS. Situated just near the zone of habitability.

Proxima Centauri b



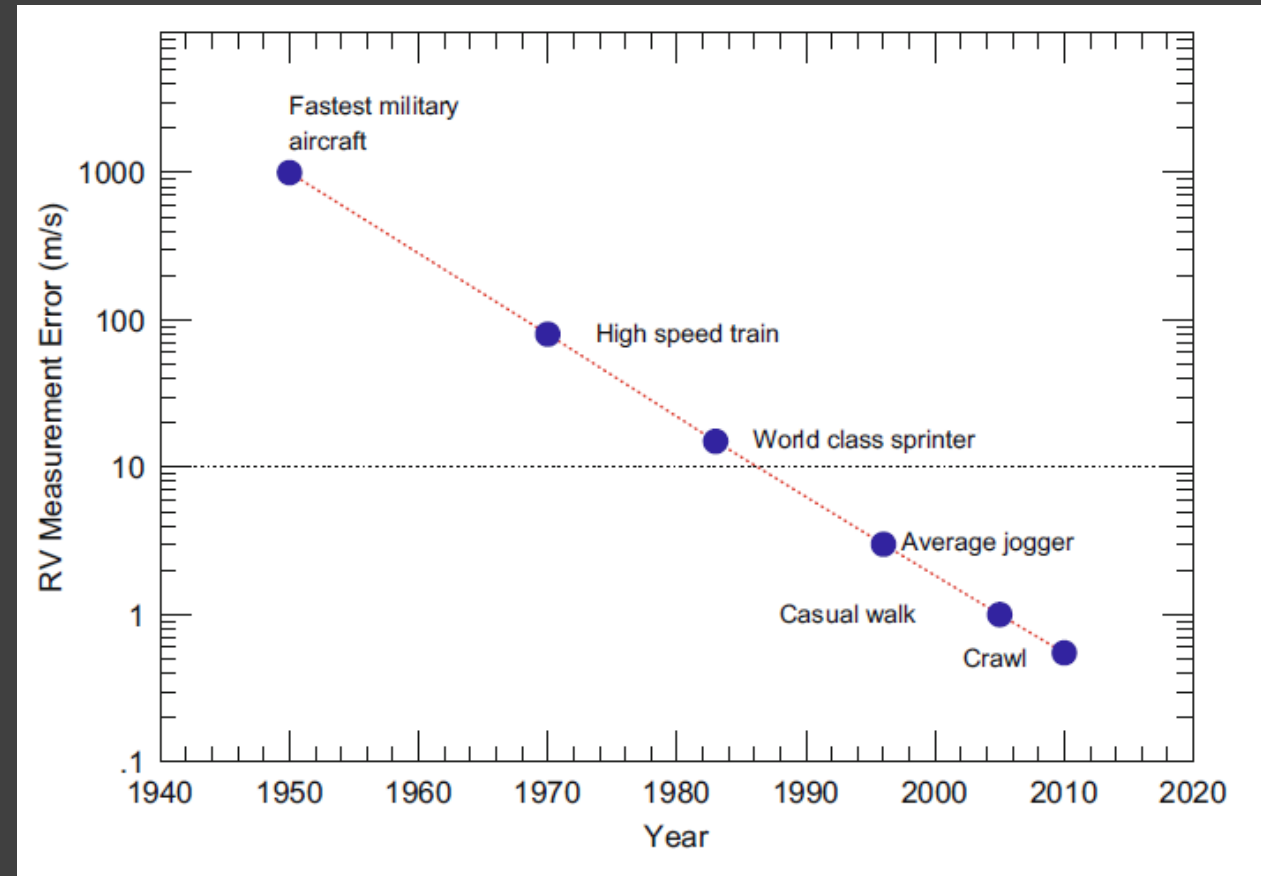
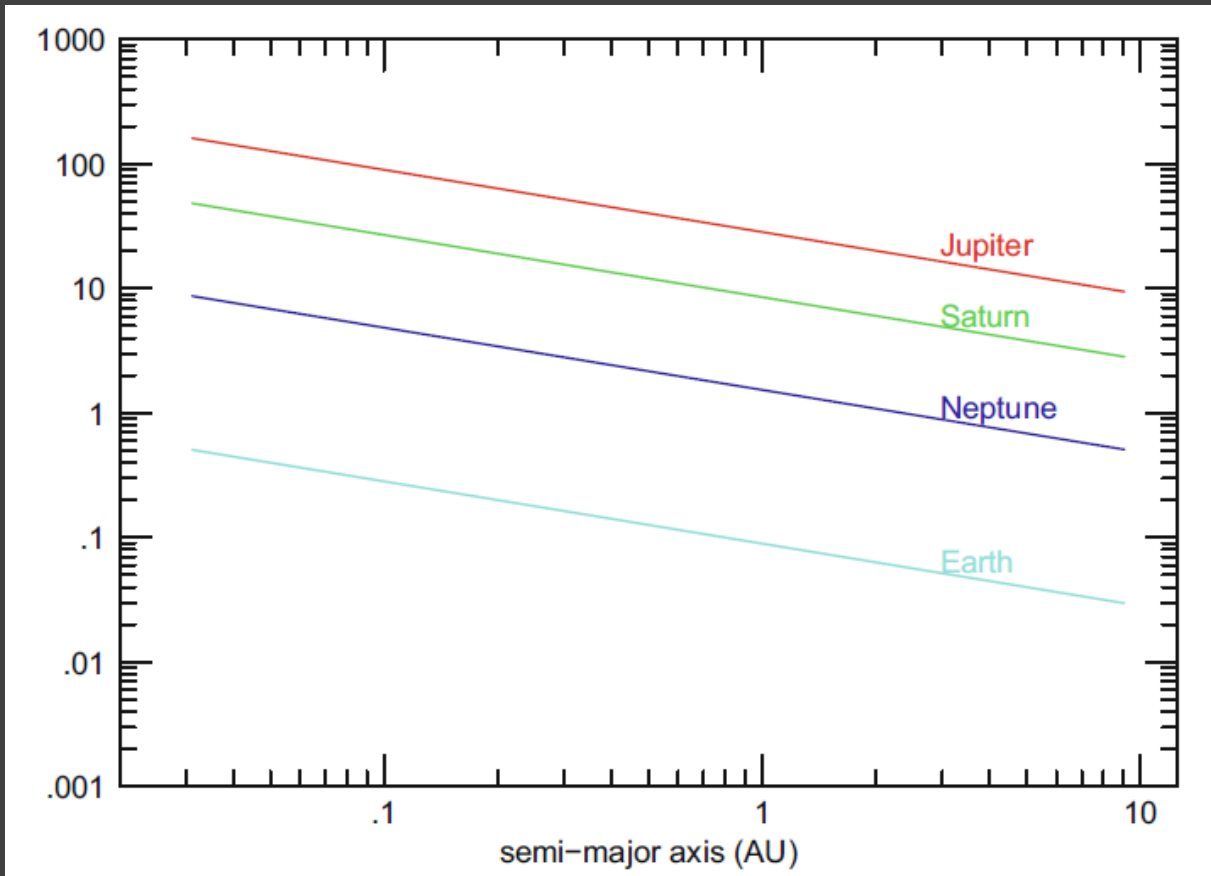
1.3 Earth masses

0.05 AU

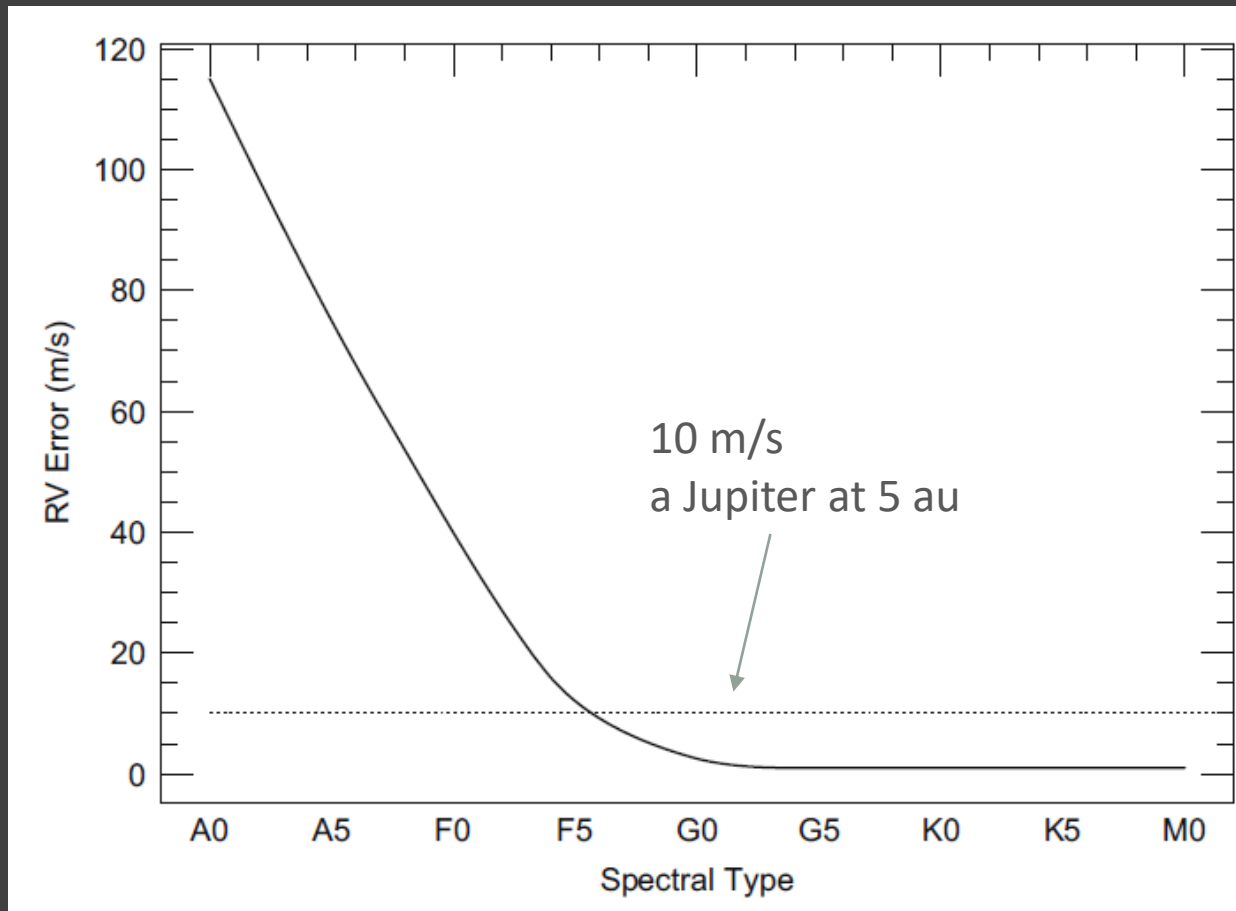
11 days

Habitability zone

Radial velocities: data and measurements



Role of a star



Difference is mainly due to

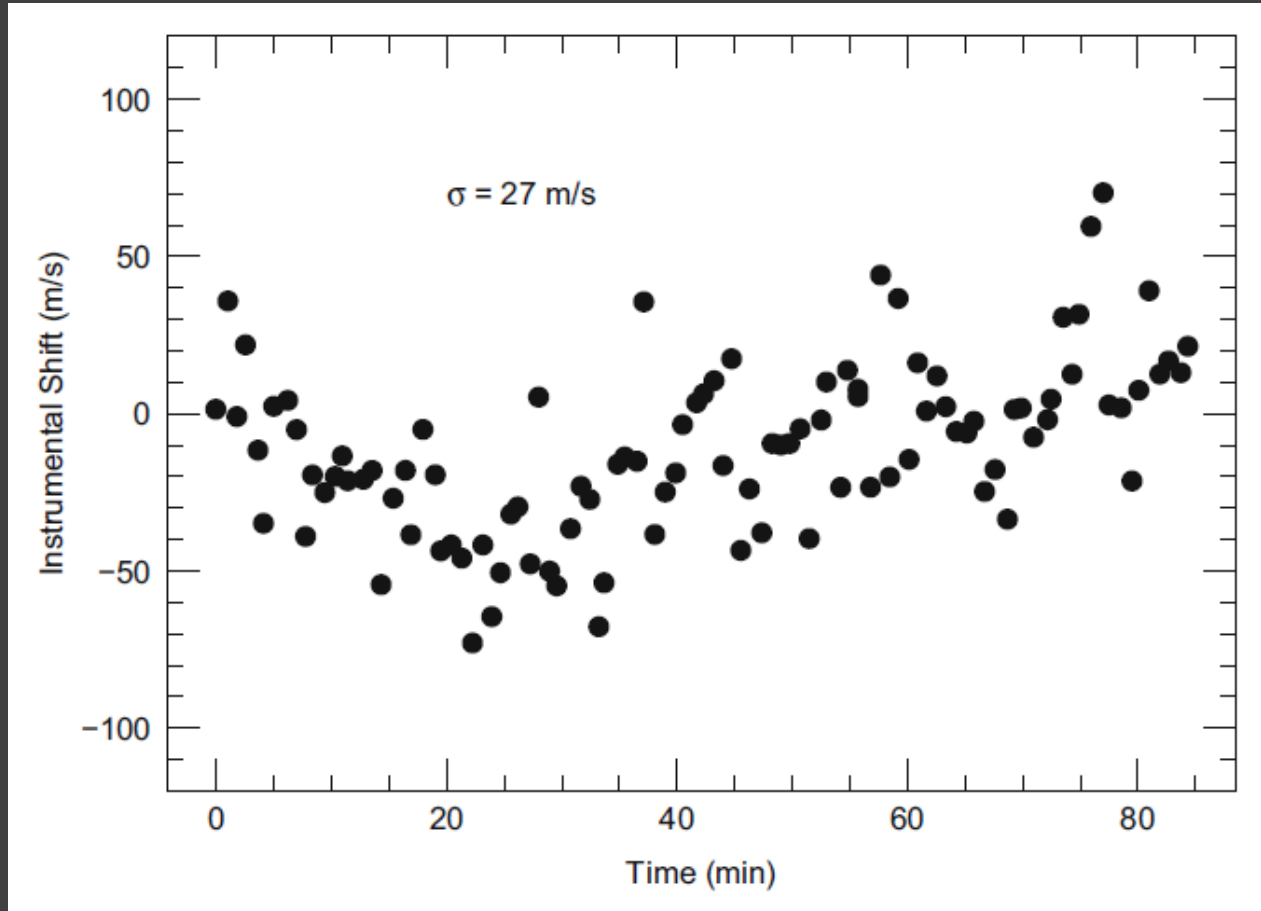
- Rapid rotation
- Smaller number of spectral lines

Without additional errors due to the instrument:

$$\sigma [\text{m/s}] = C(S/N)^{-1} R^{-3/2} B^{-1/2} (v \sin i / 2) f(\text{SpT})$$

B- band width, R – resolution ($\lambda / \Delta\lambda$)

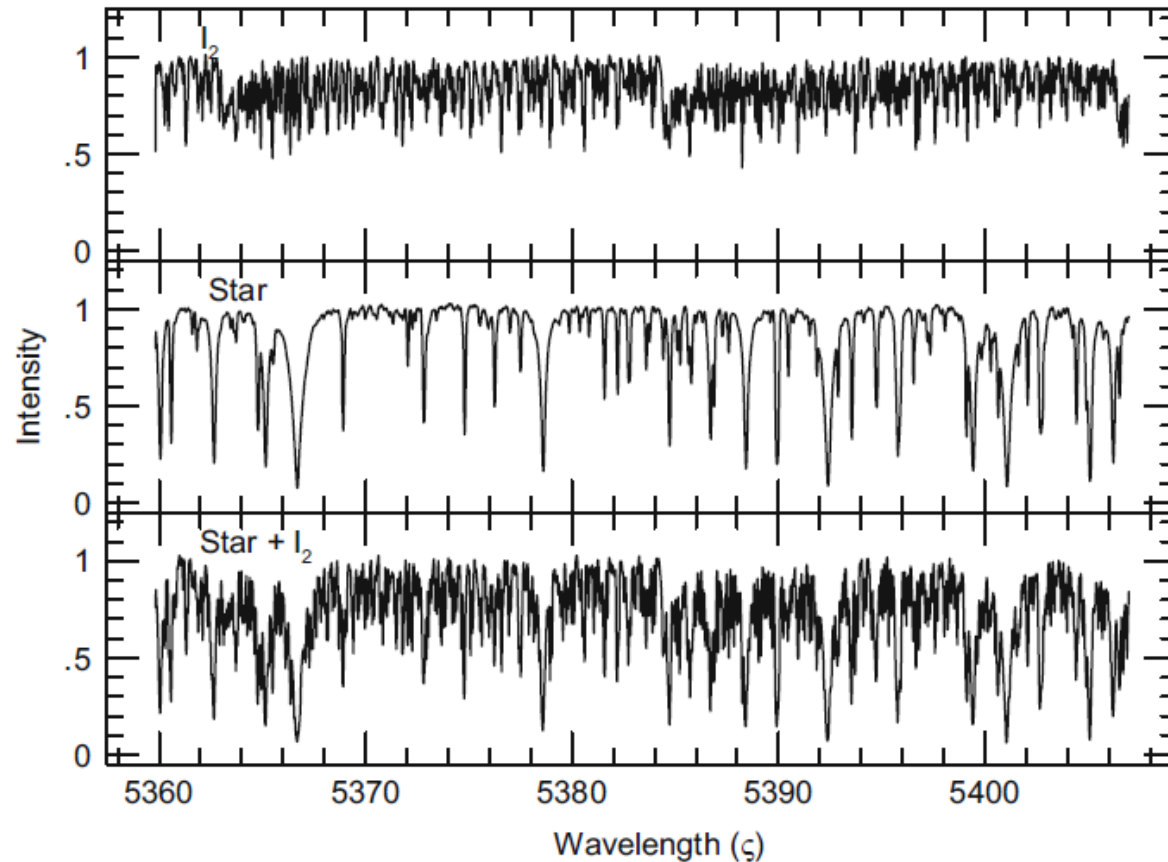
Necessity for simultaneous record of the stellar and calibration spectra



It is necessary to take the stellar and the laboratory spectra simultaneously, as the shift due to stellar velocity is very small and so the device cannot be stabilized to such level.

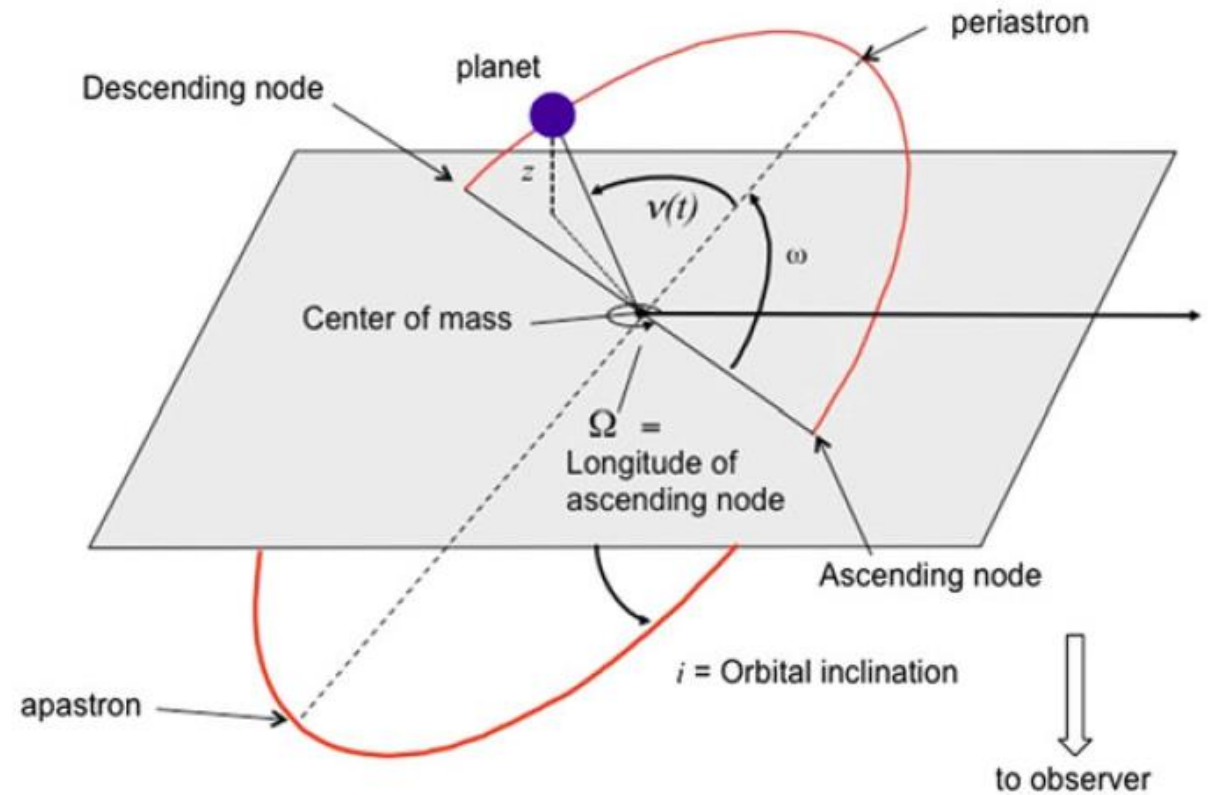
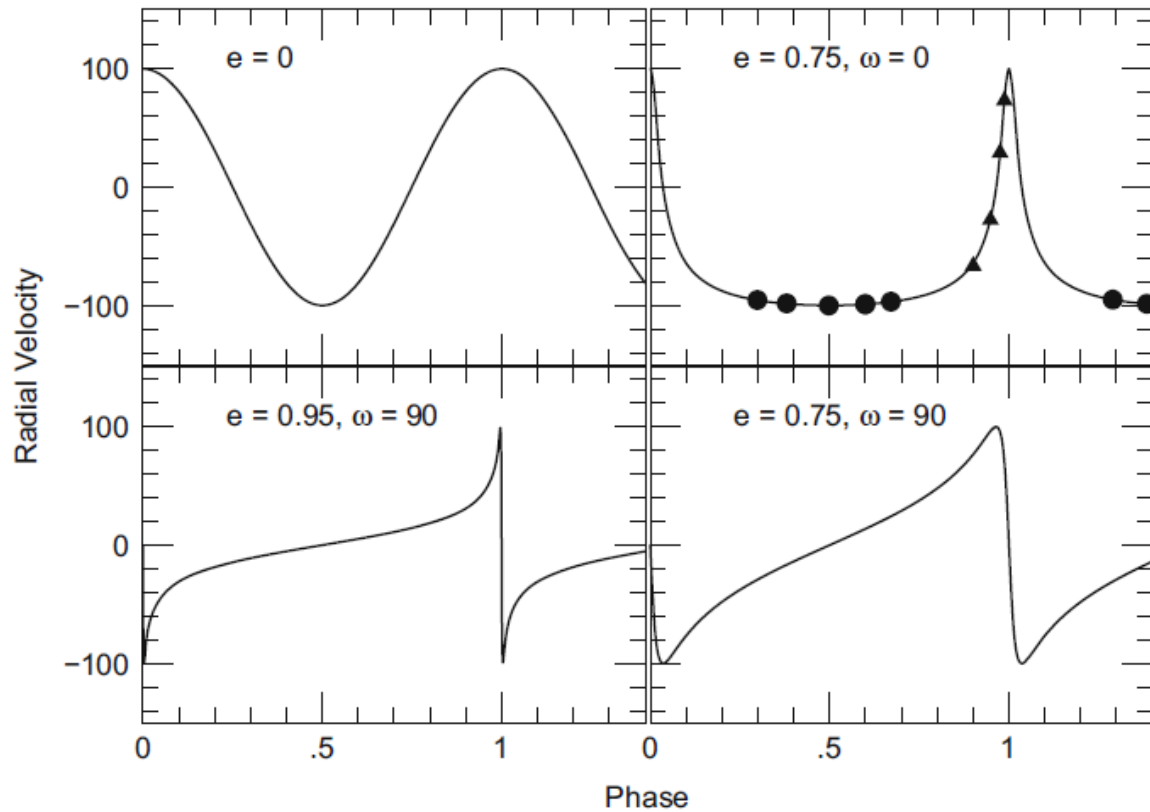
Any external mechanical influence can shift the detector so that the position of the line cannot be determined with precision high enough to detect the signal from the planet presence.

Molecular iodine cell



I_2 cell became the first effective tool to provide lines for RV measurements.

Velocity vs. phase for different orbits



Planet mass

$$f(m) = \frac{M_2^3 \sin^3 i}{(M_1 + M_2)^2} = \frac{K_1^3 P (1 - e^2)^{3/2}}{2\pi G} \approx \frac{M_2^3 \sin^3 i}{M_1^2}$$

Thus, it is necessary to know the stellar mass (M_1)

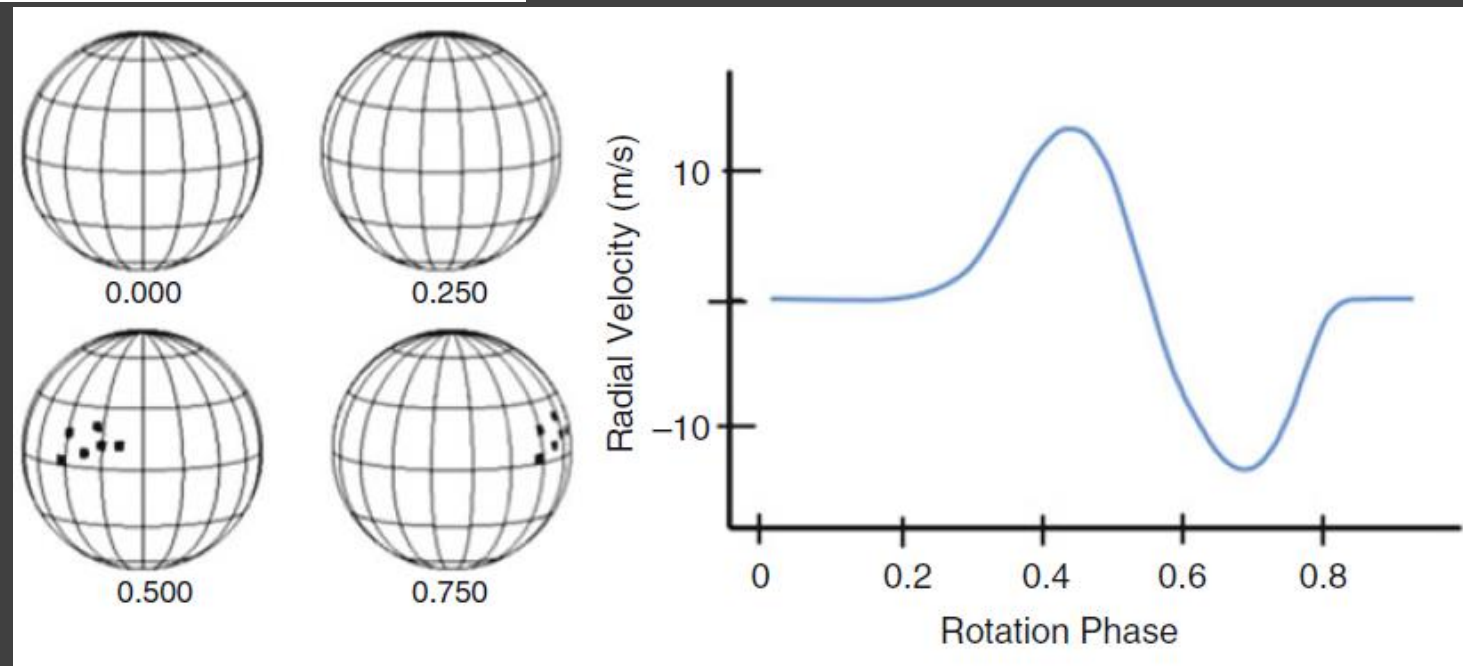
$$\langle \sin i \rangle = \frac{\int_0^\pi p(i) \sin i \, di}{\int_0^\pi p(i) \, di} = \frac{\pi}{4} = 0.79$$

For the mass function
<sin³ i> is important:

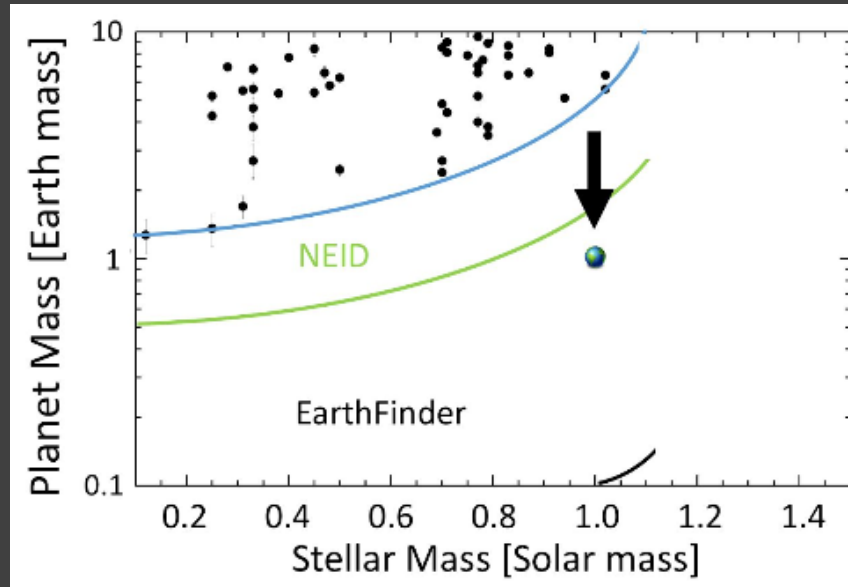
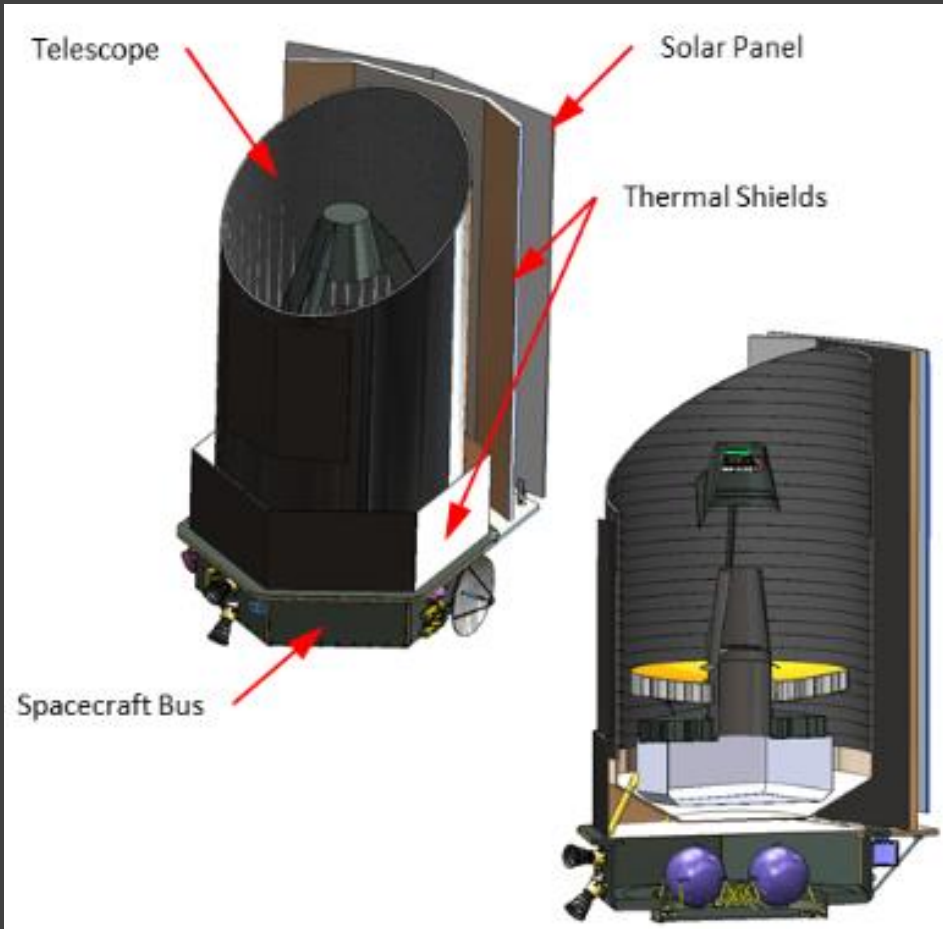
$$\frac{\int_0^\pi p(i) \sin^3 i \, di}{\int_0^\pi p(i) \, di} = 0.5 \int_0^\pi \sin^4 i \, di = \frac{3\pi}{16} = 0.59$$

Stellar noise

| Phenomenon | RV amplitude (m s^{-1}) | Time scales |
|--------------------------------|------------------------------------|---------------------------|
| Solar-like oscillations | 0.2–0.5 | $\sim 5\text{--}15$ min |
| Stellar activity (e.g., spots) | 1–200 | $\sim 2\text{--}50$ days |
| Granulation/Convection pattern | \sim few | $\sim 3\text{--}30$ years |



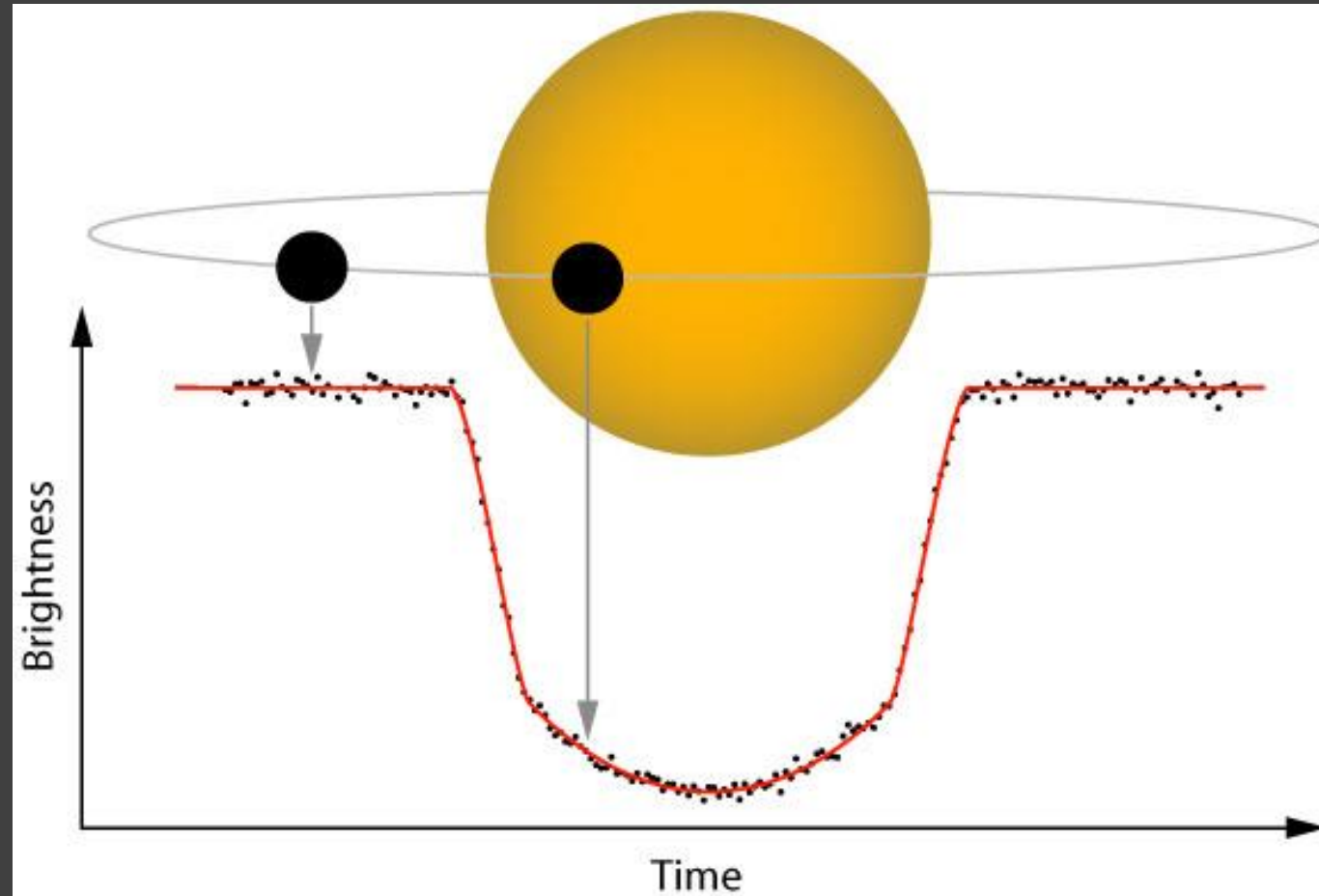
Proposals of special space mission



The nominal spacecraft design is based upon the Kepler spacecraft by Ball Aerospace, with a 1.4-m primary, with the starlight coupled into single-mode fibers illuminating three high-resolution, compact and diffraction-limited spectrometer “arms”, one covering the near-UV (200-380nm), visible(380-900 nm) and near-infrared (NIR; 900-2500 nm) respectively with a spectral resolution of greater than 150,000 in the visible and near-infrared arms.

Planet transits

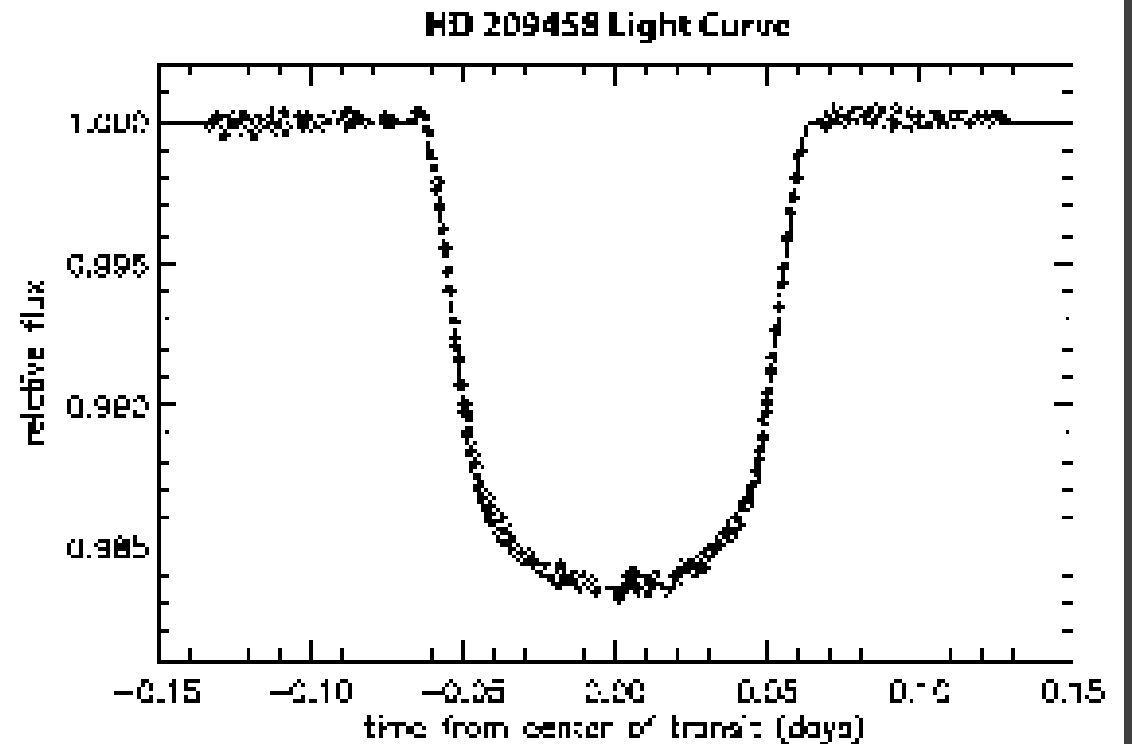
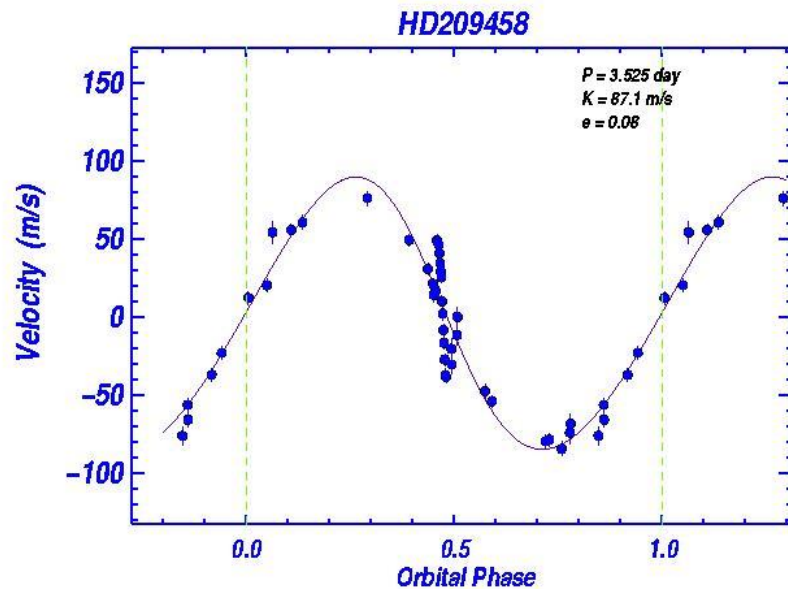
Proposed by
Otto Struve
in 1952



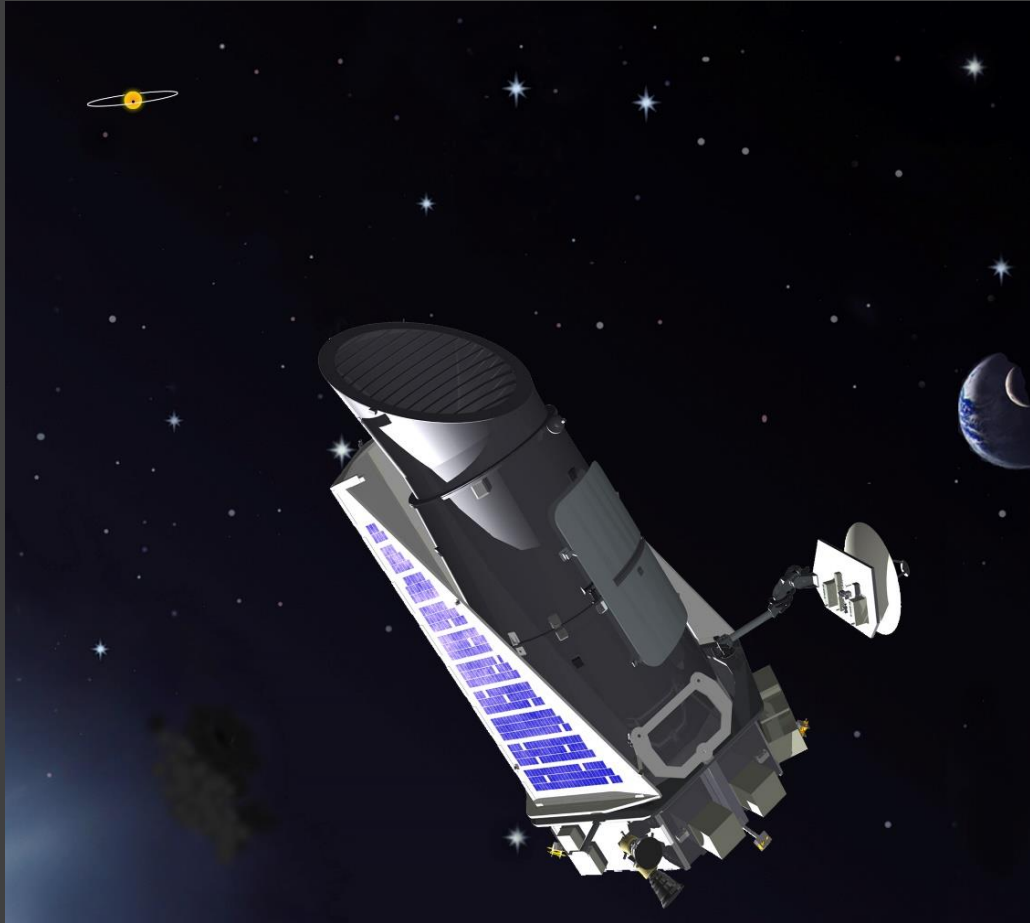
$$\frac{S_{\text{star}} - S_{\text{planet}}}{S_{\text{star}}}$$

The first transit measurement. HD 209458

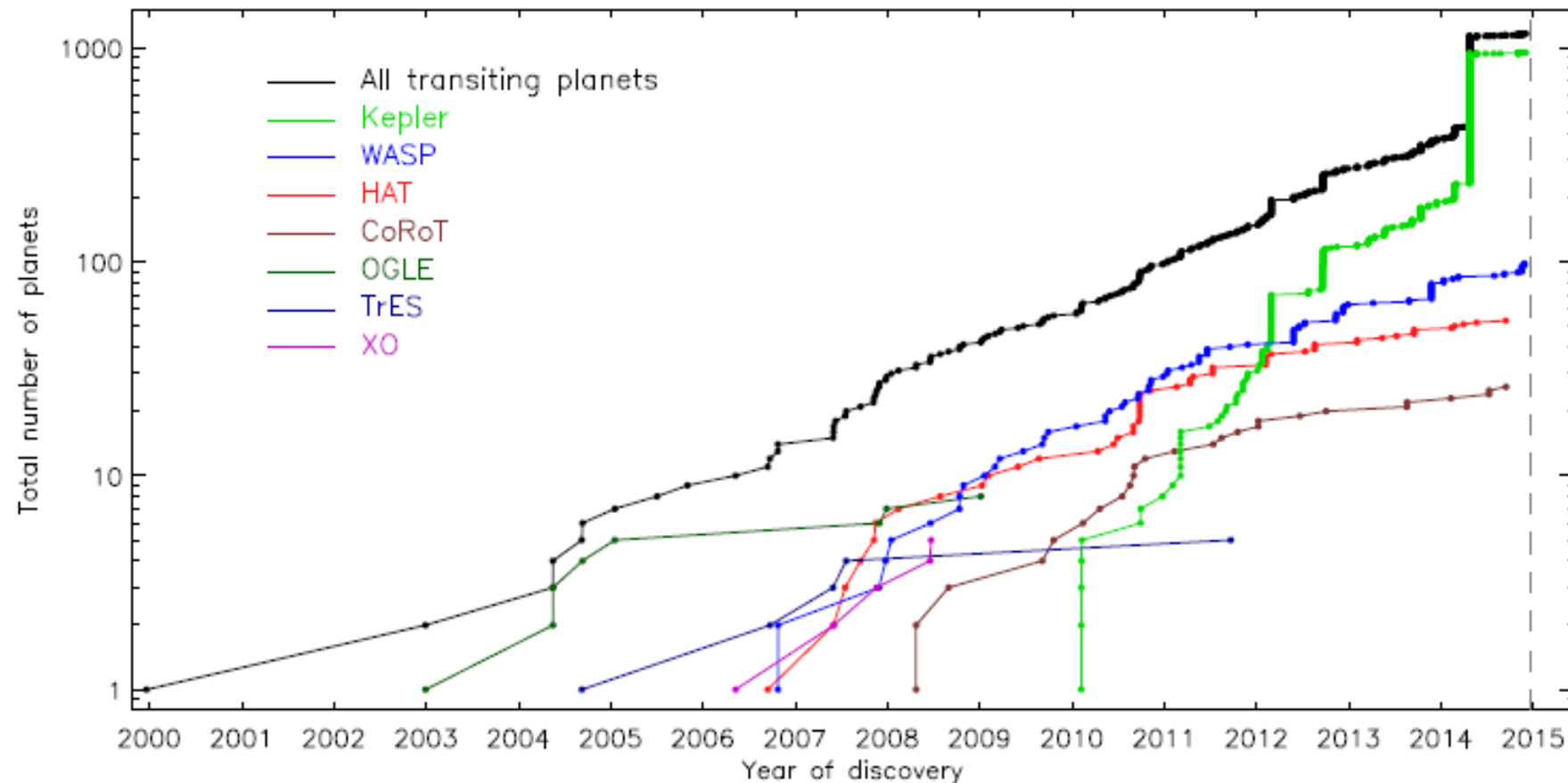
The first measurements of a transit was made from the ground for a planet discovered by RV, and so known orbital parameters.



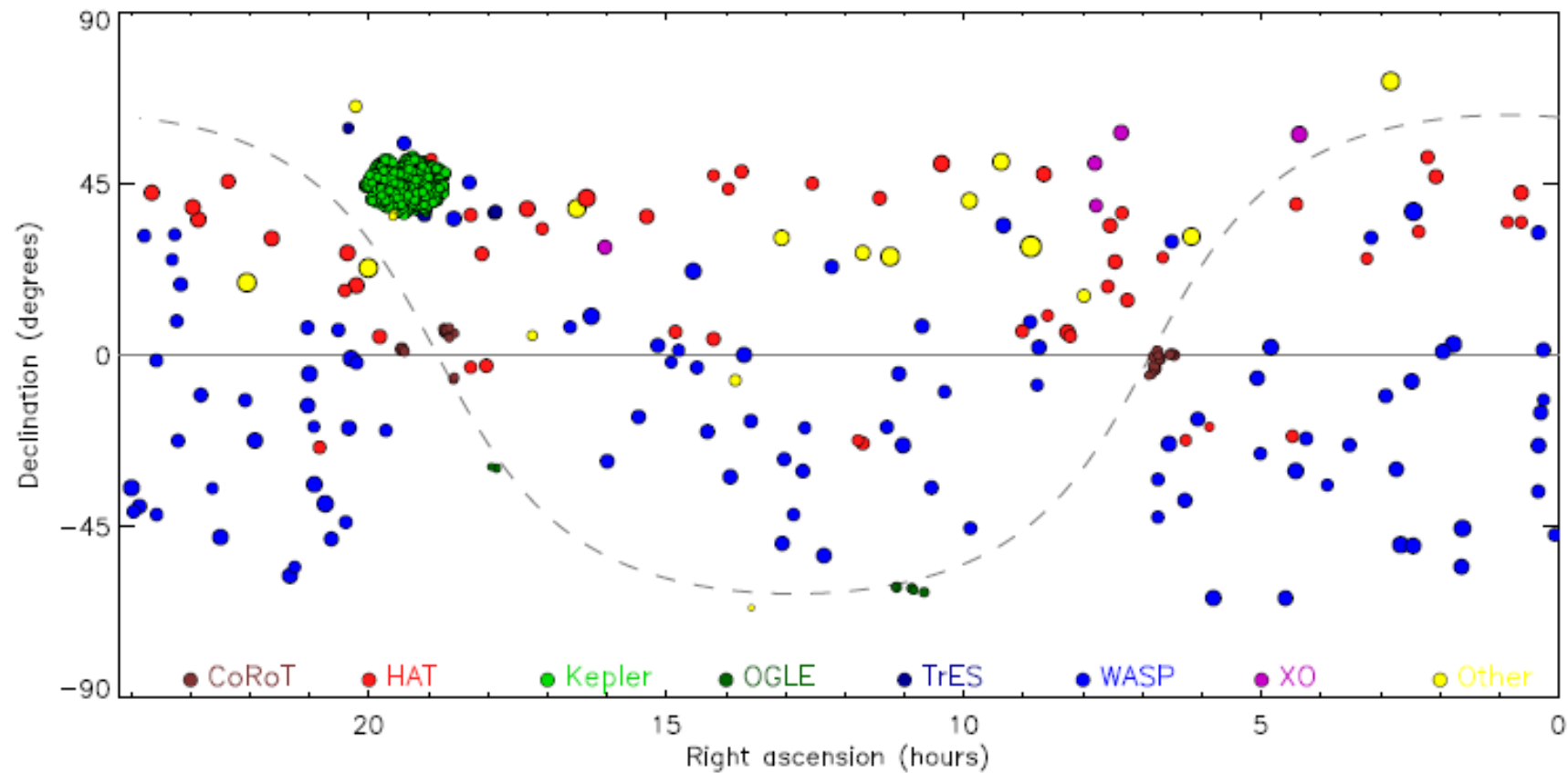
Kepler and CoRoT



Rate of discovery



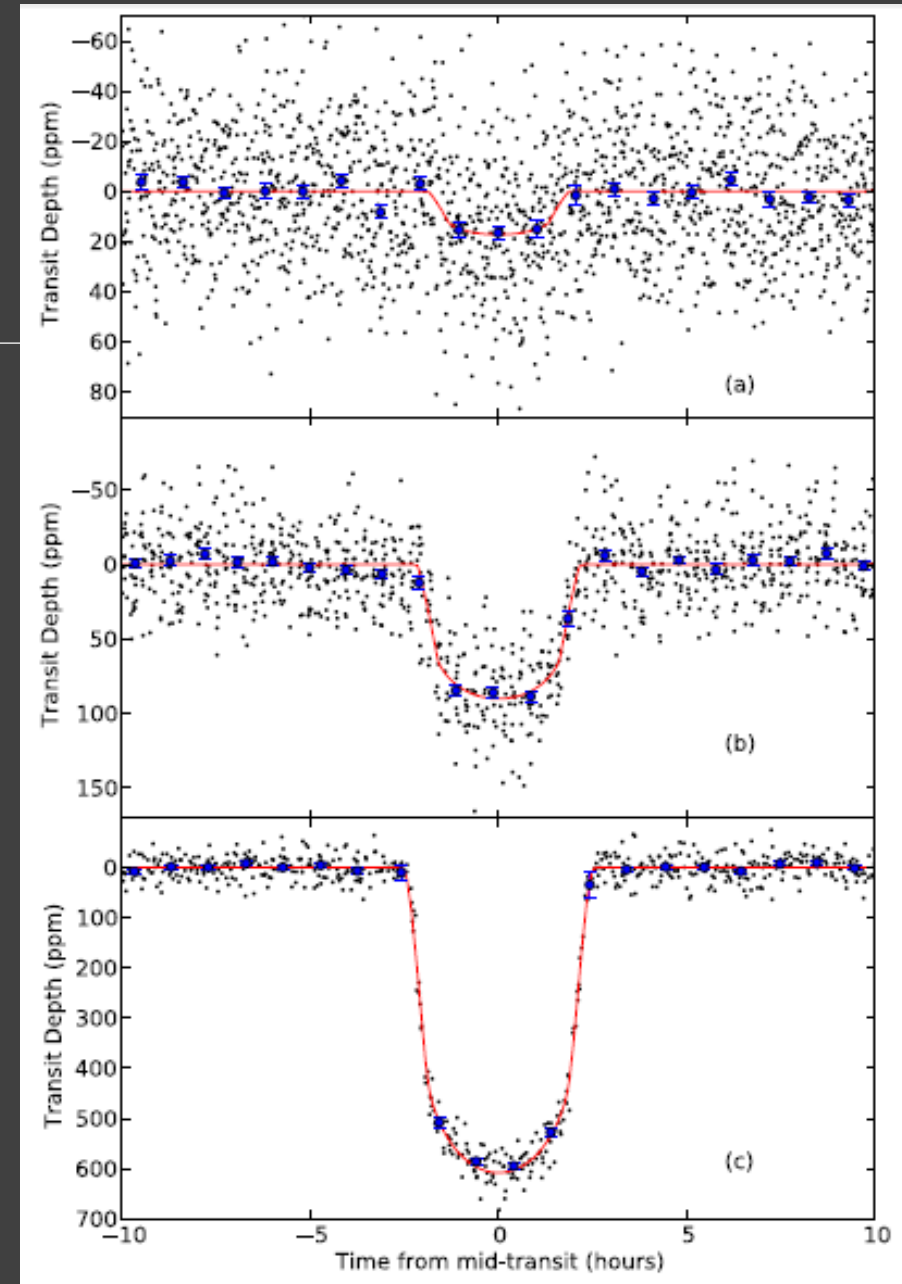
Transiting planets in the sky



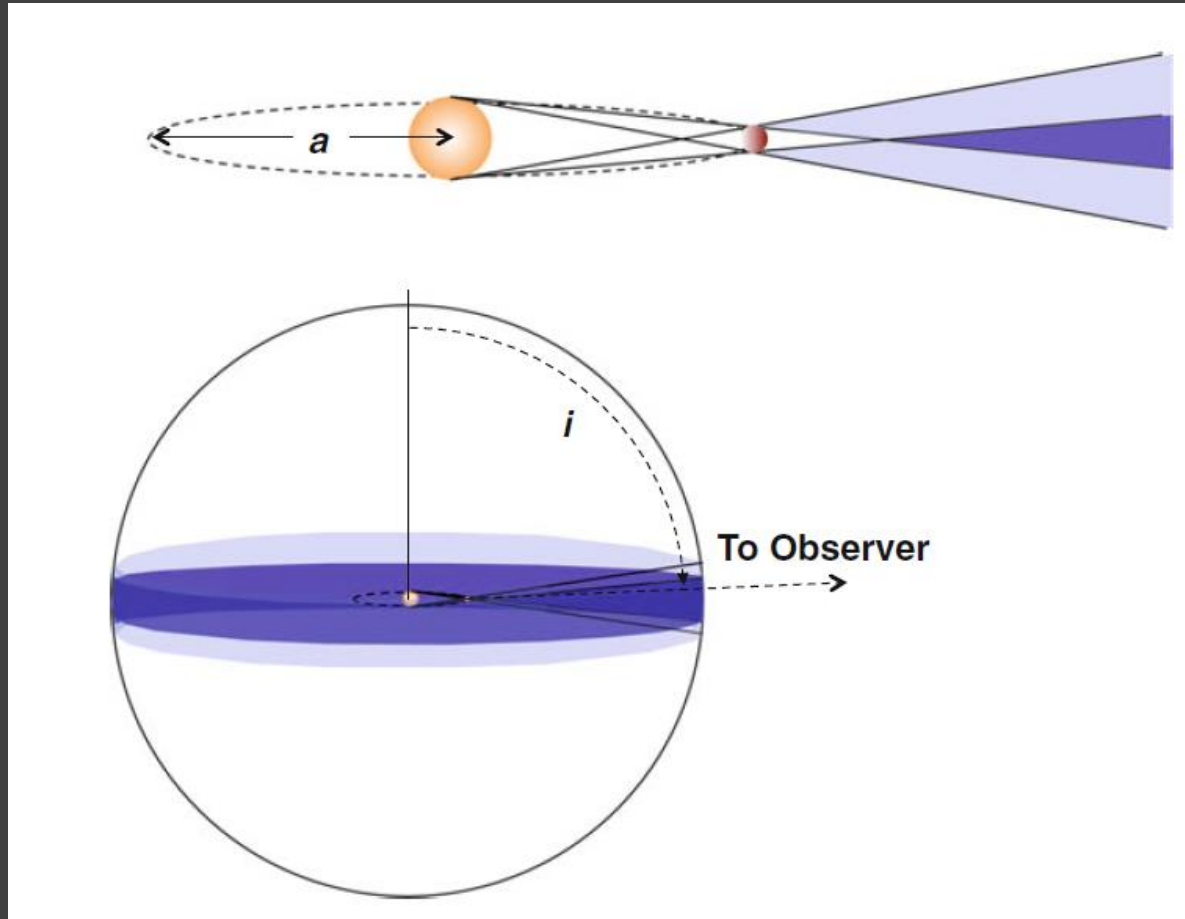
Very small planets

Kepler-37b

The first discovered exoplanet
with size smaller than Mercury

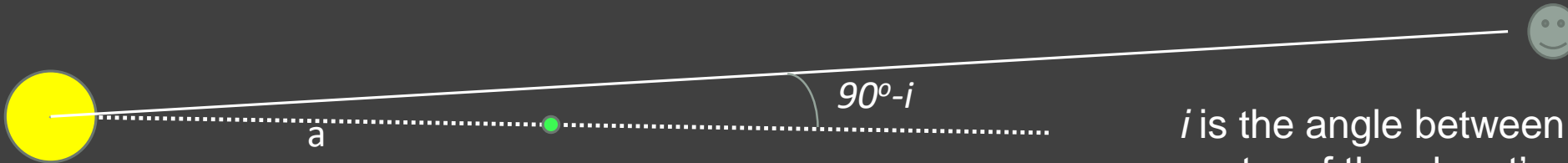


Transit probability



$$\Pr \left(\cos i < \frac{R_*}{a} \right) \simeq 0.0046 \left(\frac{R_*}{R_\odot} \right) \left(\frac{1 \text{ au}}{a} \right).$$

Transit conditions



i is the angle between the angular-momentum vector of the planet's orbit and the line of sight

$$b = \frac{a \cos i}{R_*}.$$

$$\frac{d\Omega}{4\pi} = \frac{2\pi \sin i \, di}{4\pi} = \frac{d(\cos i)}{2}.$$

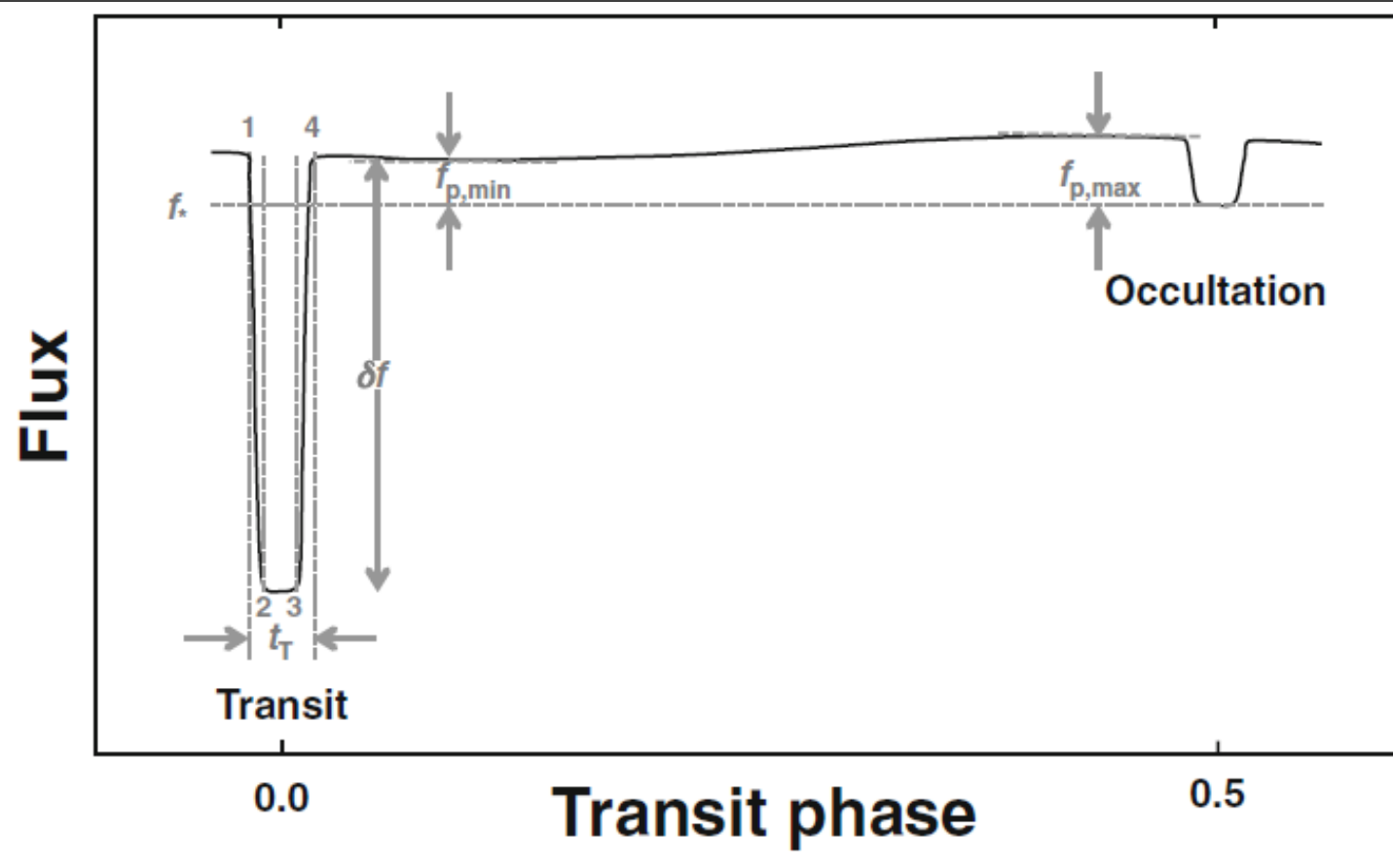
$$\Pr \left(\cos i < \frac{R_* + R_p}{a} \right) = \frac{1}{2} \int_{-(R_* + R_p)/a}^{(R_* + R_p)/a} = \frac{R_* + R_p}{a}.$$

$$R_p \ll R_*,$$

$$\Pr \left(\cos i < \frac{R_*}{a} \right) \simeq 0.0046 \left(\frac{R_*}{R_\odot} \right) \left(\frac{1 \text{ au}}{a} \right).$$

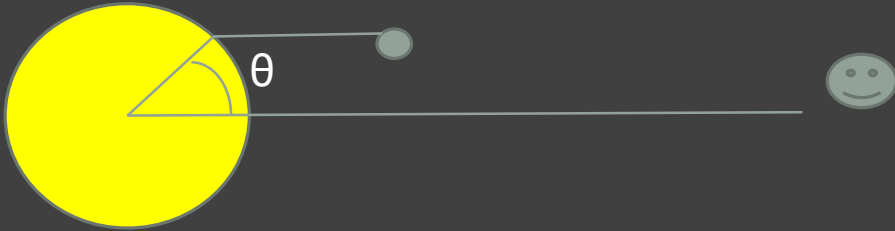
Selection in favour of close-in planets.

Transit depth



$$\frac{\Delta f}{f} \simeq \left(\frac{R_p}{R_*} \right)^2 = 0.0105 \left(\frac{R_p}{R_{\text{Jup}}} \right)^2 \left(\frac{R_*}{R_{\odot}} \right)^{-2}$$

Limb darkening



$$\mu = \cos \theta = \sqrt{1 - b^2}$$

$$I = I_0(1 - u(1 - \mu))$$

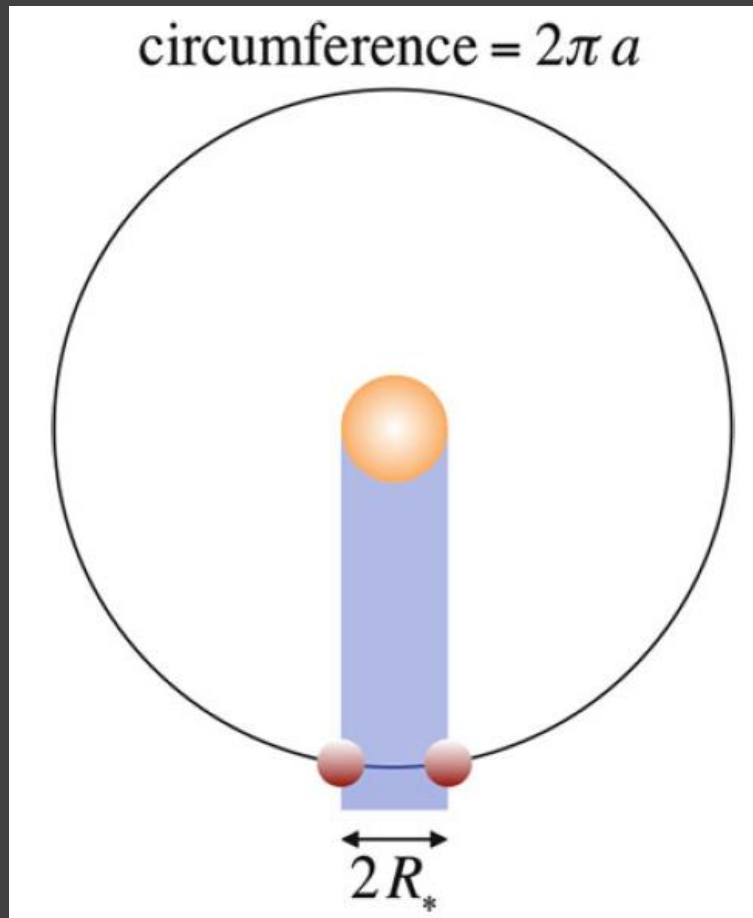
Limb darkening can be taken into account in a more precise manner

$$\frac{I(\mu)}{I_0} = 1 - \sum_{n=1}^4 u_n(1 - \mu^{n/2}).$$

$$\begin{aligned} \frac{\Delta f}{f} &= \frac{\pi R_p^2 I_0 (1 - u + u \cos \theta)}{2\pi R_*^2 I_0 \int_0^{\pi/2} (1 - u + u \cos \theta) \sin \theta \cos \theta d\theta} \\ &= \frac{3(1 - u + u\sqrt{1 - b^2})}{3 - u} \left(\frac{R_p}{R_*} \right)^2. \end{aligned}$$

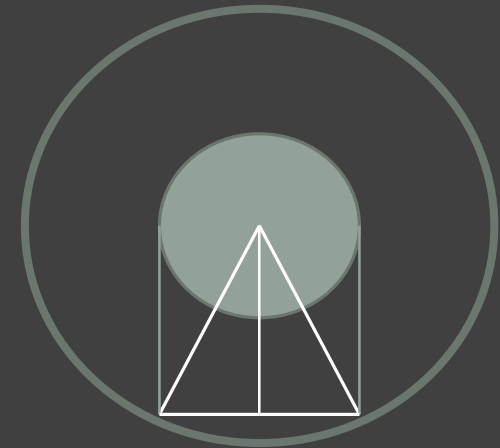
Transit duration

$$\frac{t_{tr}}{P} \simeq \frac{R_*}{a} \frac{\sqrt{(1 + R_p/R_*)^2 - b^2}}{\pi} \frac{1 + e \sin \omega}{1 - e^2}.$$



$$\frac{T}{P} = \frac{1}{\pi} \sin^{-1} \frac{R_*}{a}$$

$$\frac{T}{P} = \frac{1}{\pi} \sin^{-1} R_* \left(\frac{4\pi^2}{GM_* P^2} \right)^{1/3}$$



$$\frac{t_T}{P} = \frac{1}{\pi} \sin^{-1} \left(\frac{R_*}{a} \left\{ \frac{[1 + (R_p/R_*)]^2 - [(a/R_*) \cos i]^2}{1 - \cos^2 i} \right\}^{1/2} \right)$$

t_T – from first to last contact

For $\cos i \ll 1$

$$\frac{t_T}{P} = \frac{R_*}{\pi a} \sqrt{\left(1 + \frac{R_p}{R_*}\right)^2 - b^2}.$$

System parameters

$$T \simeq 3h \left(\frac{P}{4d} \right)^{1/3} \left(\frac{\rho_*}{\rho_\odot} \right)^{-1/3}$$

Stellar density estimate

$$\frac{dv_r}{dt} = \frac{2\pi K}{P} = \frac{GM_p}{a^2} = g_p \frac{R_p^2}{a^2} = g_p \frac{R_p^2}{R_*^2} \frac{R_*^2}{a^2},$$

K – stellar velocity

$$g_p = \frac{2\pi K}{P} \left(\frac{R_*}{R_p} \right)^2 \left(\frac{a}{R_*} \right)^2$$

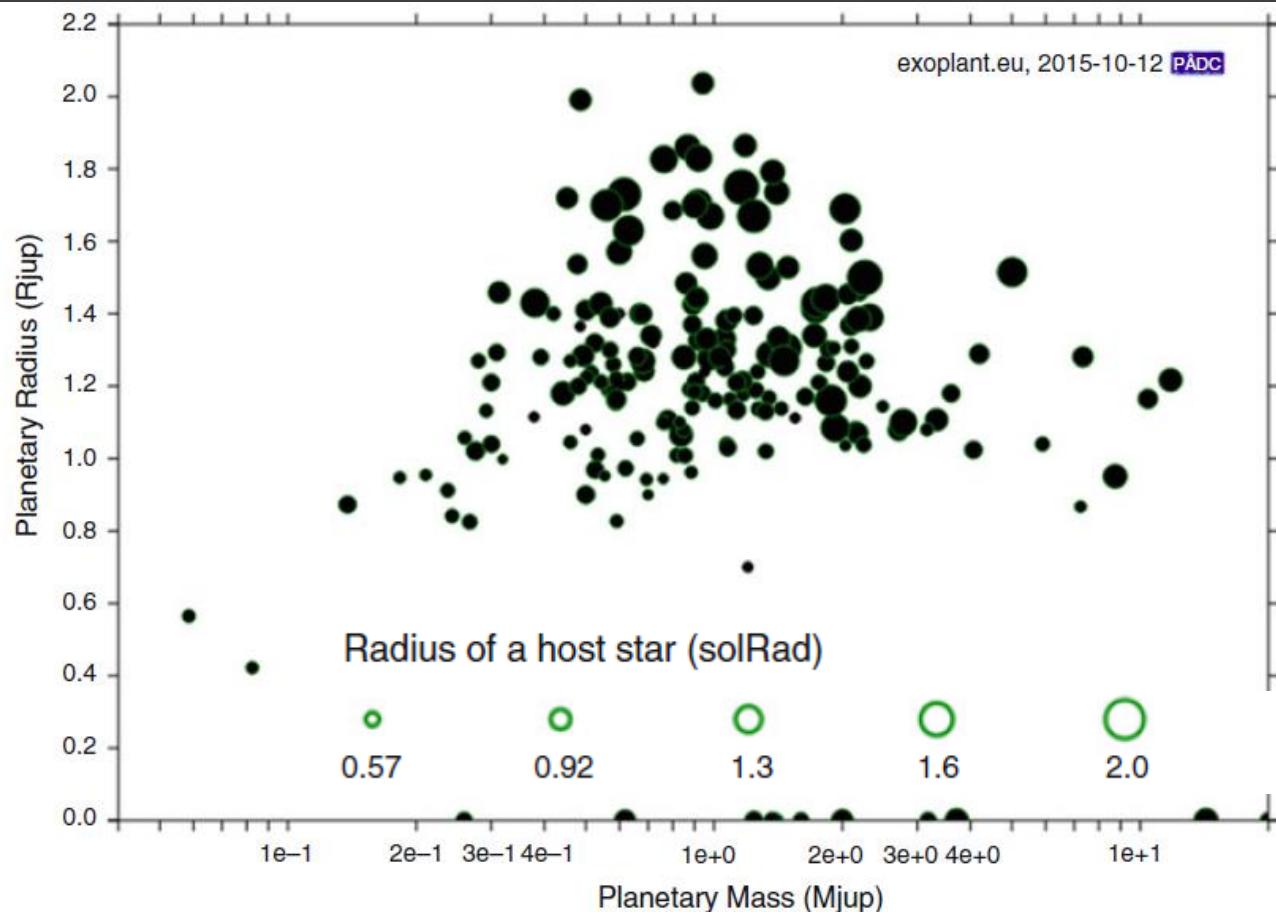
Planet density

$$\rho_p = \frac{3g_p}{4\pi GR_p} = \frac{3g_p}{4\pi GR_*} \left(\frac{R_*}{R_p} \right)$$

$$R_* = \theta d = \theta / \hat{\pi}:$$

$$\rho_p = \frac{3g_p \hat{\pi}}{4\pi G \theta} \left(\frac{R_*}{R_p} \right)$$

Ground based searches with small cameras



It is expected to have one hot Jupiter per 82 sq. degrees at $V < 12$

$$3600 \times \frac{180}{\pi} \frac{1}{f} = \frac{206265}{f} \text{ arcsec/mm},$$

Thus one source per 82 sq.deg corresponds to $f=174 \text{ mm}$

For 200-mm camera we have:

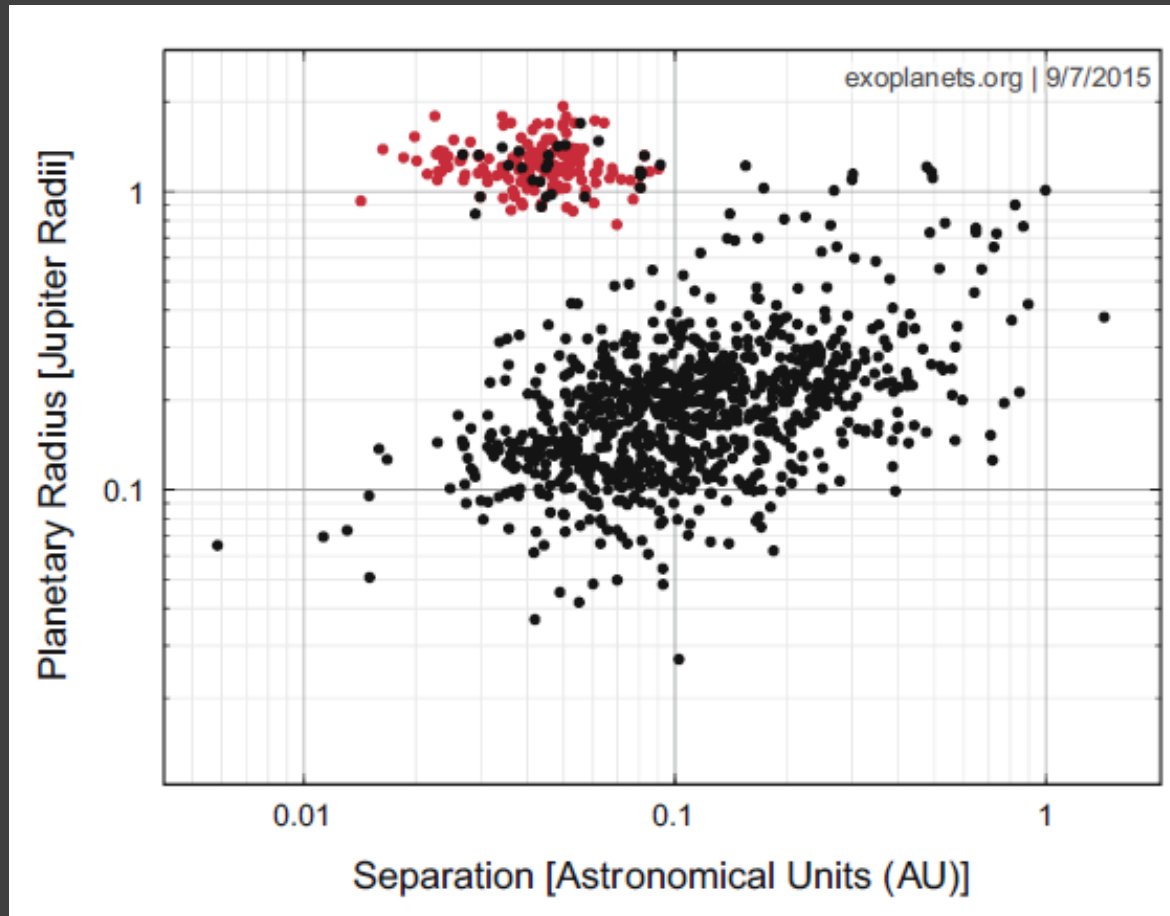
$$3600 \times \frac{180}{\pi} \frac{1}{f} = 1031 \text{ arcsec/mm},$$

$$0.0135 \times 1031 = 13.9 \text{ arcsec/pixel}$$

FOV is:
which gives
52 sq. deg.

$$\frac{2048 \times 13.9}{3600} = 7.9 \text{ degrees},$$

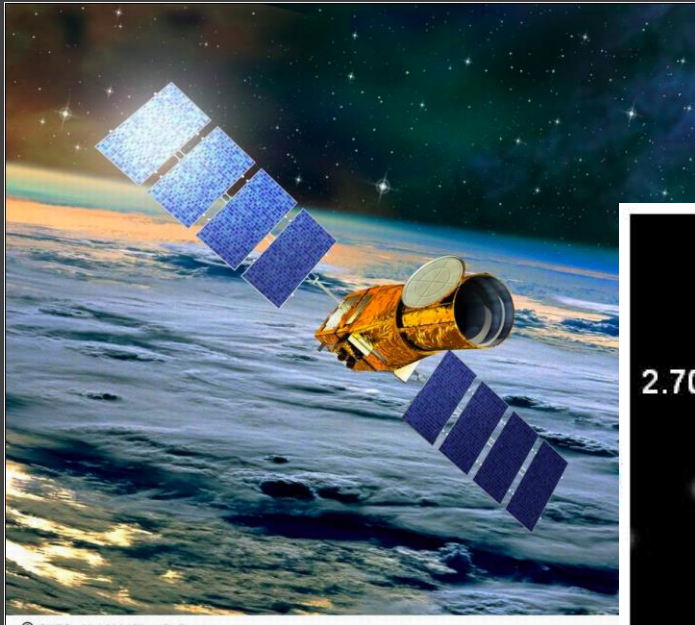
Space surveys vs. ground based



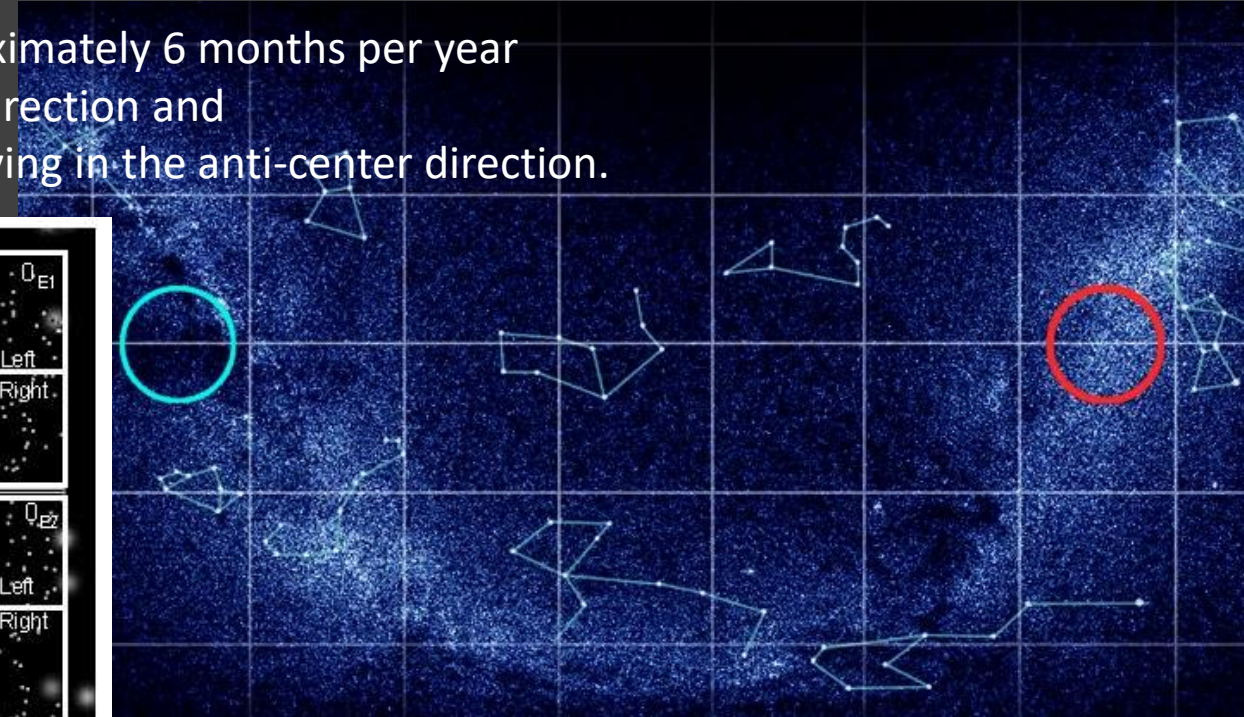
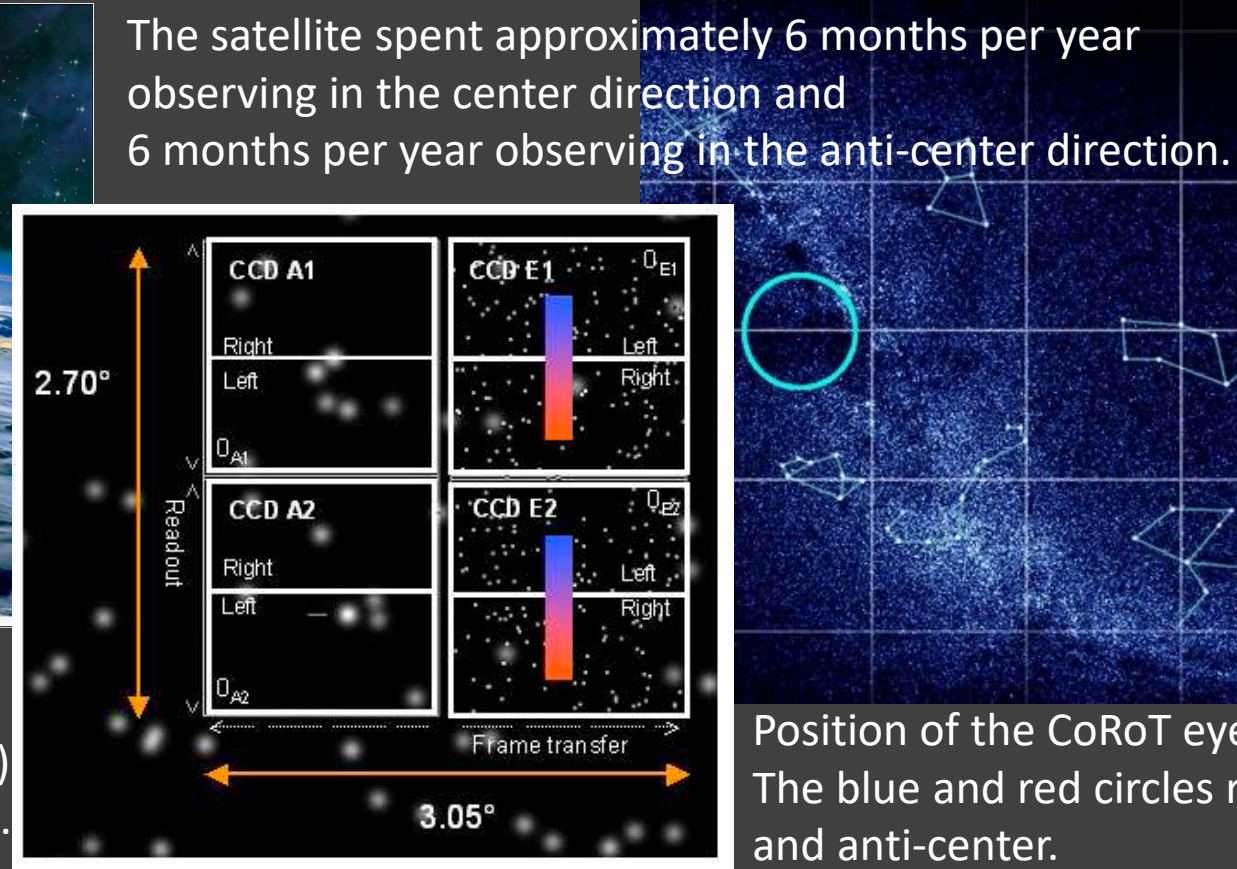
Hot jupiters are rare, but easy to detect from Earth. Space surveys (here – Kepler) show mostly different types of planets.

CoRoT

December 2006 – November 2012
27-cm telescope



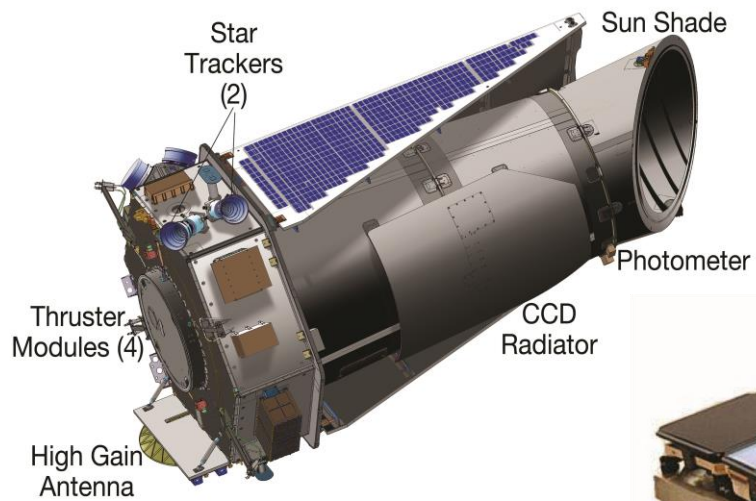
Focal planet arrangement
of the asteroseismology (A1, A2)
and the exoplanet (E1, E2) CCDs.



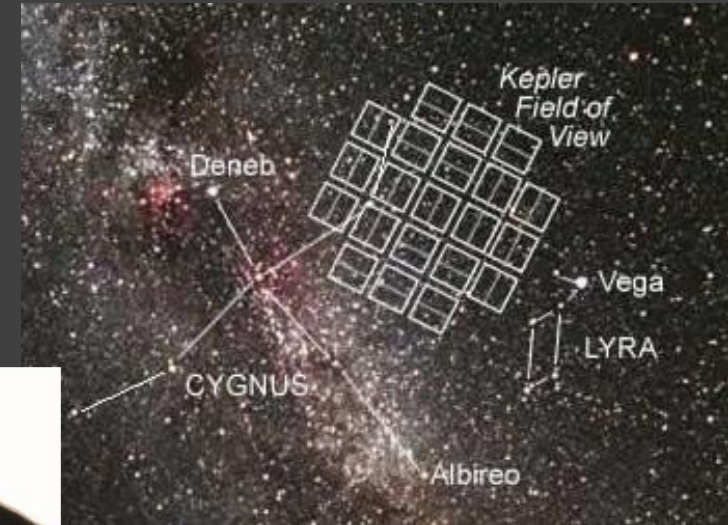
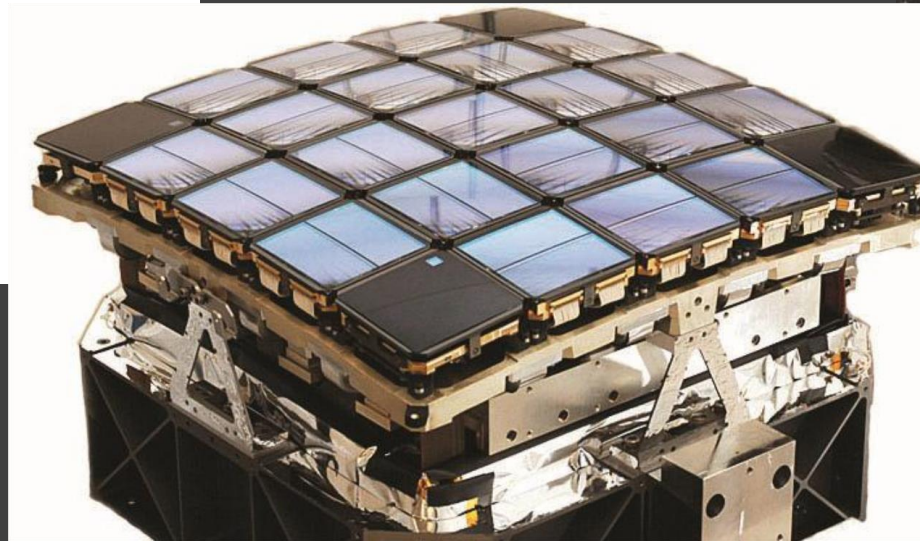
Position of the CoRoT eyes in the sky.
The blue and red circles represent the center
and anti-center.

Kepler

2009-2013 + K2-mission
0.95 m telescope

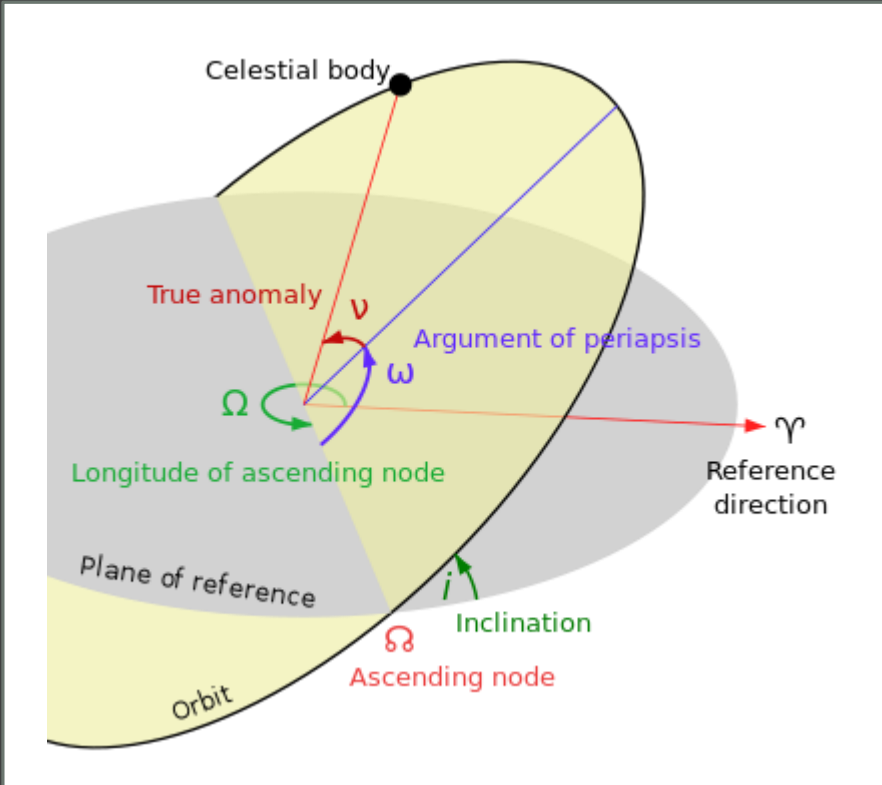


Monitoring of ~150 000 stars

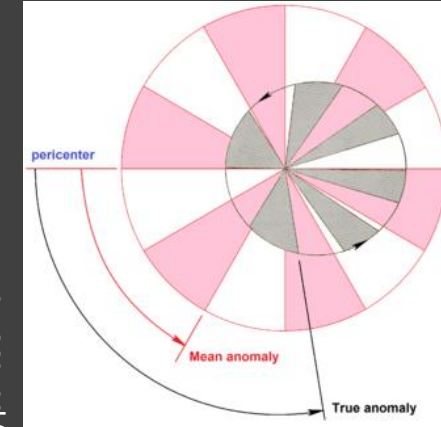
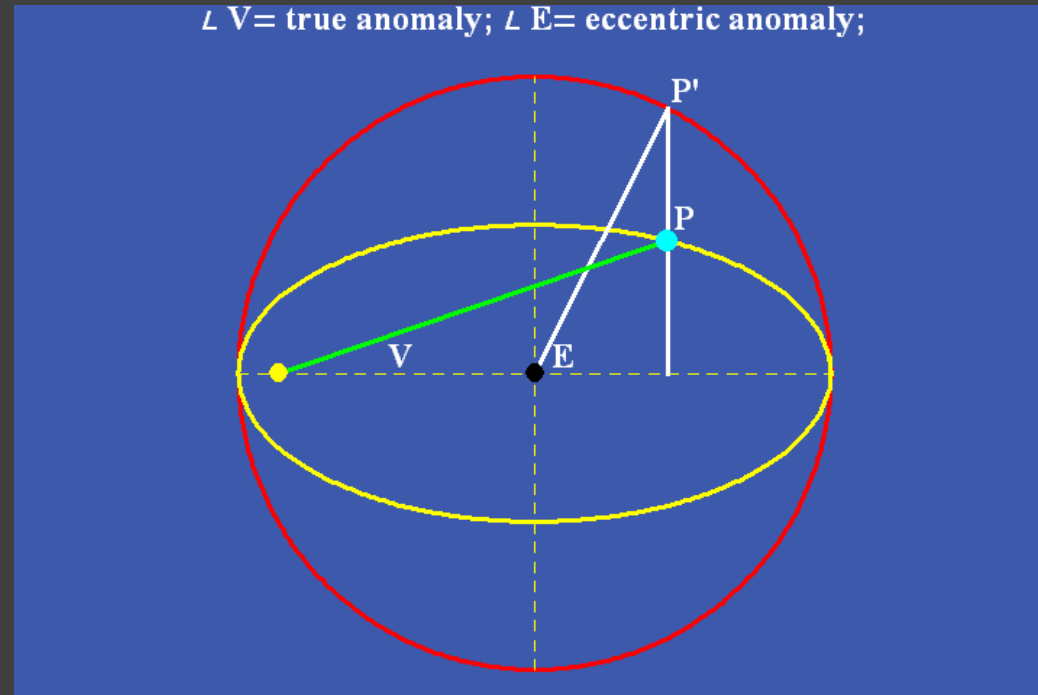


Field of view ~115 sq. degrees

Orbital elements



v – true anomaly
 ω – argument of periapsis
 E - eccentric anomaly
 M – mean anomaly



<http://www.wlym.com/antidummies/part66.html>

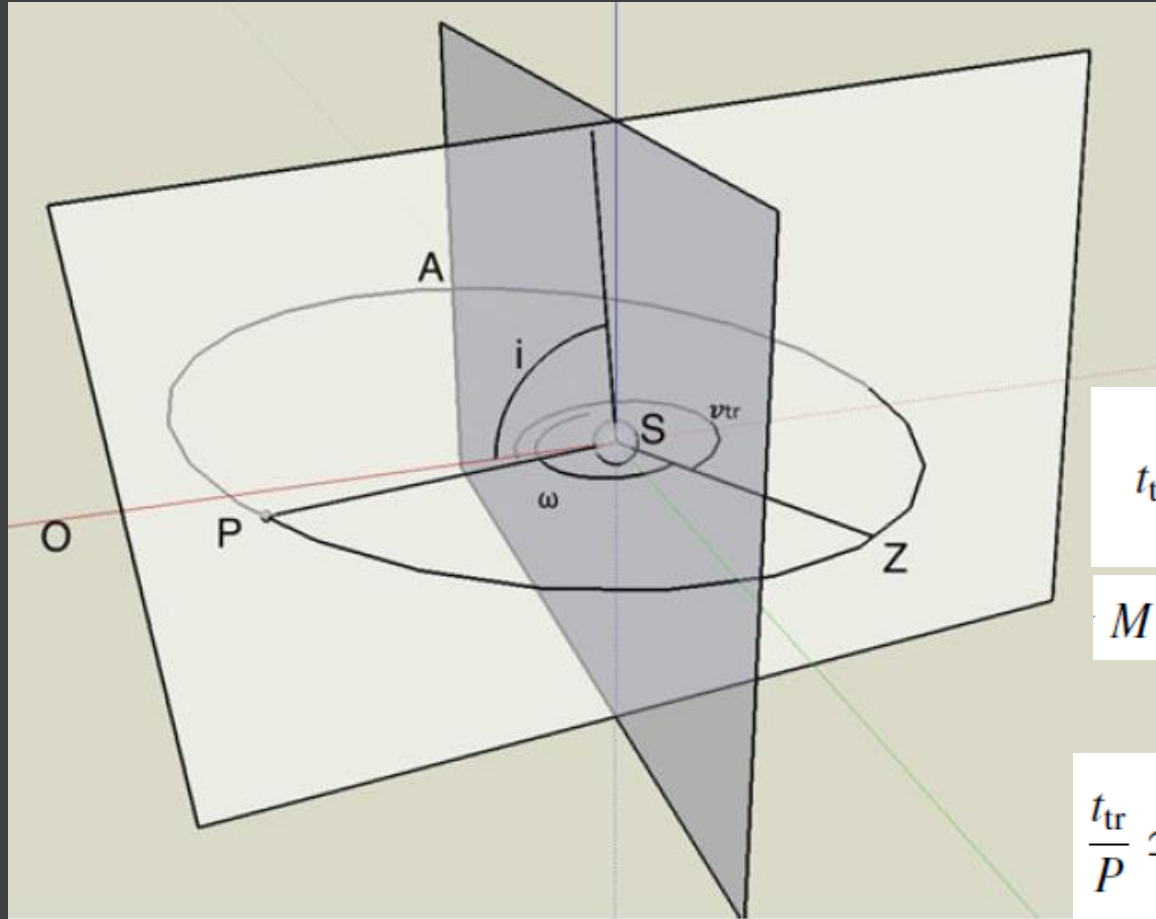
Orbital parameters



$$d = r \sin \alpha$$

$$z = d/R_{\text{star}}$$

$$p = R_p/R_{\text{star}}$$



$$v_{\text{tr}} = \frac{\pi}{2} - \omega$$

$$v_{\text{occ}} = \frac{3\pi}{2} - \omega,$$

$$E = 2 \tan^{-1} \left[\sqrt{\frac{1-e}{1+e}} \tan \frac{v}{2} \right]$$

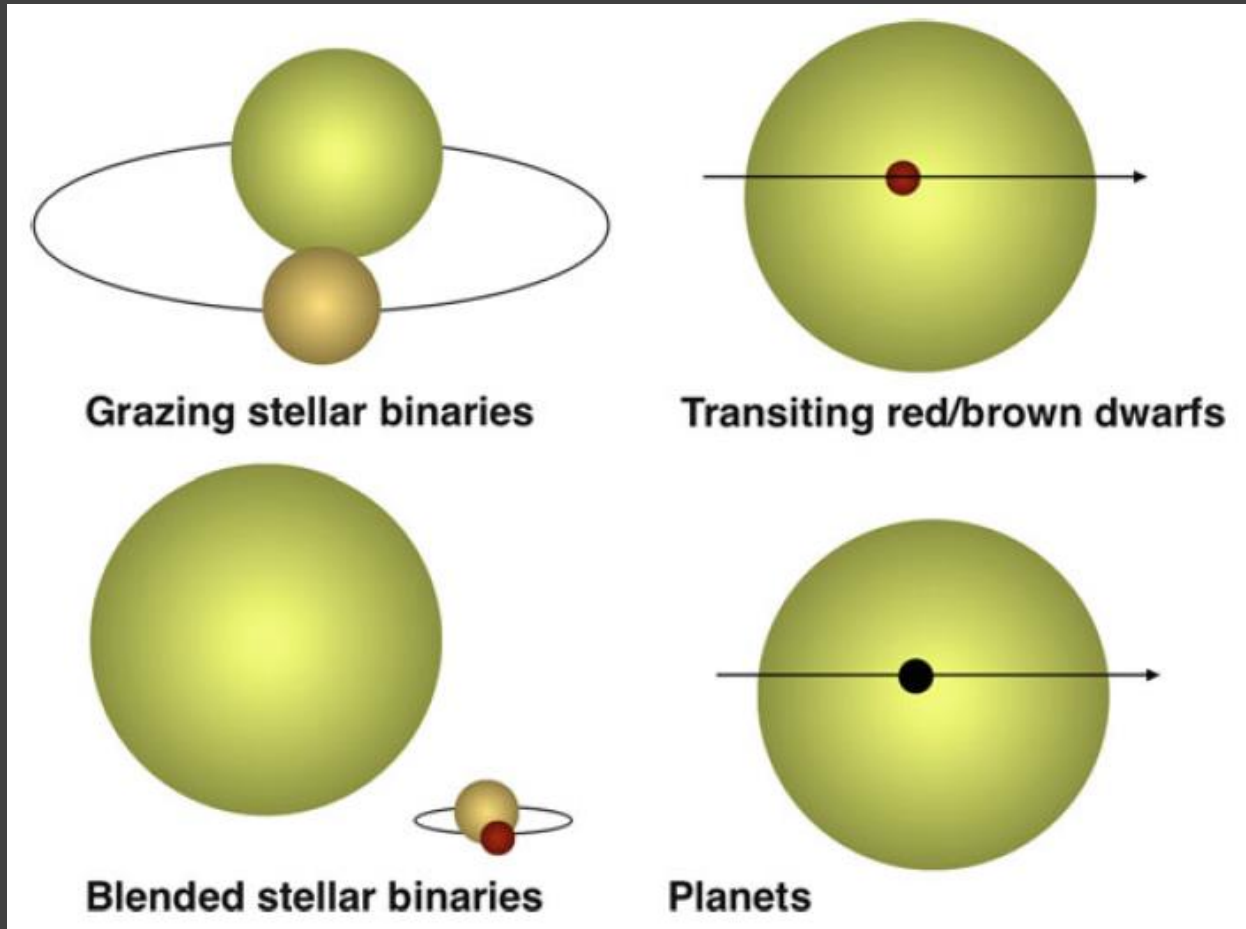
$$t_{\text{tr}} - t_0 = \frac{P}{2\pi} M_{\text{tr}} = \frac{P}{2\pi} (E_{\text{tr}} - e \sin E_{\text{tr}}).$$

$$M = E - e \sin E, \quad E_{i+1} = M + e \sin E_i.$$

$$E_1 = M,$$

$$\frac{t_{\text{tr}}}{P} \simeq \frac{R_*}{a} \frac{\sqrt{(1 + R_p/R_*)^2 - b^2}}{\pi} \frac{1 + e \sin \omega}{1 - e^2}.$$

Transits and transit-like events



Spectral lines and planet/star mass ratio

$$\dot{v}_r \simeq \frac{GM_*}{a^2} = \frac{2\pi K}{P} \frac{M_*}{M_p}.$$

Observations of spectral line in the planet atmosphere can allow to measure important parameters of the system!

Measurements of the radial acceleration (due to observations of spectral lines in the planet atmosphere) allow to measure stellar mass.

$$\frac{T}{P} = \frac{1}{\pi} \sin^{-1} \frac{R_*}{a}$$

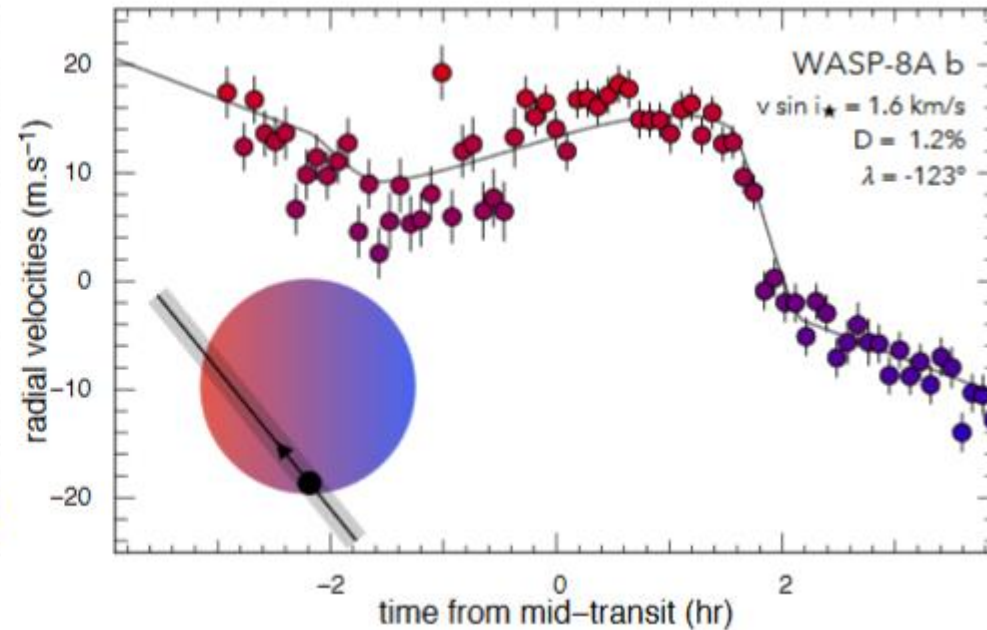
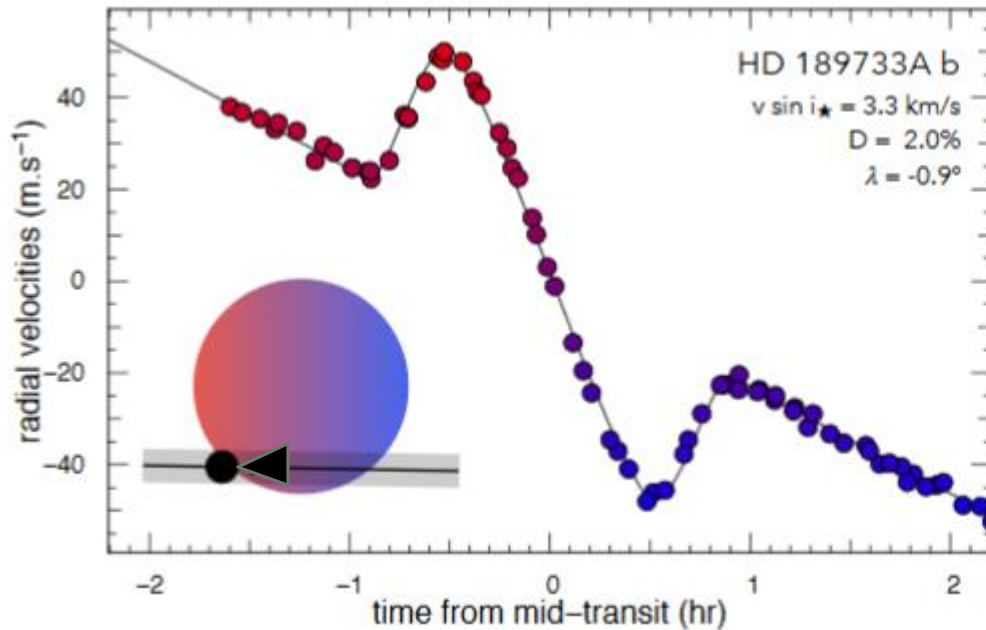
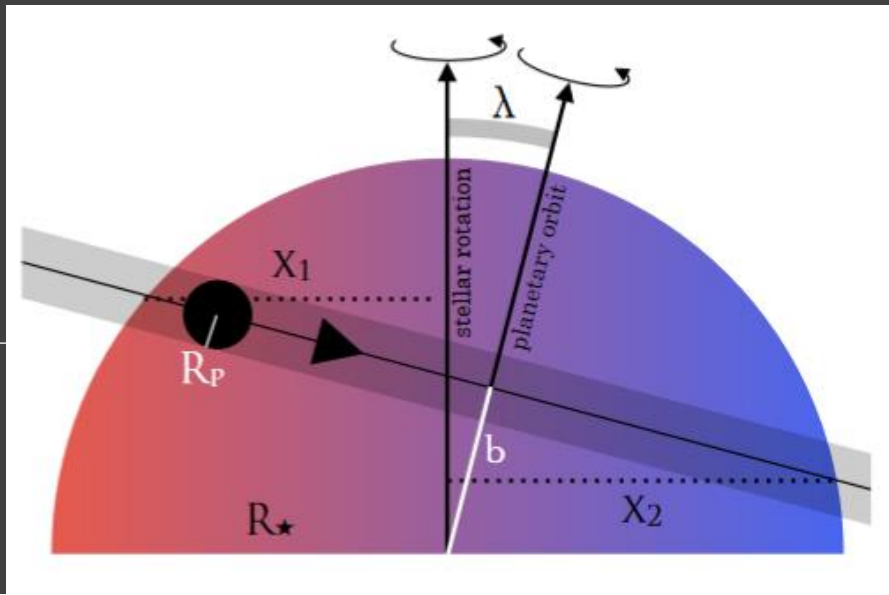
$$\delta v_r \simeq \frac{P}{\pi} \frac{R_*}{a} \frac{2\pi K}{P} \frac{M_*}{M_p}.$$

If narrow spectral lines in the planet atmosphere can be observed during transit then it is possible to derive $M_{\text{star}}/M_{\text{planet}}$

Rossiter–McLaughlin effect

$$A_{\text{RM}} \simeq \frac{2}{3} D v \sin i_{\star} \sqrt{1 - b^2}$$

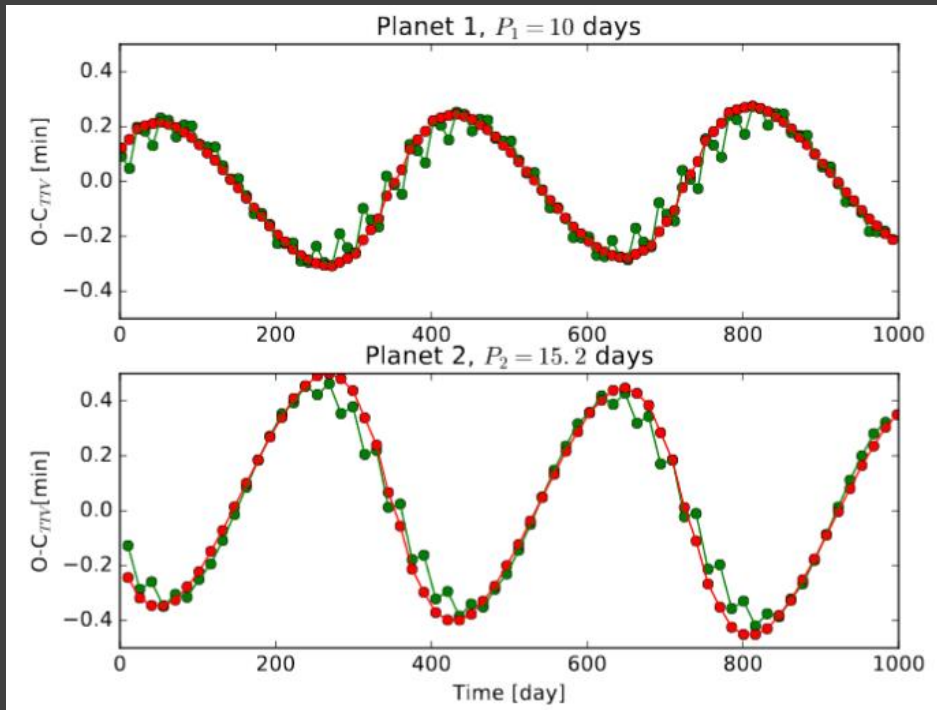
$$D = (R_p/R_{\star})^2$$



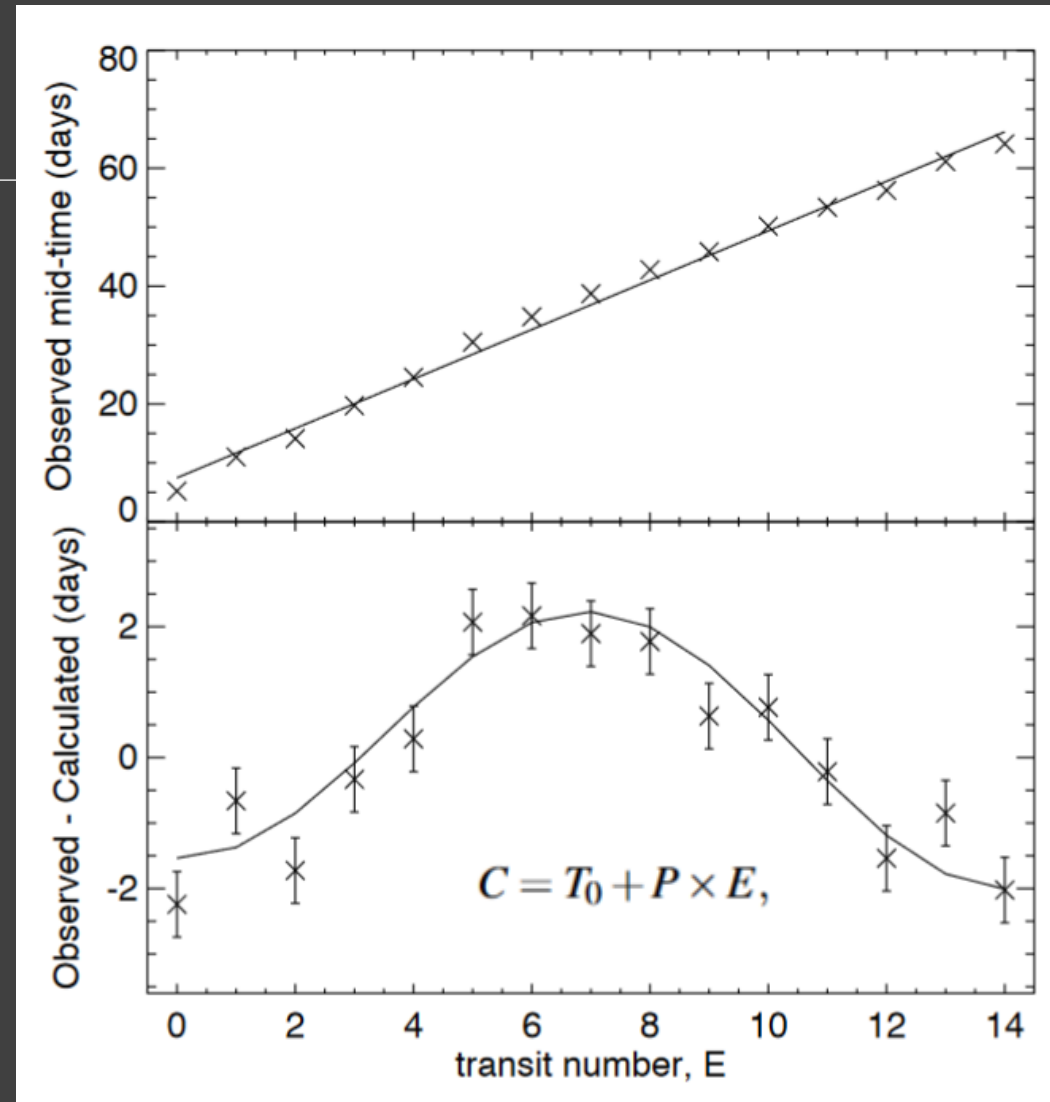
Transit timing variations

$$\delta t_1 = P_1 \frac{m_2}{m_0} f_{12}(\alpha_{12}, \theta_{12}), \quad \alpha_{ij} = \min(a_i/a_j, a_j/a_i)$$

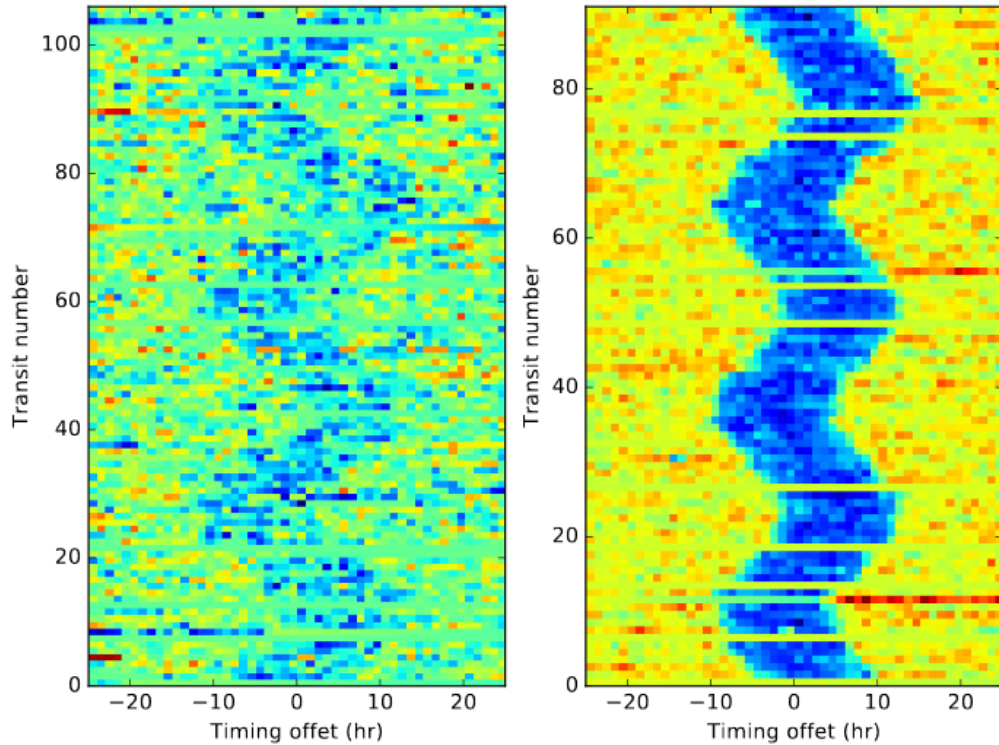
$$\delta t_2 = P_2 \frac{m_1}{m_0} f_{21}(\alpha_{12}, \theta_{21}), \quad \theta_{ij} = (\lambda_i, e_i, \omega_i, I_i, \Omega_i, \lambda_j, e_j, \omega_j, I_j, \Omega_j)$$



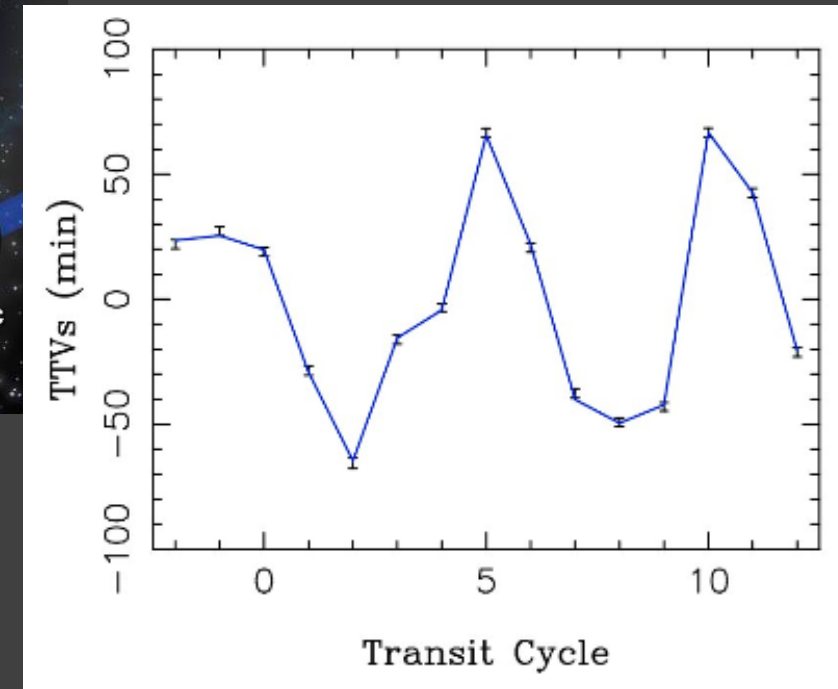
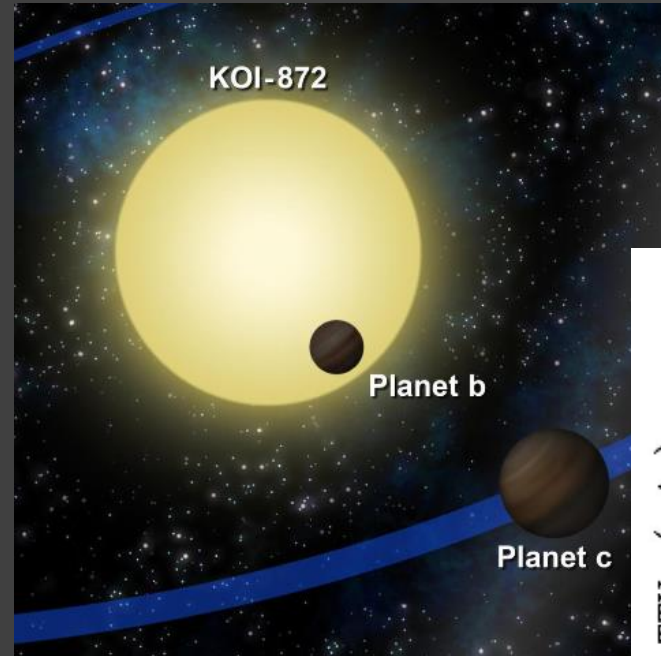
Transit-timing variations of two low-eccentricity planets with larger mass ratio (green) compared with two smaller mass planets with larger eccentricity $e_1=e_2=0.04$



Transit timing variations (TTV)

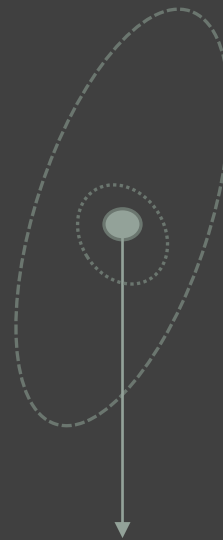
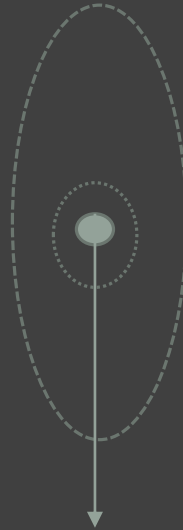
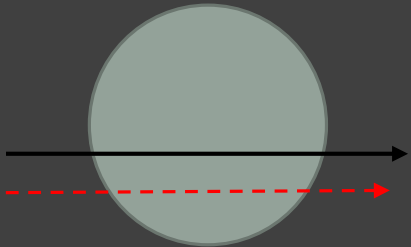
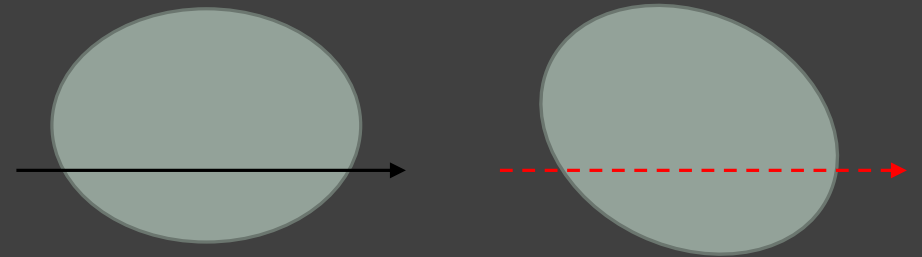


River plot



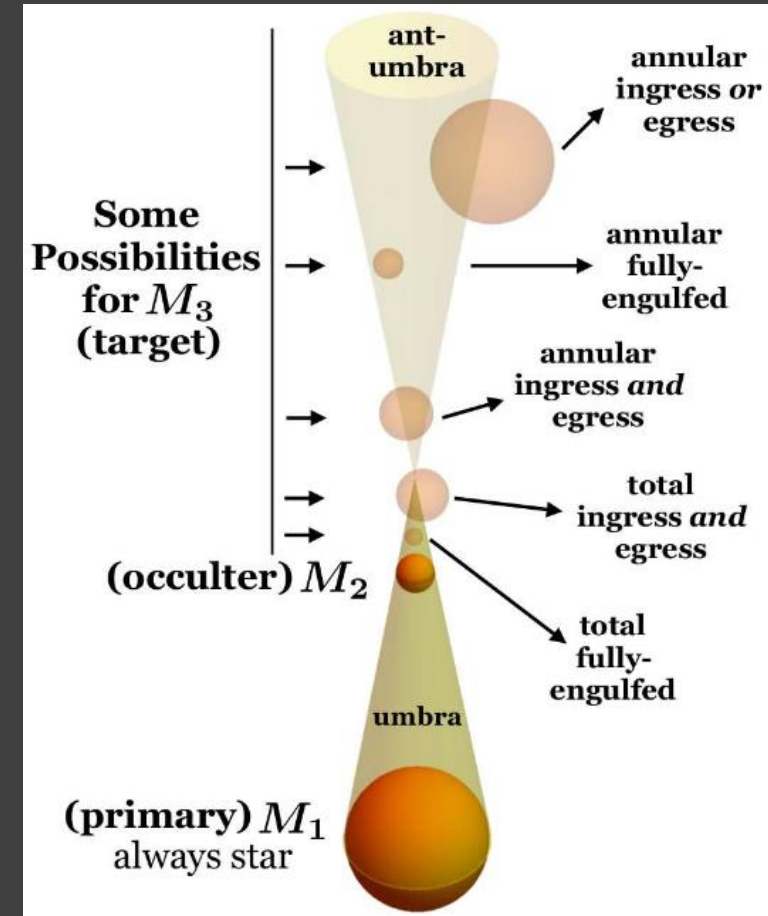
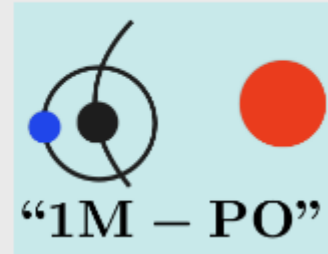
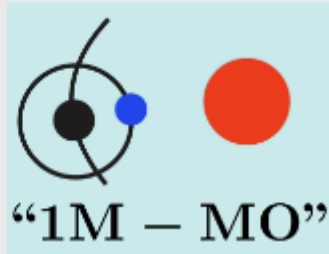
Transit duration variations (TDV)

- Torque due to the rotational oblateness of the star;
- Eccentricity variations due to a resonant interaction;
- Inclination changes due to secular precession of the orbital plane.

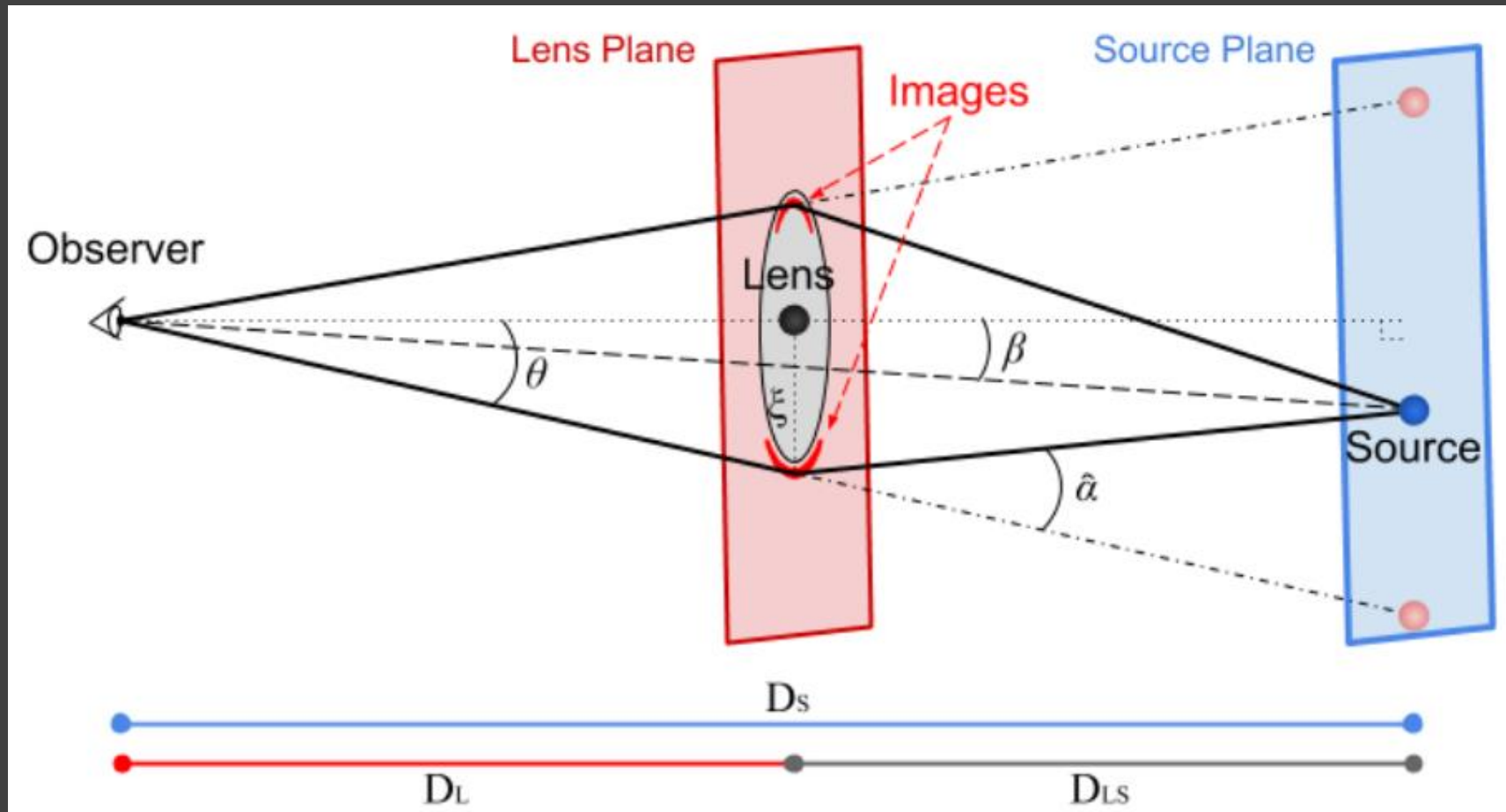


Calculations of transits in 3 body systems

$$\{a, e, i, \Omega, w, \Pi(t)\} \rightarrow \{x(t), y(t), z(t)\} \rightarrow \vec{r}(t)$$

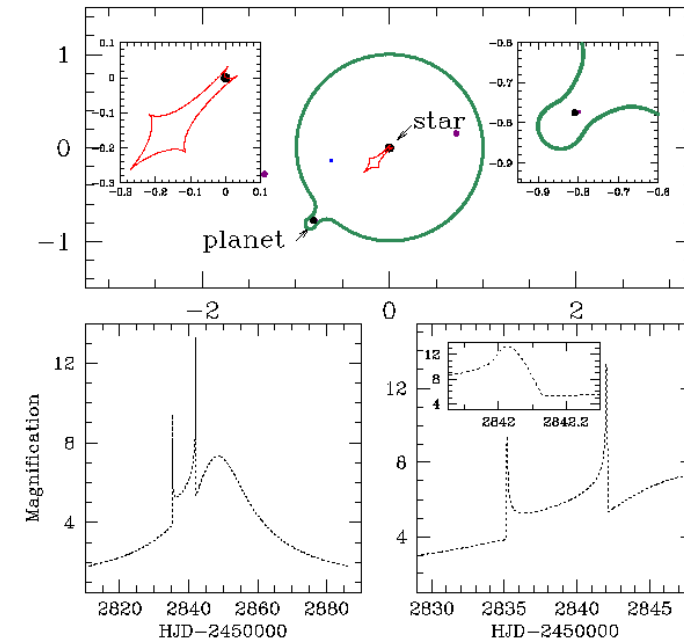
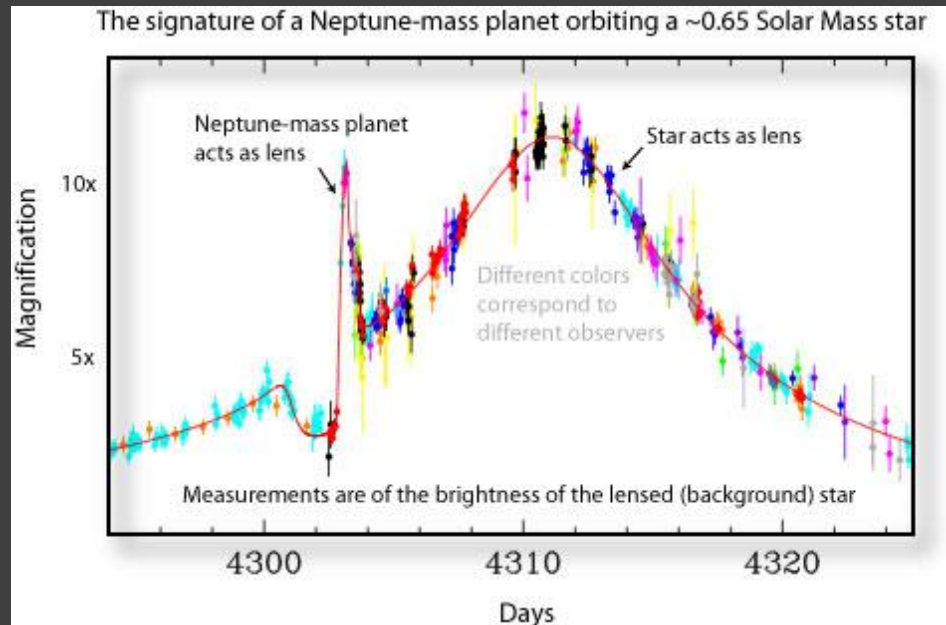


Microlensing



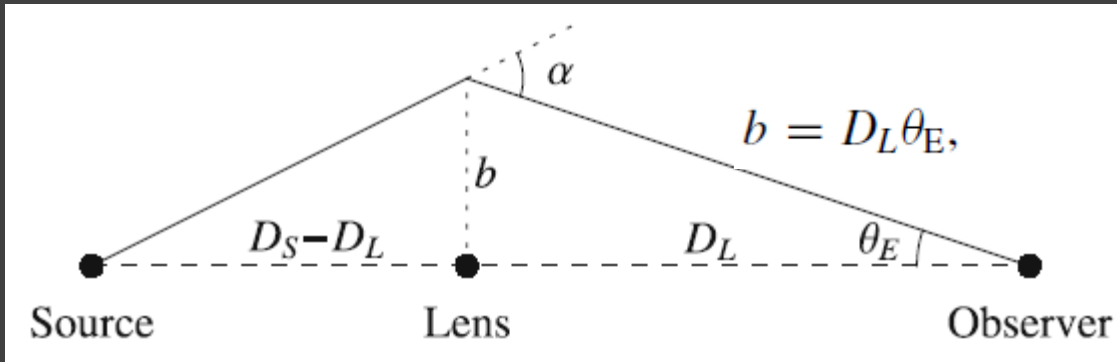
Exoplanet detection via microlensing

- Sensitive to low mass planets (down to $0.1 M_{\text{earth}}$)
- Sensitive to wide orbits (1-4 AU)
- Sensitive to free-floating planets



<https://www3.nd.edu/~bennett/ma53-ogle235/technical.gif>

Gravitational microlensing - 1



Probability of microlensing is small.
For stars it is $\sim 10^{-5} - 10^{-6}$ per year.
For planets it is lower, as $\theta_E \sim M^{1/2}$
and $M_{\text{planet}}/M_{\text{star}} \sim 10^{-4}$

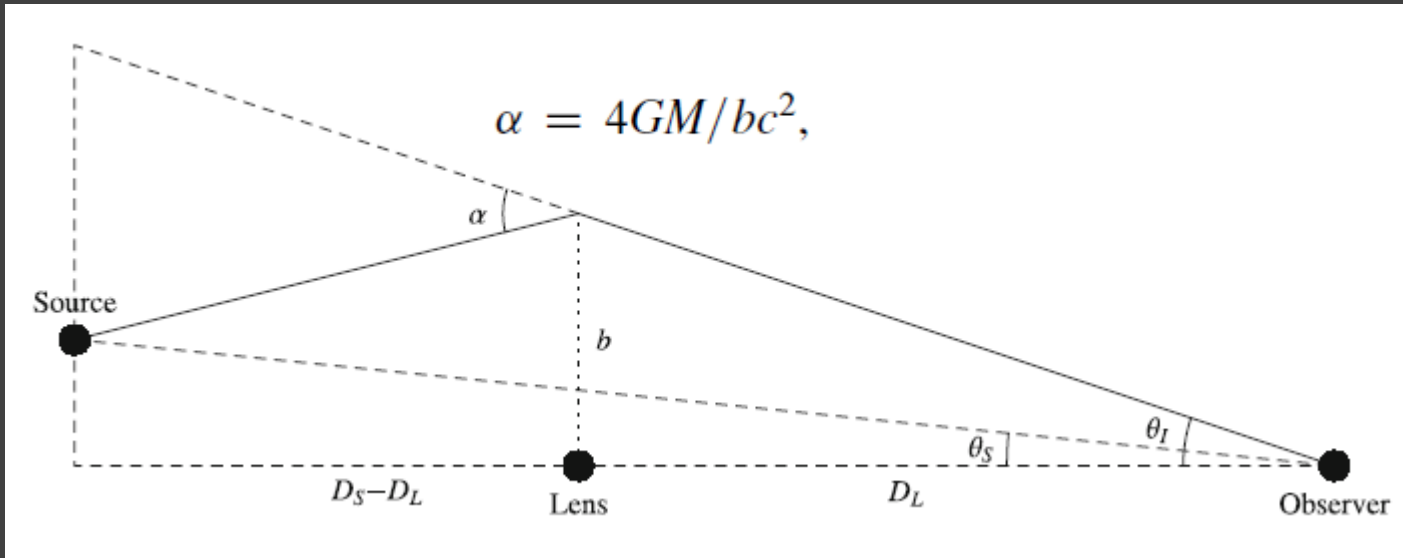
$$\alpha = b/D_L + b/(D_S - D_L).$$

$$\theta_E = \sqrt{\kappa M \pi_{\text{rel}}}; \quad \kappa \equiv \frac{4G}{c^2 \text{AU}} \simeq 8.14 \frac{\text{mas}}{M_{\odot}},$$

$$\pi_{\text{rel}} = \text{AU}(D_L^{-1} - D_S^{-1})$$

$$\tau = \int dD_L \pi (D_L \theta_E)^2 n(D_L) \sim \frac{4\pi G M n}{c^2} D^2 = \frac{4\pi G \rho}{c^2} D^2 \sim \frac{GM_{\text{tot}}}{Dc^2} \sim \frac{v^2}{c^2}$$

Gravitational microlensing - 2



$$(\theta_I - \theta_S)D_S = \alpha(D_S - D_L)$$

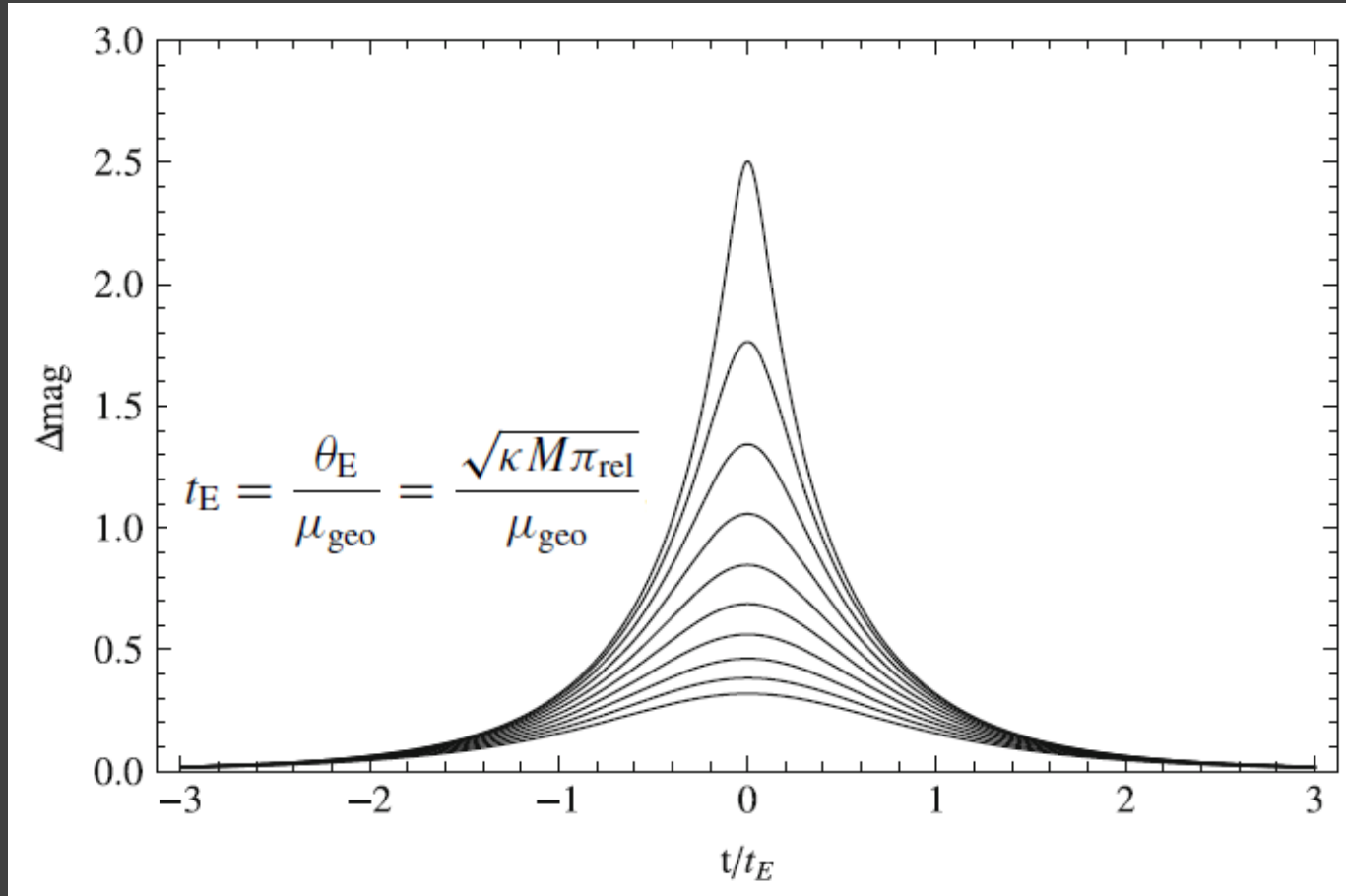
$$\theta_I(\theta_I - \theta_S) = \frac{4GM\pi_{\text{rel}}}{c^2 \text{AU}} \equiv \theta_E^2.$$

$$u_{\pm} = \frac{u \pm \sqrt{u^2 + 4}}{2}; \quad u \equiv \frac{\theta_S}{\theta_E} \quad u_{\pm} \equiv \frac{\theta_{I,\pm}}{\theta_E}.$$

$$A_{\pm} = \pm \frac{u_{\pm}}{u} \frac{\partial u_{\pm}}{\partial u} = \frac{A \pm 1}{2}$$

$$A = \frac{u^2 + 2}{u\sqrt{u^2 + 4}} = (1 - Q^{-2})^{-1/2}; \quad Q \equiv 1 + \frac{u^2}{2},$$

Light curves for point lenses



$$F(t) = f_s A(\mathbf{u}(t; t_0, u_0, t_E), \rho) + f_b;$$

$$\mathbf{u}(t; t_0, u_0, t_E) = (\tau(t), \beta) = \left(\frac{t - t_0}{t_E}, u_0 \right).$$

Finite size lense

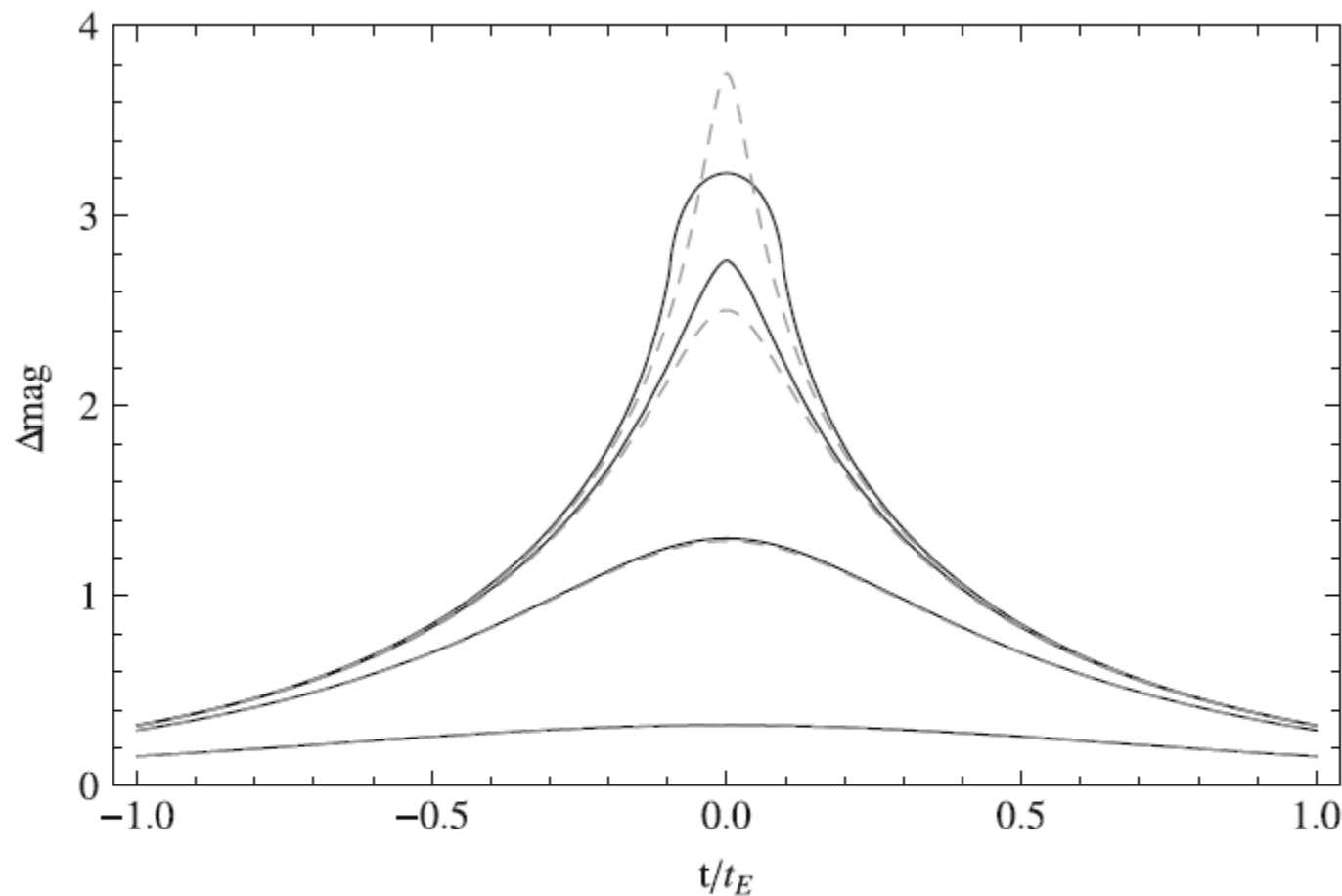
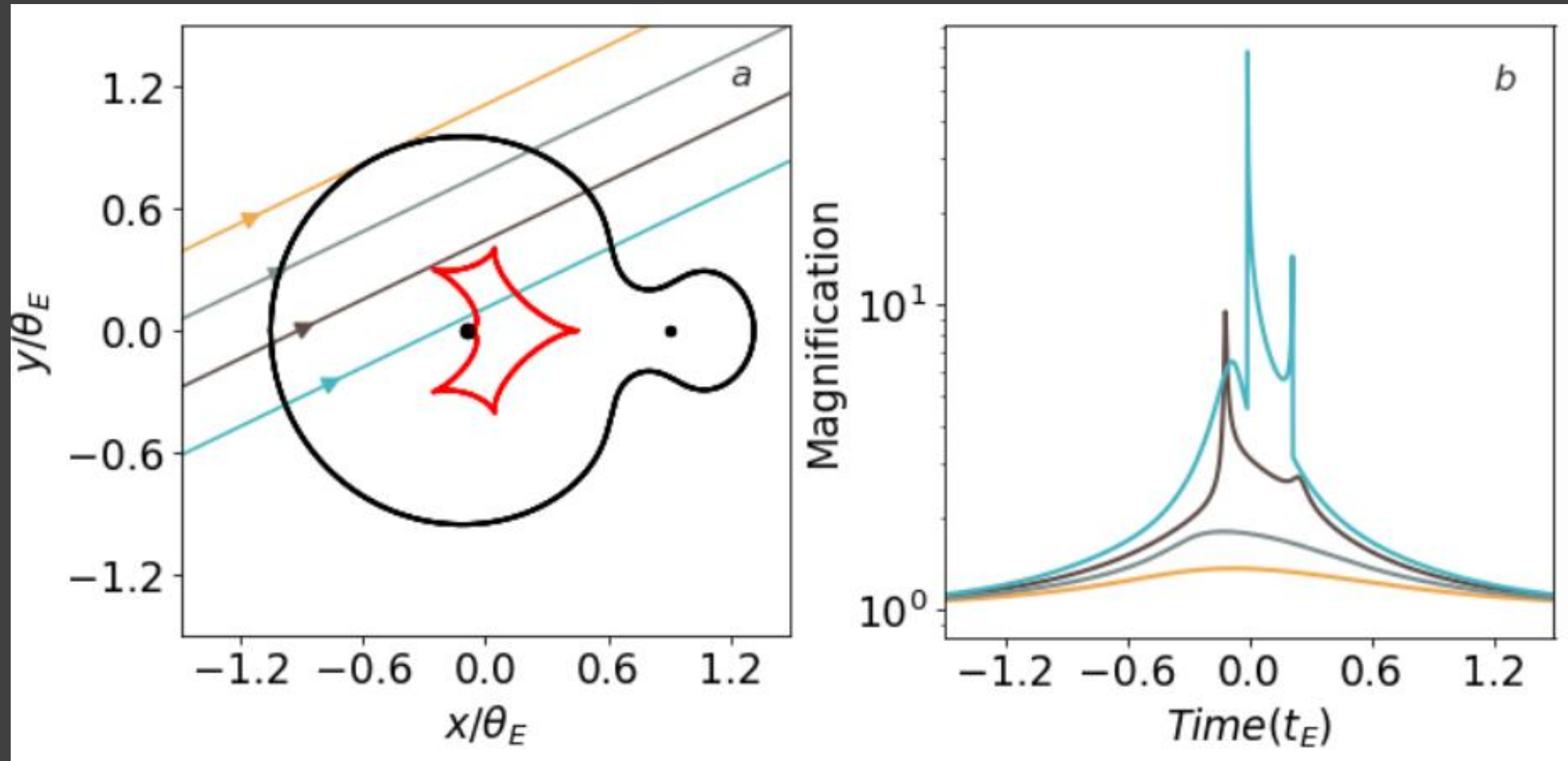


Fig. 3.4 Magnification as a function of time in microlensing events for an impact parameters $u_0 = 10^{-n}$ with $n \in \{-1.5, -1, -0.5, 0\}$. The angular source size is $0.1\theta_E$. Note that when the impact parameter is greater than the source radius, the magnification is higher than the corresponding Paczynski curve (*dashed*). When the impact parameter is smaller than the source radius (source passing right behind the lens), the magnification saturates

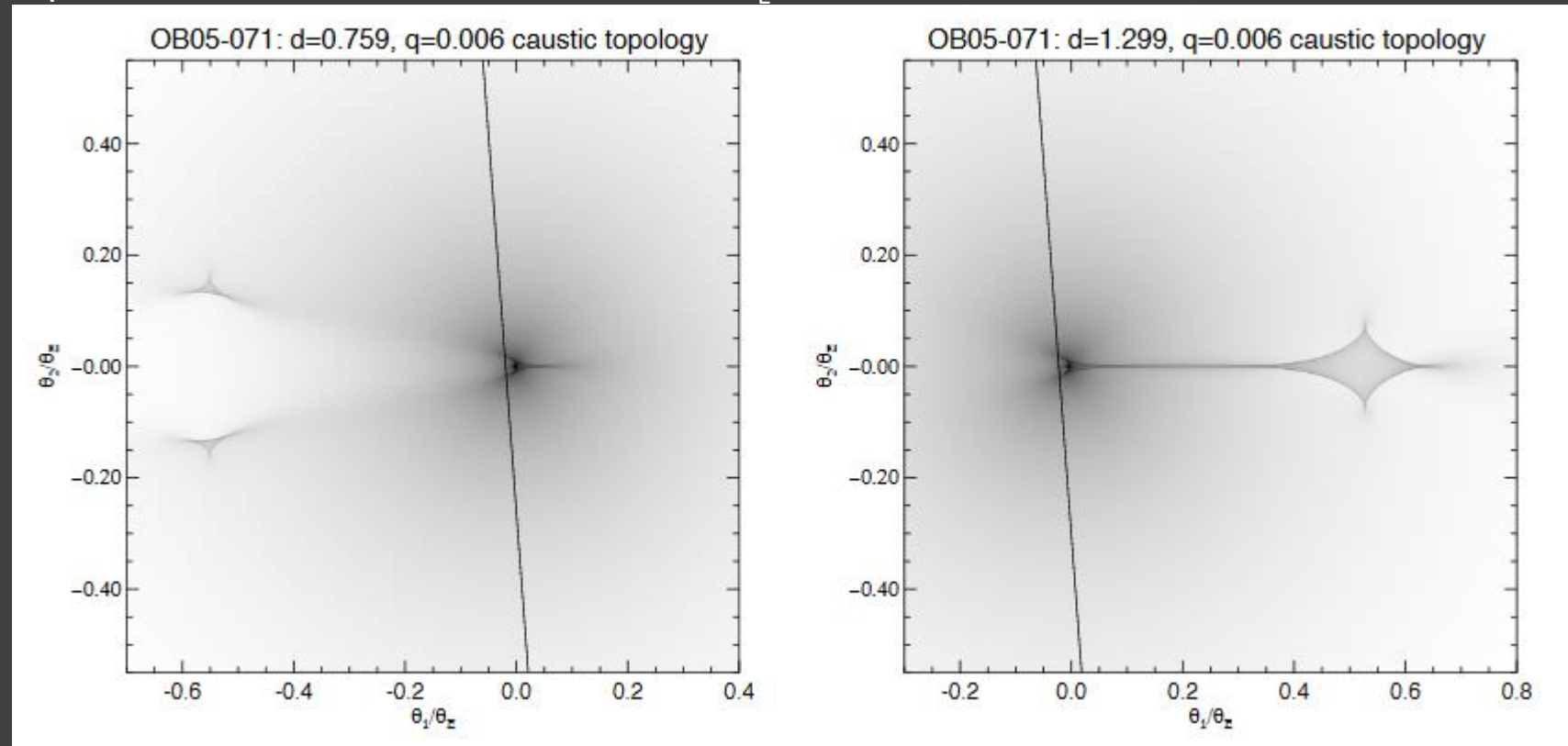
Light curves form different trajectories



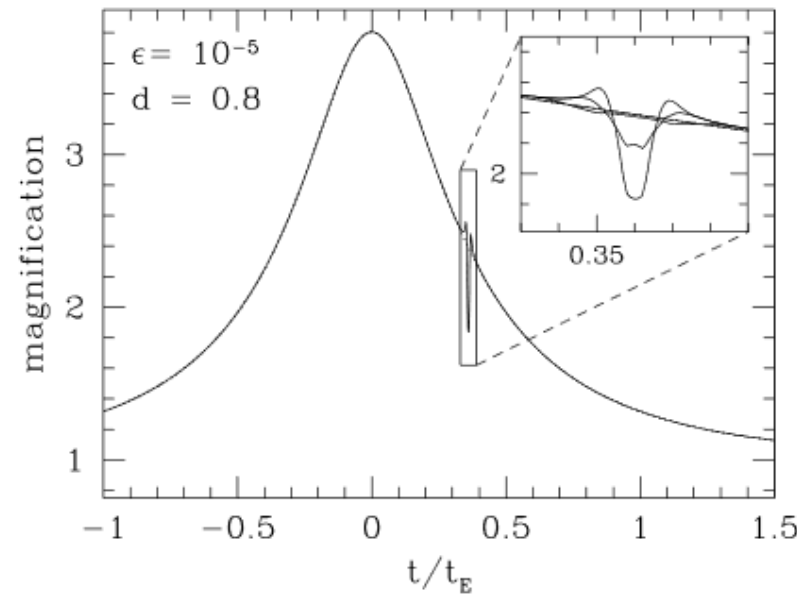
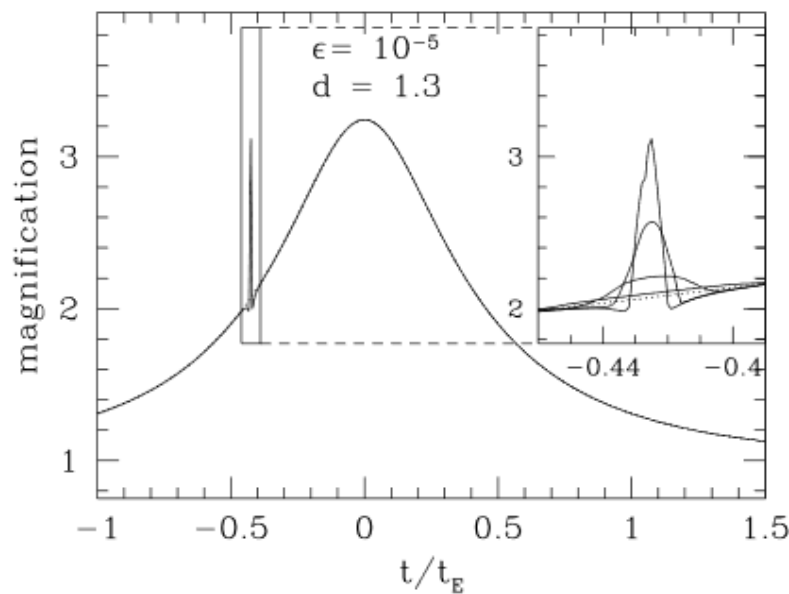
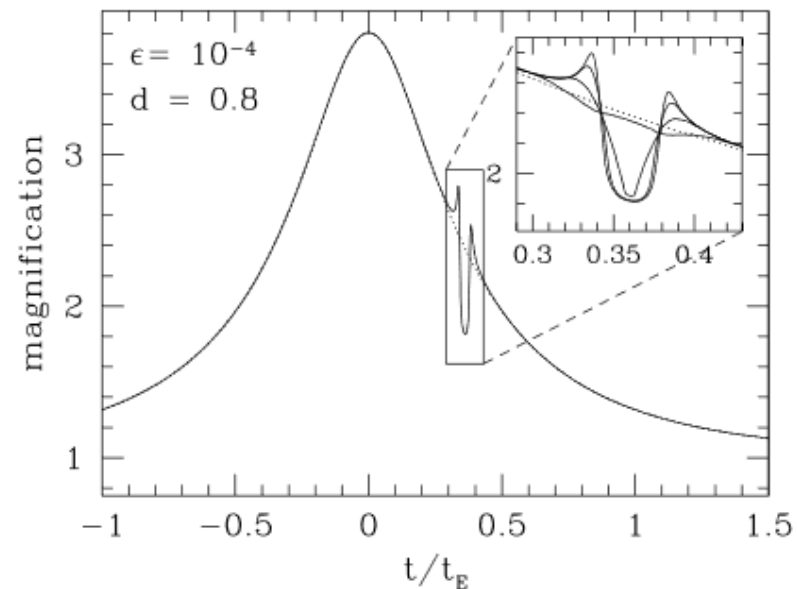
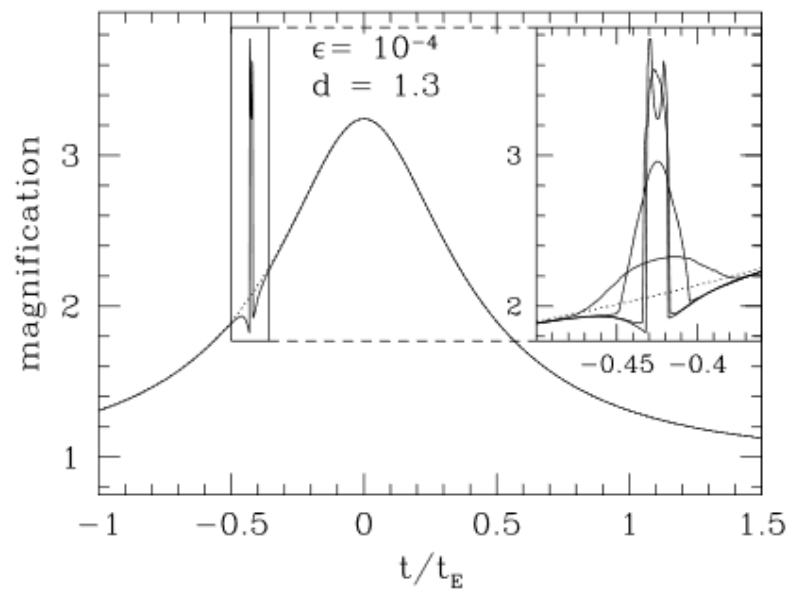
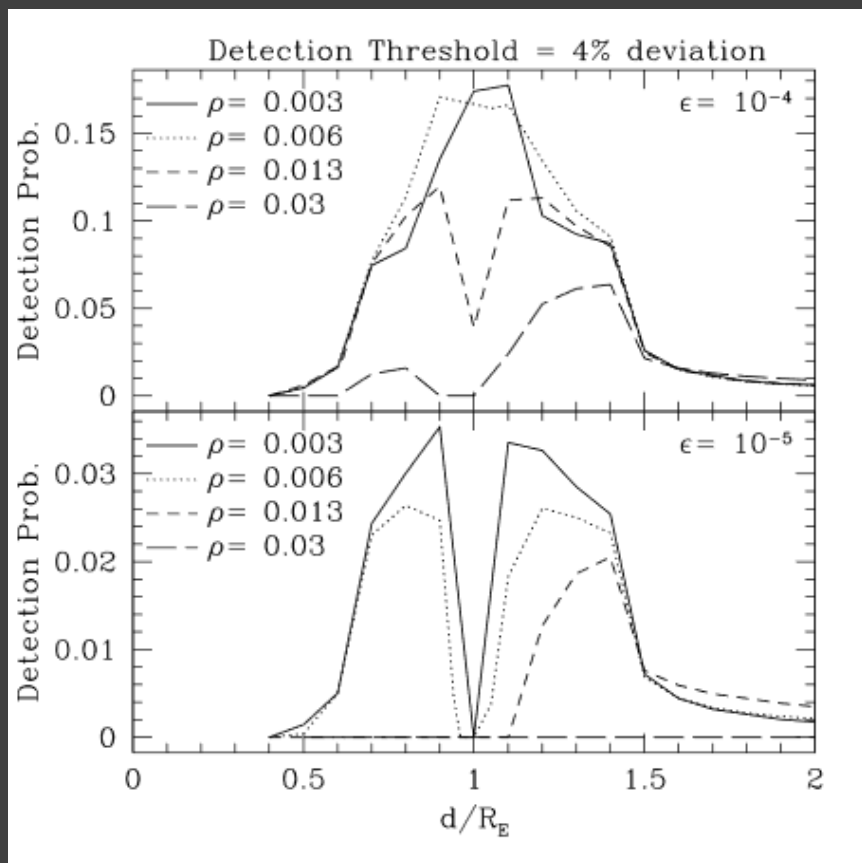
Binary lense

s – separation of components in units of the Einstein radius θ_E .
 q - mass ratio.

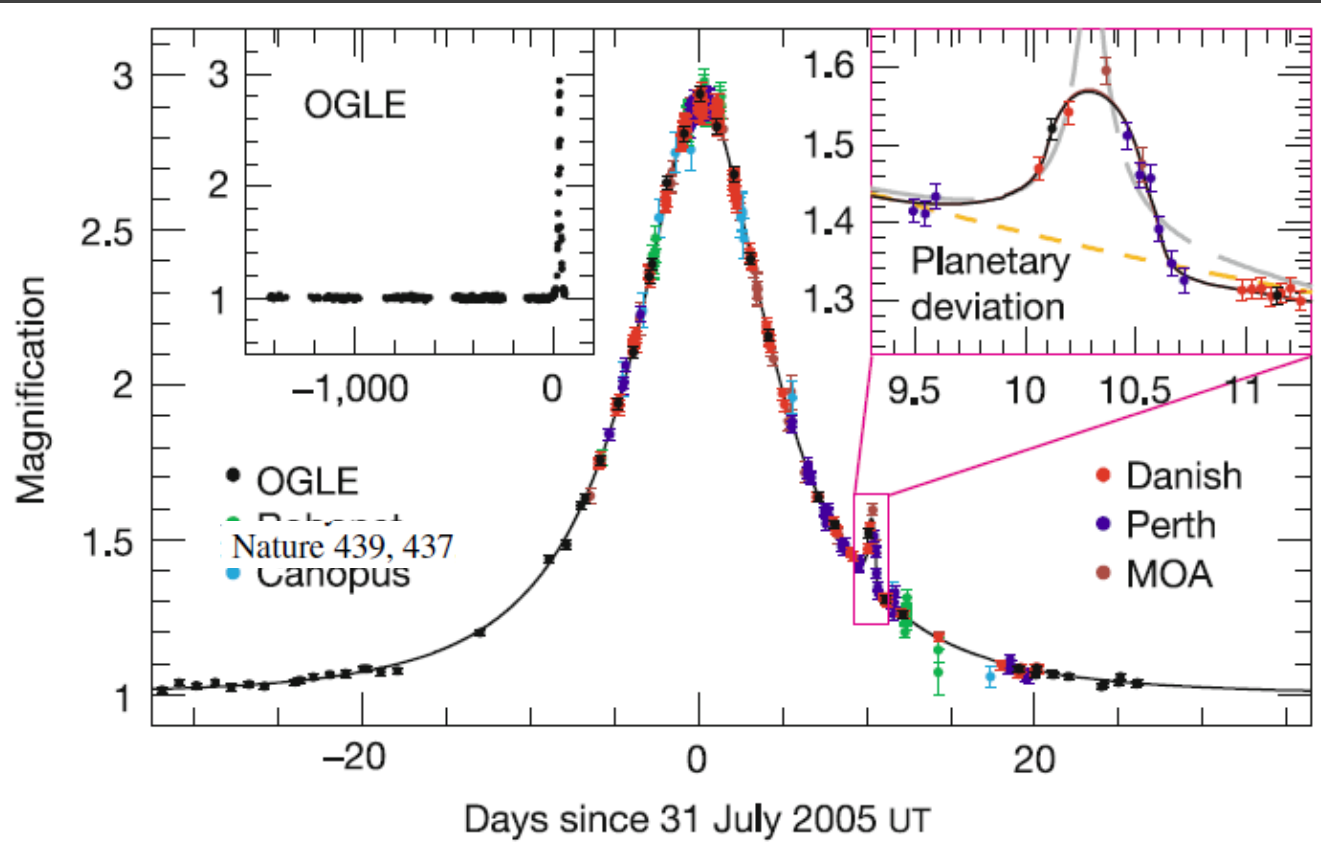
$$r_{\perp} = s\theta_E D_L,$$



Light curves



Cold Neptune



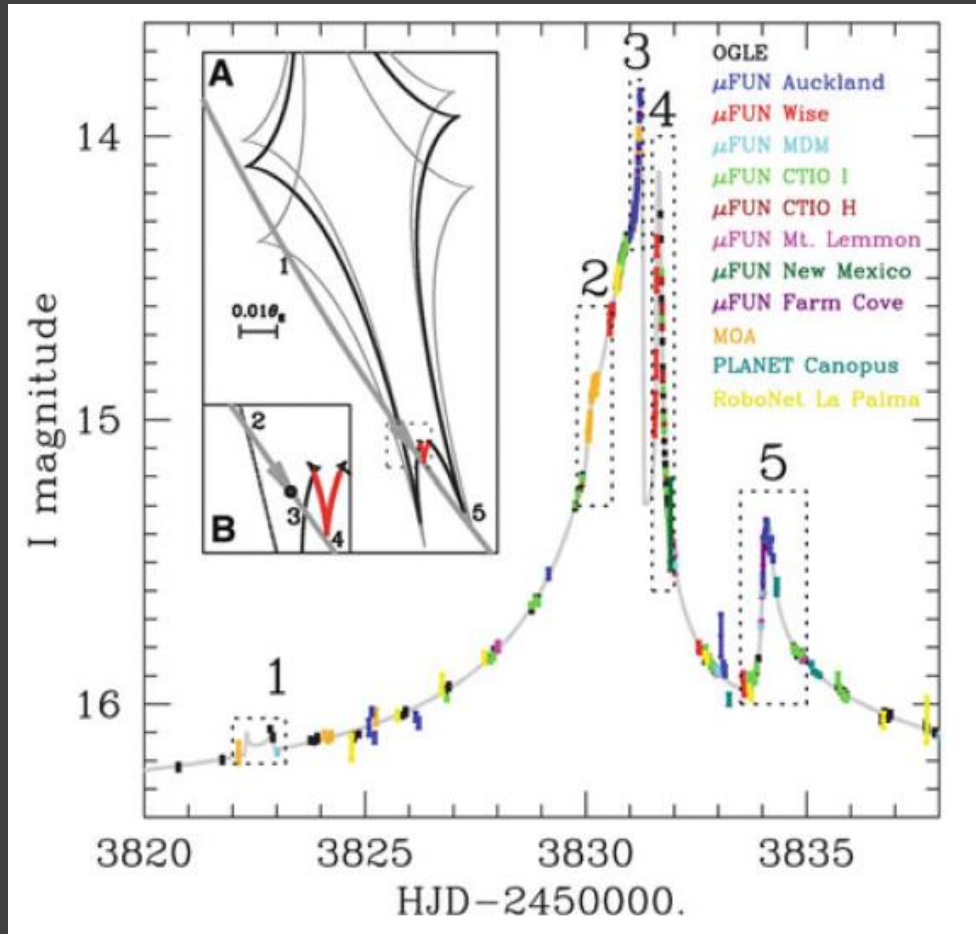
$$A_p = \frac{2}{\rho_p^2} = 2 \left(\frac{\theta_{E,p}}{\theta_*} \right)^2$$

$$\frac{t_p}{t_E} = \frac{\theta_*}{\theta_E}$$

$$q = \frac{m_p}{M} = \frac{\theta_{E,p}^2}{\theta_E^2} = \frac{\theta_{E,p}^2}{\theta_*^2} \frac{\theta_*^2}{\theta_E^2} = \frac{A_p}{2} \frac{t_p^2}{t_E^2} \simeq 1.0 \times 10^{-4}$$

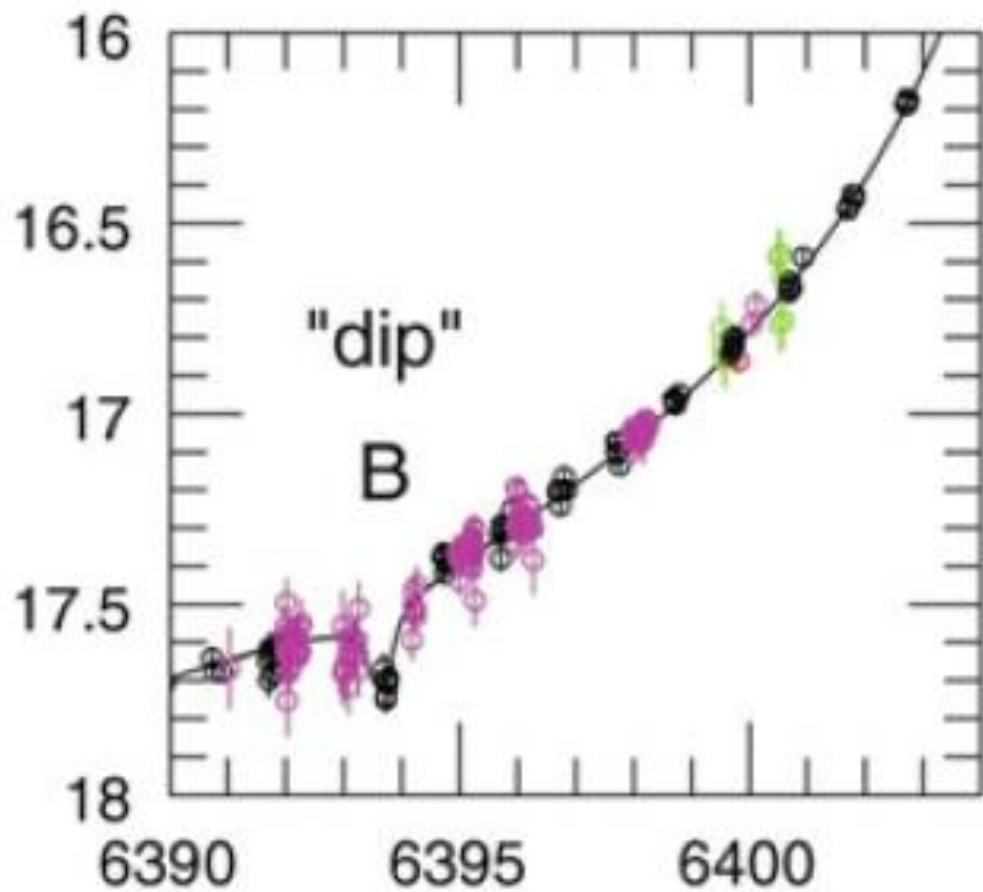
$$r_{\perp} = s \theta_E D_L = 2.2 \text{ AU} \frac{D_L}{8 \text{ kpc}}$$

Solar system – like system

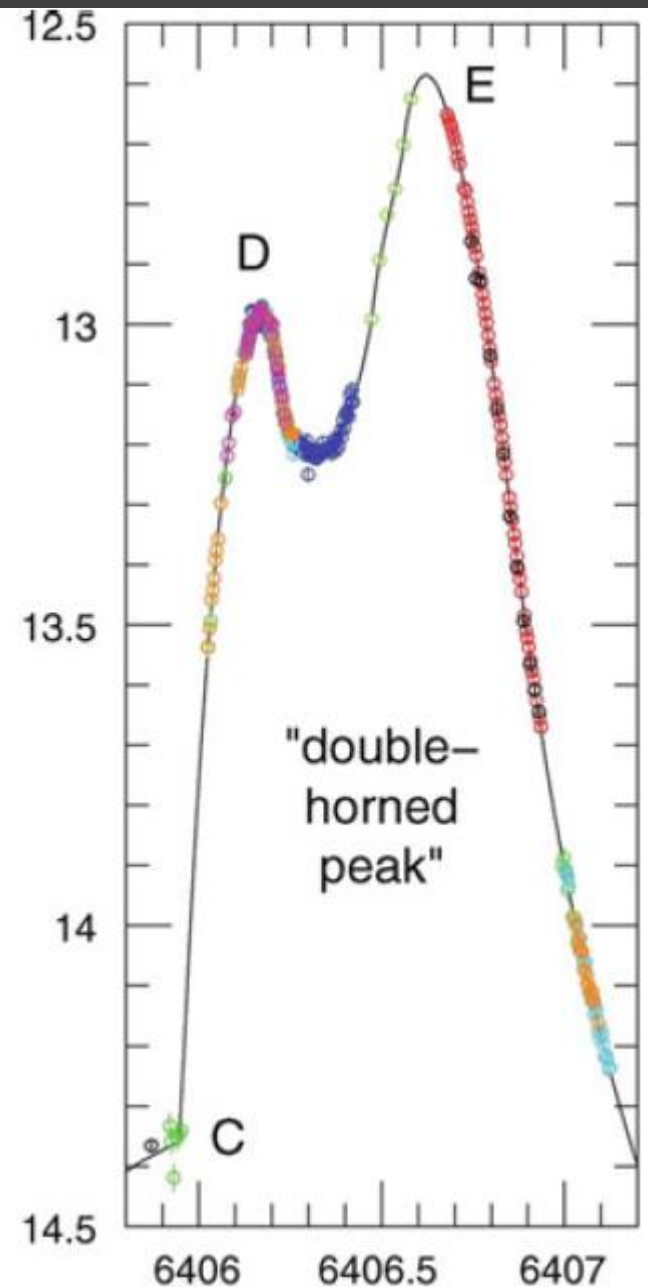


Jupiter and Saturn analogues.
Distances are slightly smaller
consistent with smaller mass
of the host star.

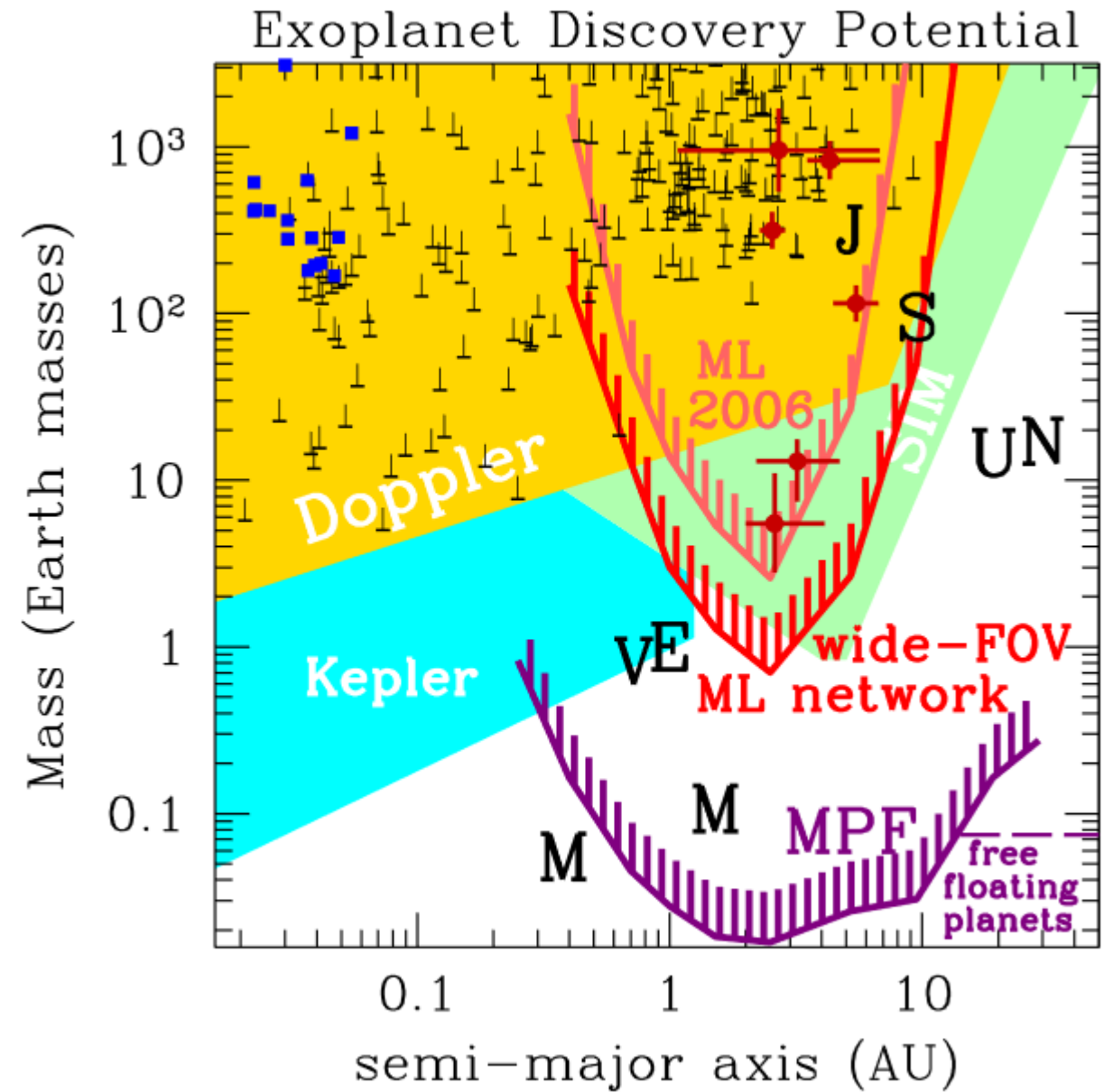
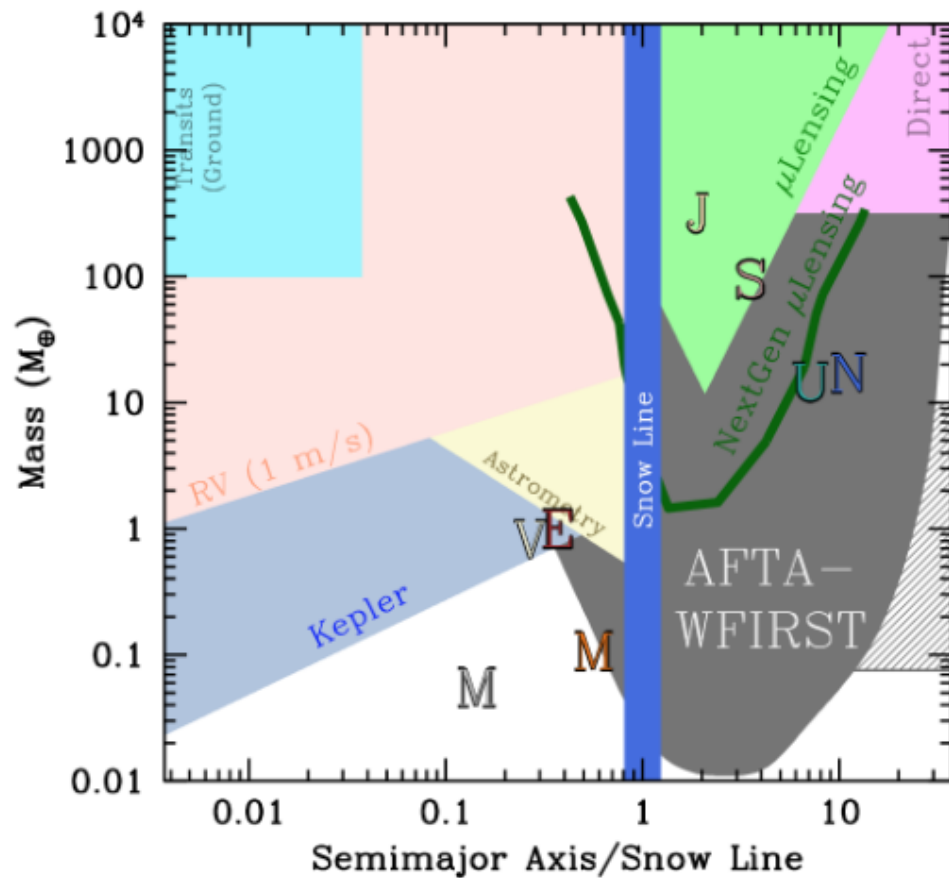
Dips due to planets



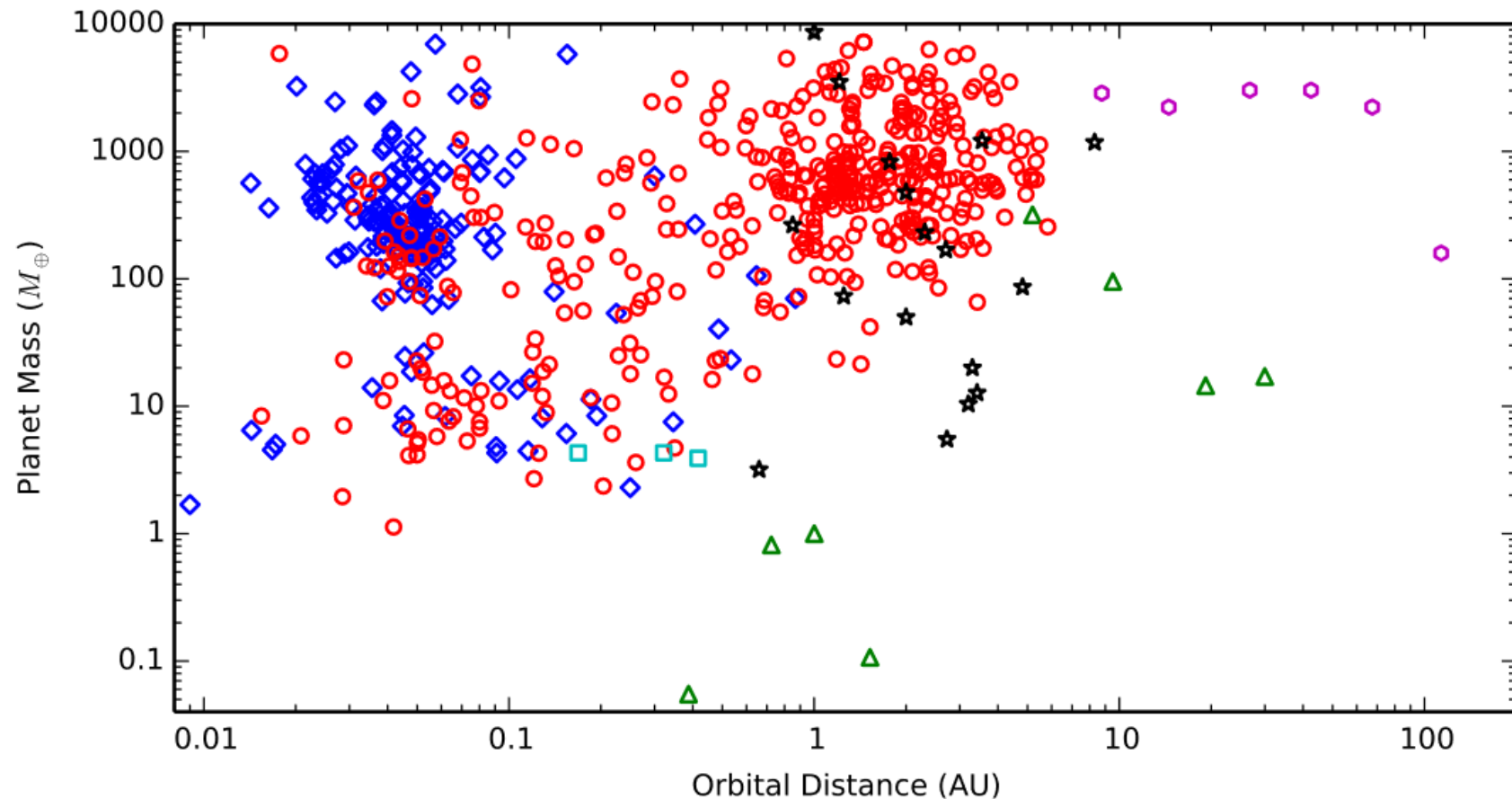
A terrestrial-mass planet in a binary. The planet orbits a red dwarf (1 AU), which orbits another star (15 AU)



Comparison of three methods



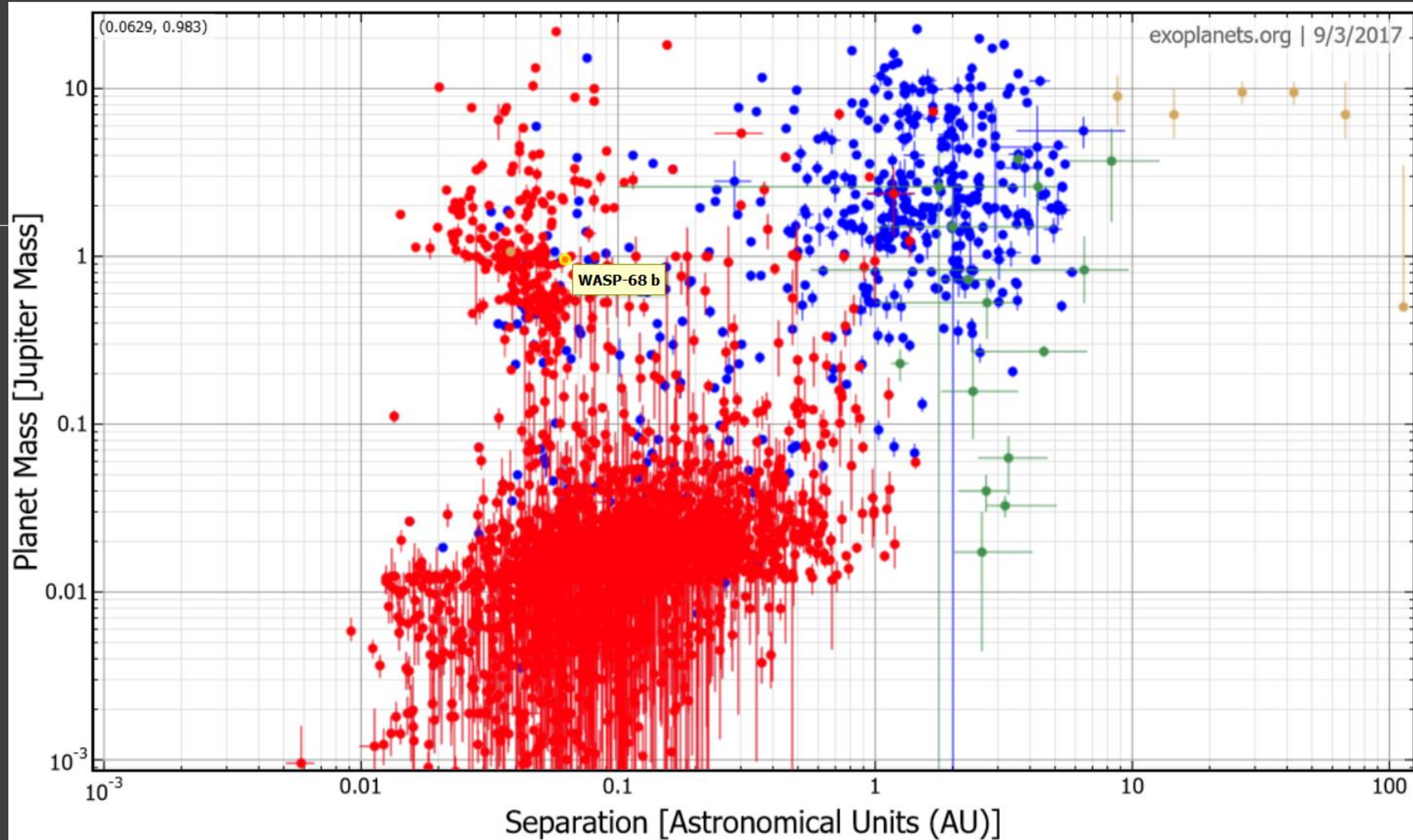
Discoveries by different methods



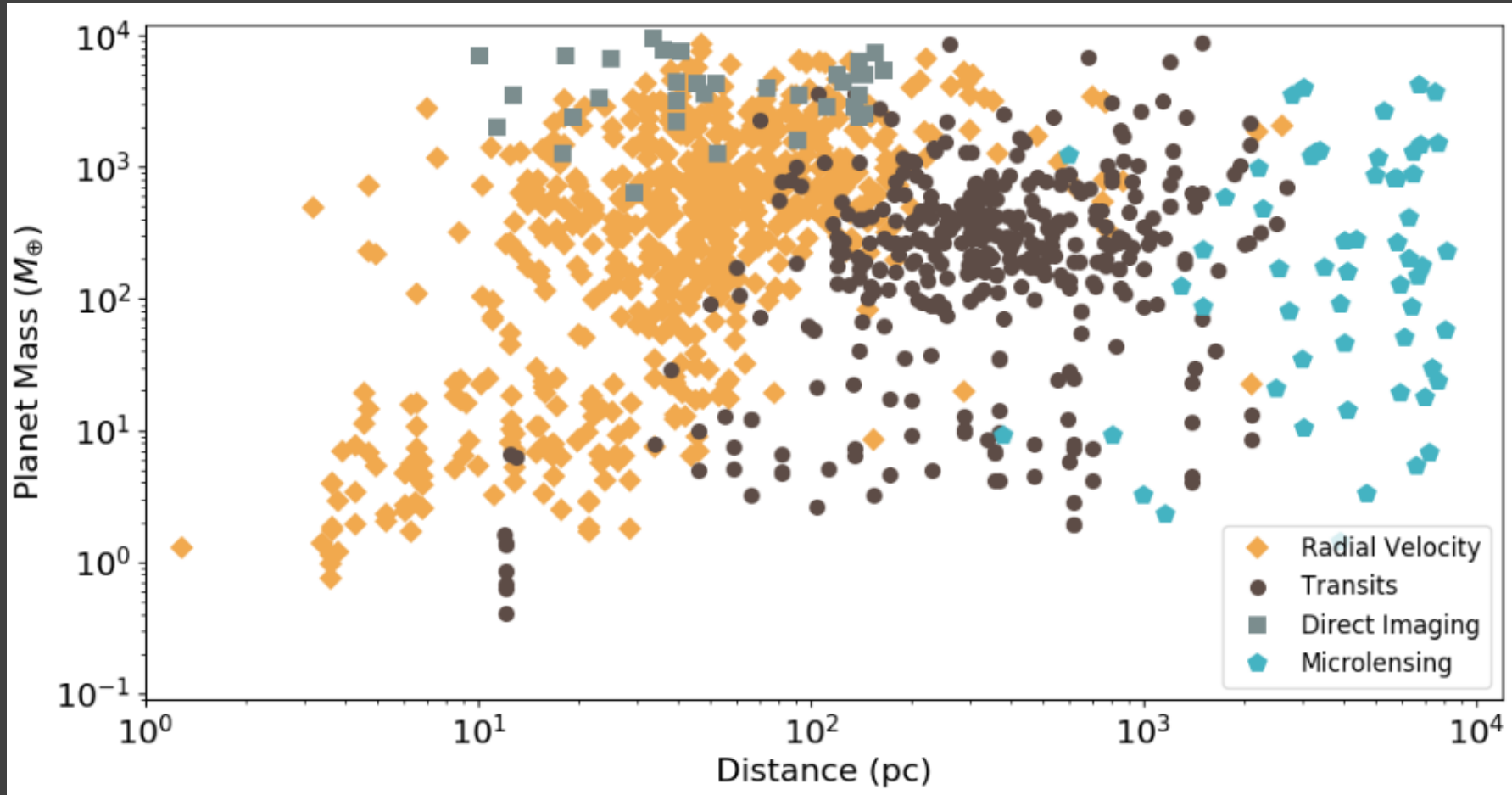
RV = red circles,
transit = blue diamonds,
imaging = magenta hex.,
gravlens = black stars,
psr time = cyan squares.

Planets in the Solar
System are green
triangles.

Blue- RV
Red – Trans.
Green – lense
Orange –
imaging

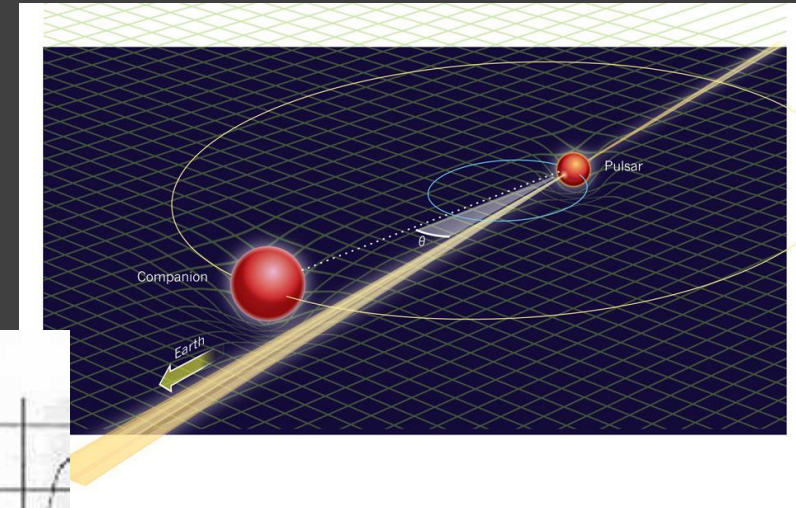
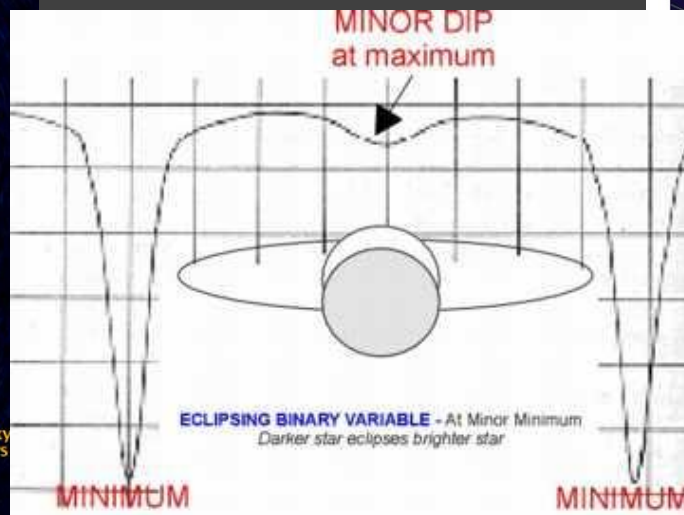
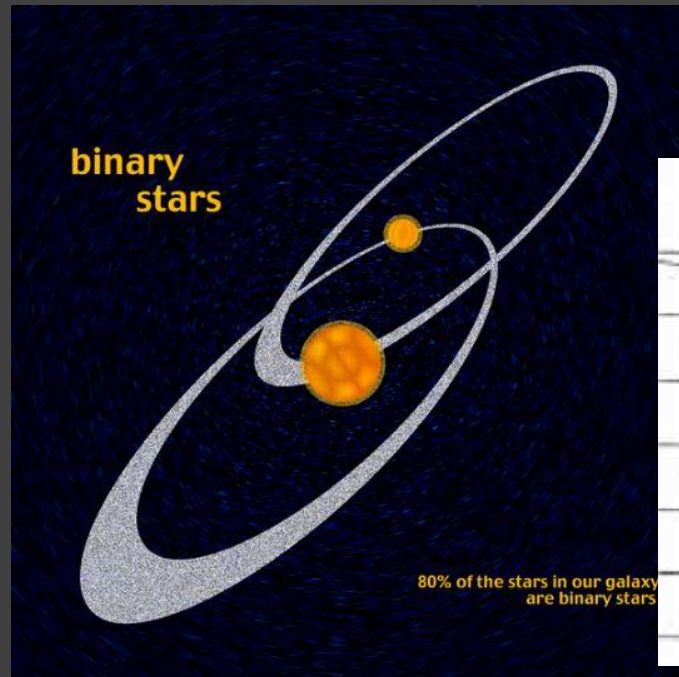


Microlensing wins in distance!



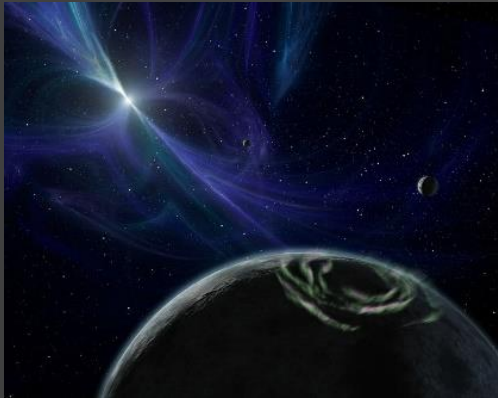
Timing

Observations of a periodic process
(radio pulsar, binary system, pulsating star)
allows to identify a perturber

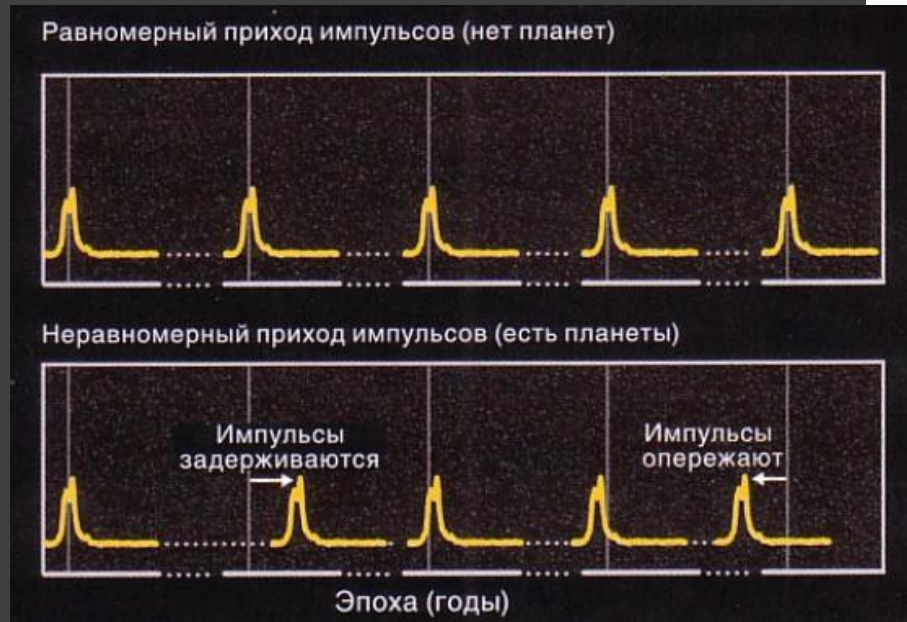


Planets around a radio pulsar

Wolszczan, Frail 1992



PSR B1257+12
Millisecond pulsar



Three light planets

| Companion (in order from star) | Mass | Semimajor axis (AU) | Orbital period (days) |
|-----------------------------------|------------------------------|------------------------|--------------------------|
| A (b) | $0.020 \pm 0.002 M_{\oplus}$ | 0.19 | 25.262 ± 0.003 |
| B (c) | $4.3 \pm 0.2 M_{\oplus}$ | 0.36 | 66.5419 ± 0.0001 |
| C (d) | $3.9 \pm 0.2 M_{\oplus}$ | 0.46 | 98.2114 ± 0.0002 |

Time delay

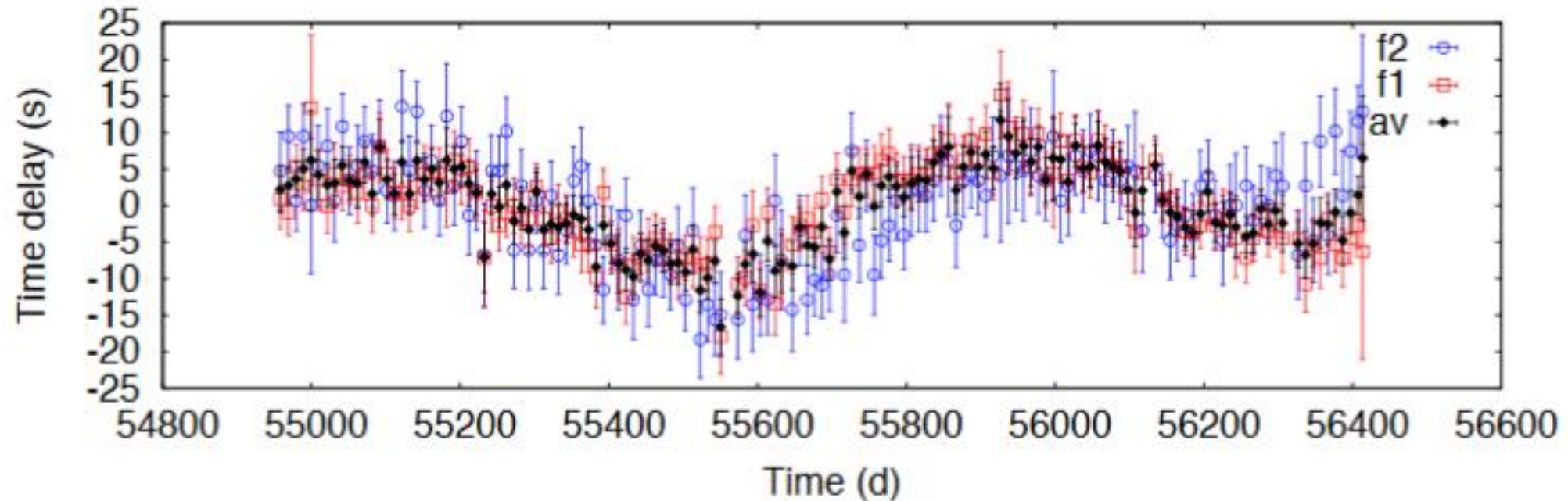
$$A \simeq \frac{a \sin i}{c} \frac{m_p}{M_{\star}},$$

$$\tau(t) = -\frac{1}{c} \int_0^t v_{\text{rad}}(t') dt'$$

$$v_{\text{rad}}(t) = -c \frac{d\tau}{dt}$$

See 1708.00896,
details in 1404.5649

Time delays for KIC 7917485



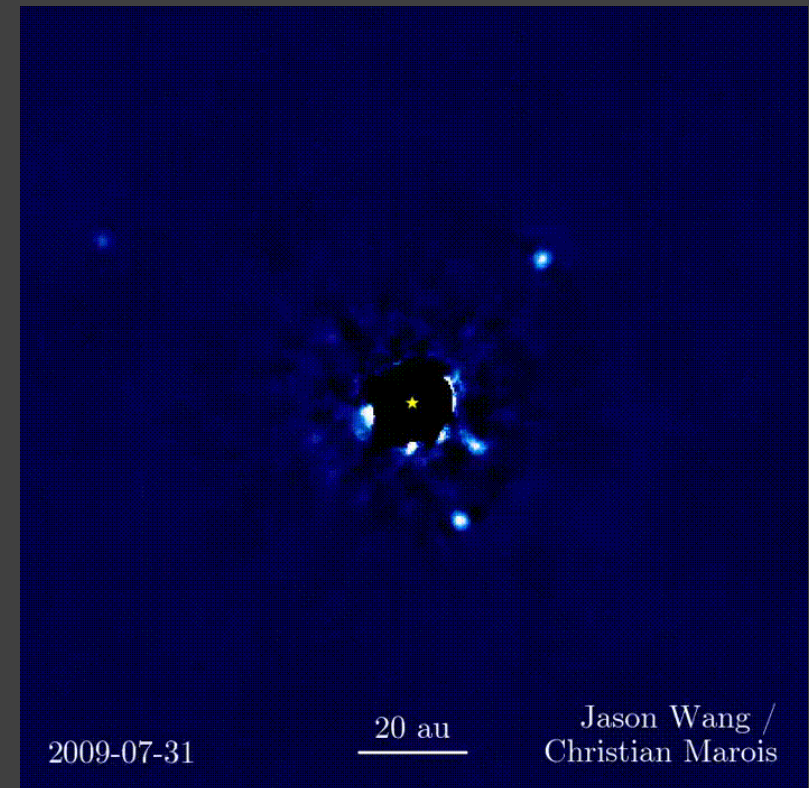
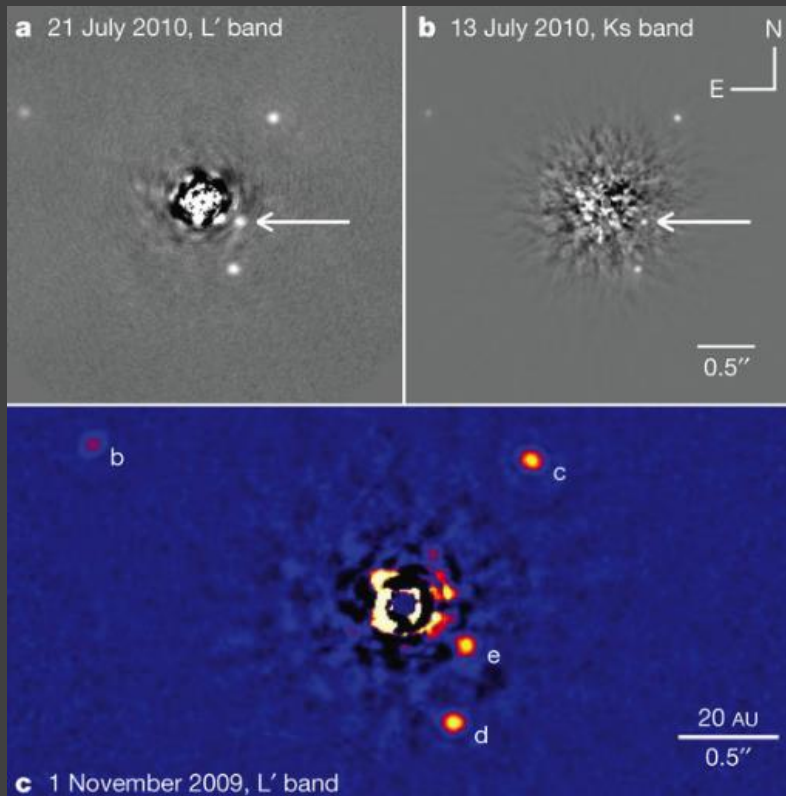
δ Scuti-type star
Planet: $M \sim 11 M_{\text{Jup}}$
Porb ~ 840 days

Pulsations 1.18 and 1.56 hours.
 $\Delta t \sim 7$ sec
Habitable zone!

Direct imaging

Now it is possible to see self-luminous planets (10^{-5} in flux) at $>\sim 1$ arcsec.

For comparison: Solar system analogue at 10 pc gives for Jupiter 10^{-9} in flux and 0.5 arcsec.

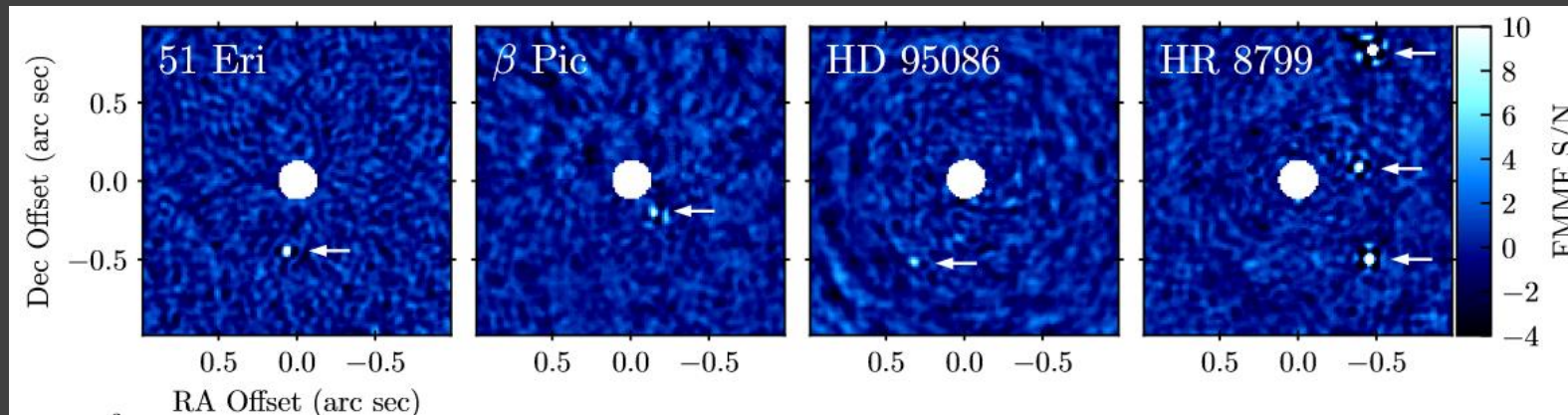
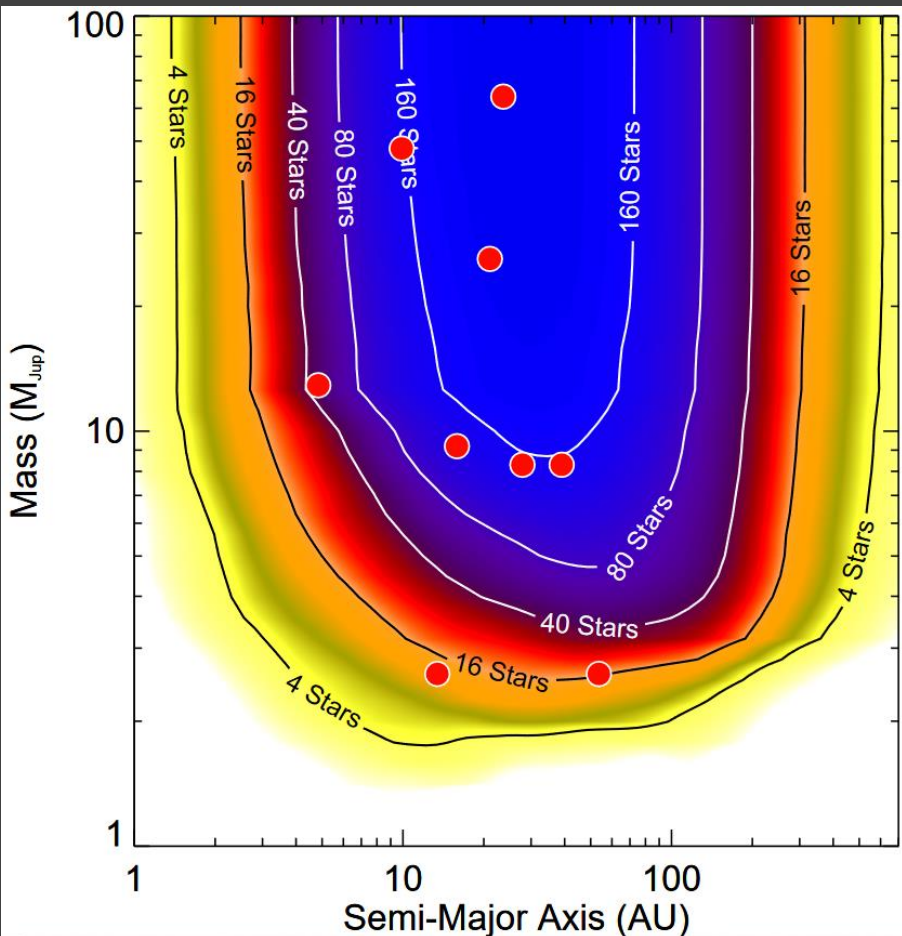


Telescope properties

| Instrument | Telescope | Wavelength (μm) | Ang. resol. (mas) | Coronagraph |
|-----------------------|-------------|---------------------------------|----------------------|----------------|
| ACS | HST | 0.2–1.1 | 20–100 | Lyot |
| STIS | HST | 0.2–0.8 | 20–60 | Lyot |
| NAOS–CONICA | VLT | 1.1–3.5 | 30–90 | Lyot/FQPM |
| VISIR | VLT | 8.5–20 | 200–500 | — |
| SINFONI–SPIFFI | VLT | 1.1–2.45 | 28–62 | — |
| SPHERE | VLT | 0.95–2.32 | 24–62 | Lyot/APLC/FQPM |
| PUEO | CFHT | 0.75–2.5 | 4–140 | Lyot |
| CIAO | SUBARU | 1.1–2.5 | 30–70 | Lyot |
| OSIRIS | Keck I | 1.0–2.4 | 20–100 | — |
| AO–NIRC2 | Keck II | 0.9–5.0 | 20–100 | Lyot |
| ALTAIR–NIRI | Gemini N. | 1.1–2.5 | 30–70 | Lyot |
| GPI | Gemini S. | 0.9–2.4 | 24–62 | Lyot/APLC |
| PALM-3000 PHARO | Hale 200'' | 1.1–2.5 | 60–140 | Lyot/FQPM |
| PALM-3000 Project1640 | Hale 200'' | 1.06–1.76 | 43–71 | APLC |
| AO–IRCAL | Shane 120'' | 1.1–2.5 | 100–150 | — |

$$\Theta = (a/d)(1+e) = 1 \text{ arcsec } (a/\text{AU})(d/\text{pc})^{-1} (1+e)$$

GPIES survey (300 stars)

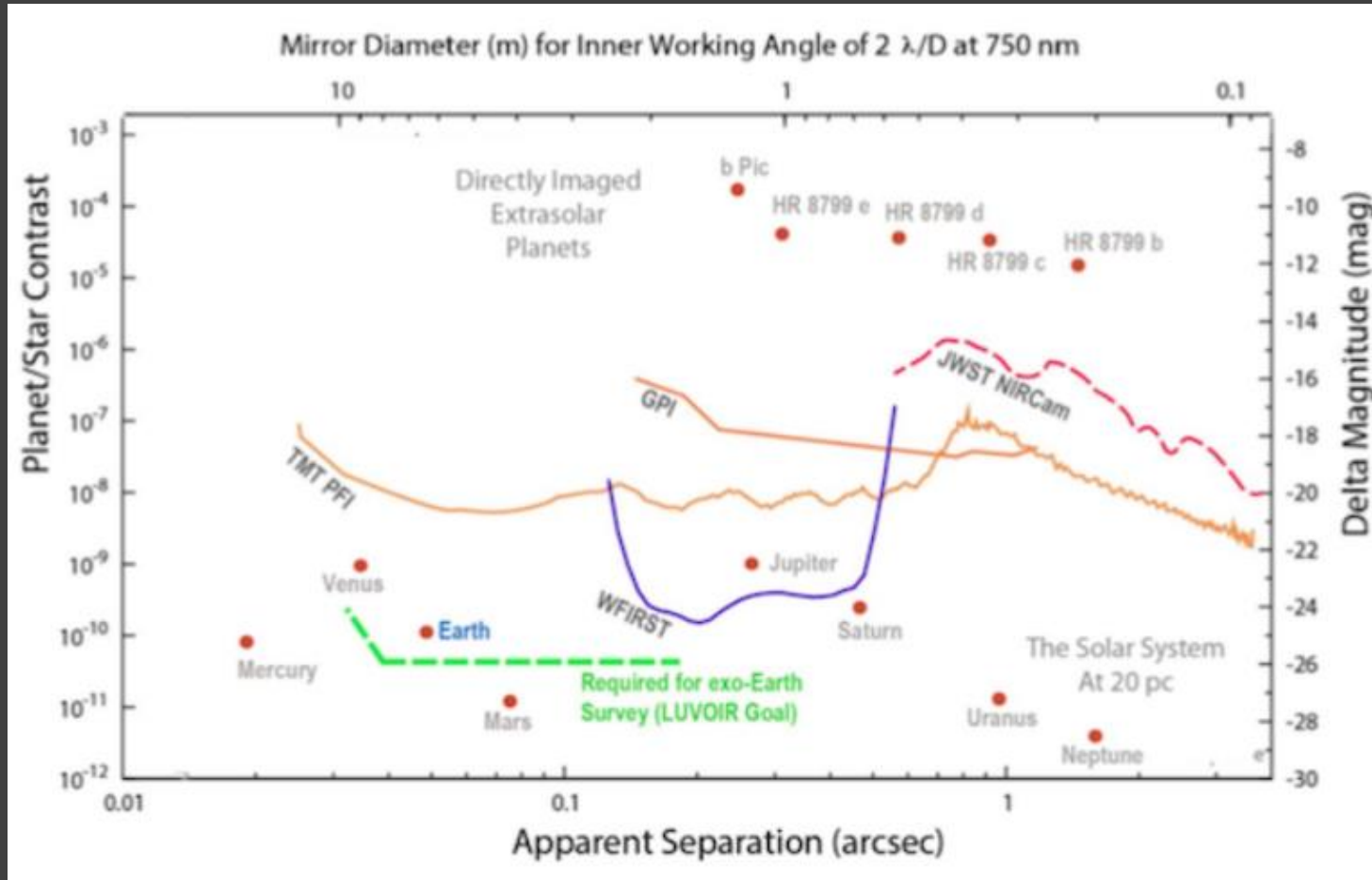


Gemini Planet Imager Exoplanet Survey

10-100 AU

6 planets + 3 brown dwarfs detected

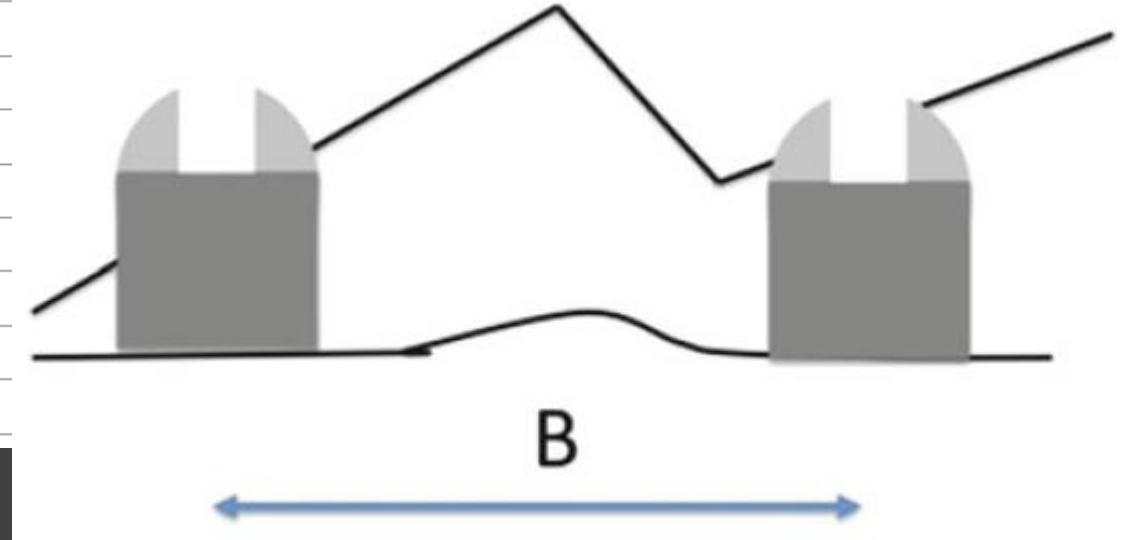
Direct imaging: present and future



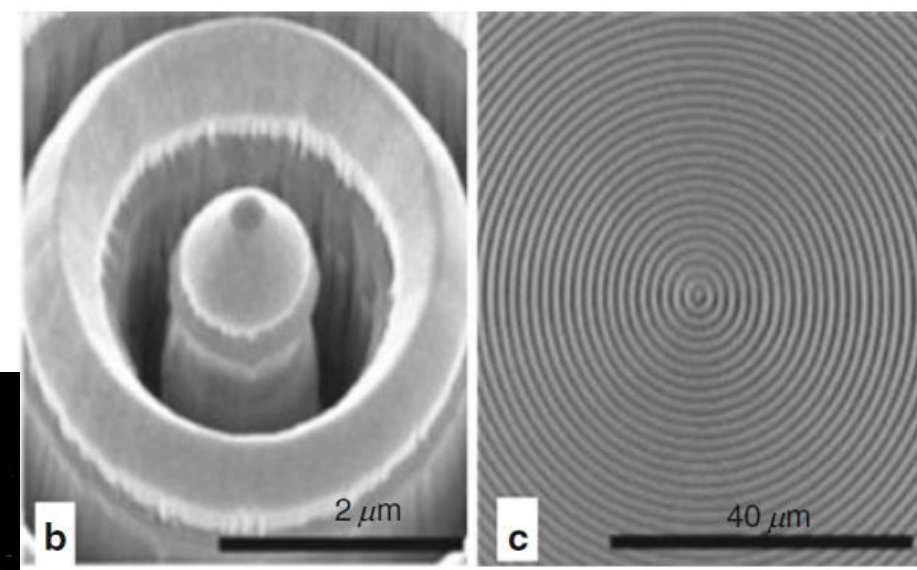
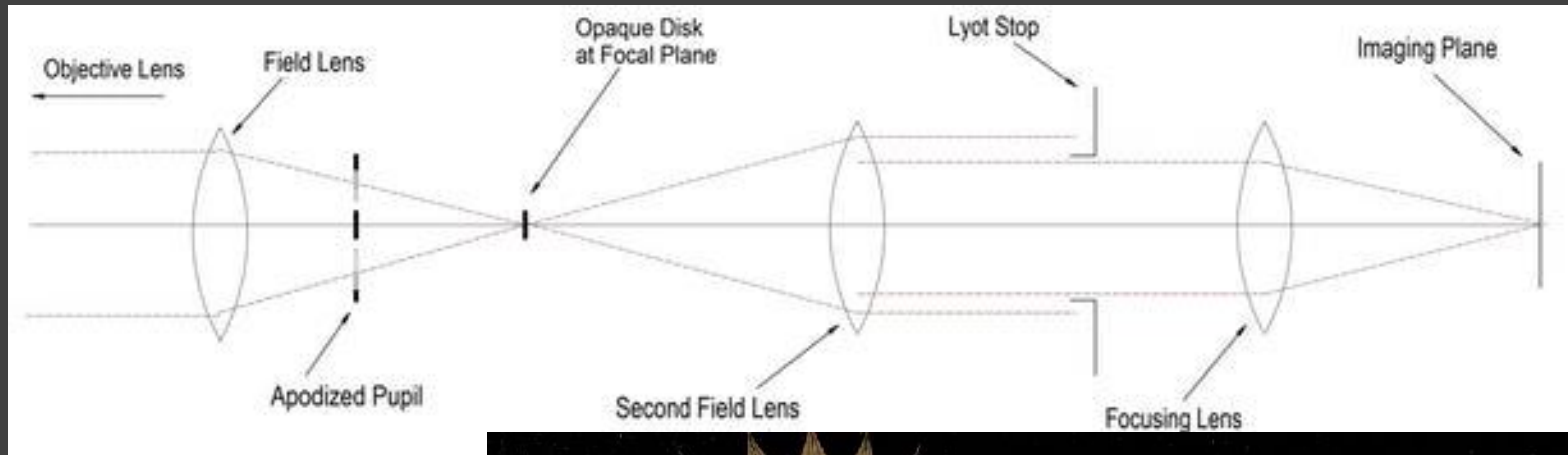
Ground optical interferometers

| Instrument | Interf. | Baseline (m) | Bands | Ang. res. (mas) | Spec. res. | Aperture |
|------------|---------|-----------------|--------|--------------------|------------|----------|
| AMBER | VLTI | 16–200 | J,H,K | 0.6–14 | 35–15,000 | 3 |
| MIDI | VLTI | 16–200 | N | 4–80 | 20–220 | 2 |
| PIONIER | VLTI | 16–200 | H,K | 1.5–45 | 15 | 4 |
| V2 | Keck I | 85 | H,K,L | 2–5 | 25–1800 | 2 |
| Nuller | Keck I | 85 | N | 10–16 | 40 | 2 |
| Mask | Keck | 1–10 | J to L | 13–400 | None | 2 |
| Classic | CHARA | 34–330 | H,K | 0.5–7 | None | 2 |
| FLUOR | CHARA | 34–330 | K | 0.7–7 | None | 2 |
| MIRC | CHARA | 34–330 | J,H | 0.4–5 | 40–400 | 4 |
| BLINC | MMT | 4 | N | 250 | None | 2 |
| LMIRCAM | LBTI | 14–23 | L,M | 27–72 | None | 2 |
| NOMIC | LBTI | 14–23 | N | 72–200 | None | 2 |

Better resolution,
but smaller aperture

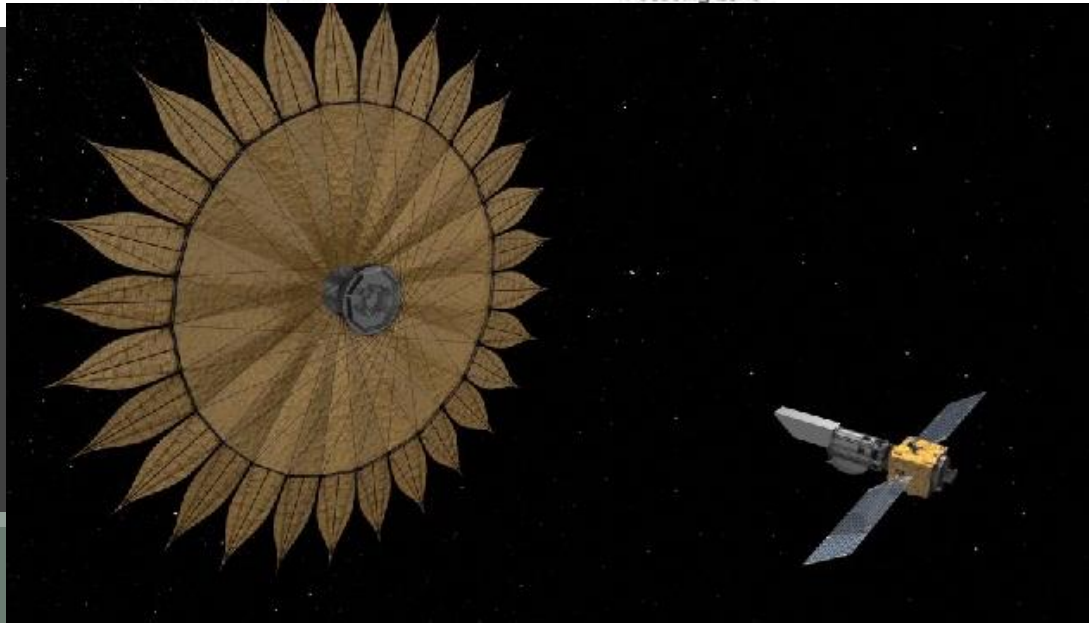


Coronagraphs

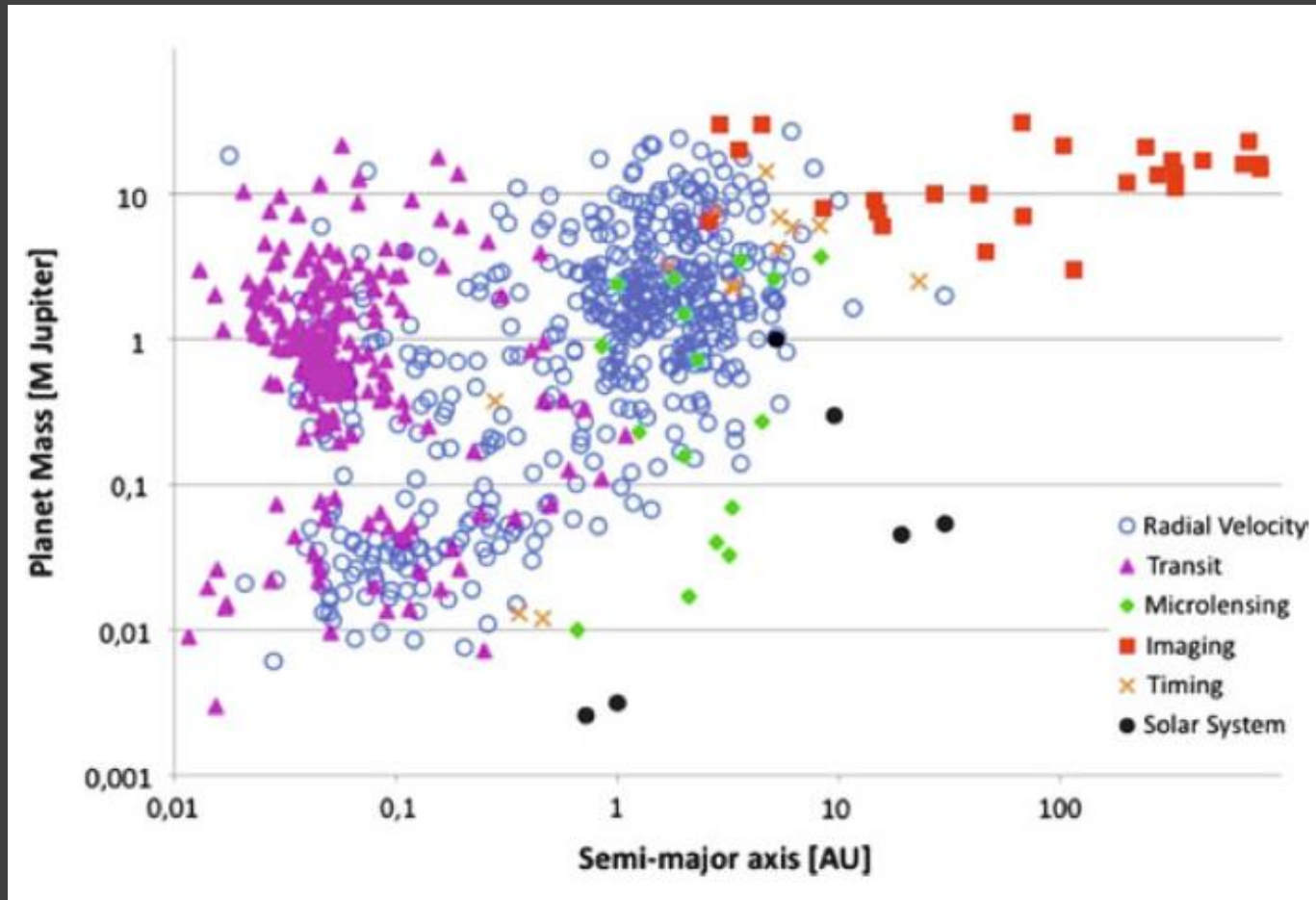


Riccardo Claudi (in Bozza et al. 2016)

To obtain planet images different kinds of coronagraphs are used.



Imaging vs. other methods



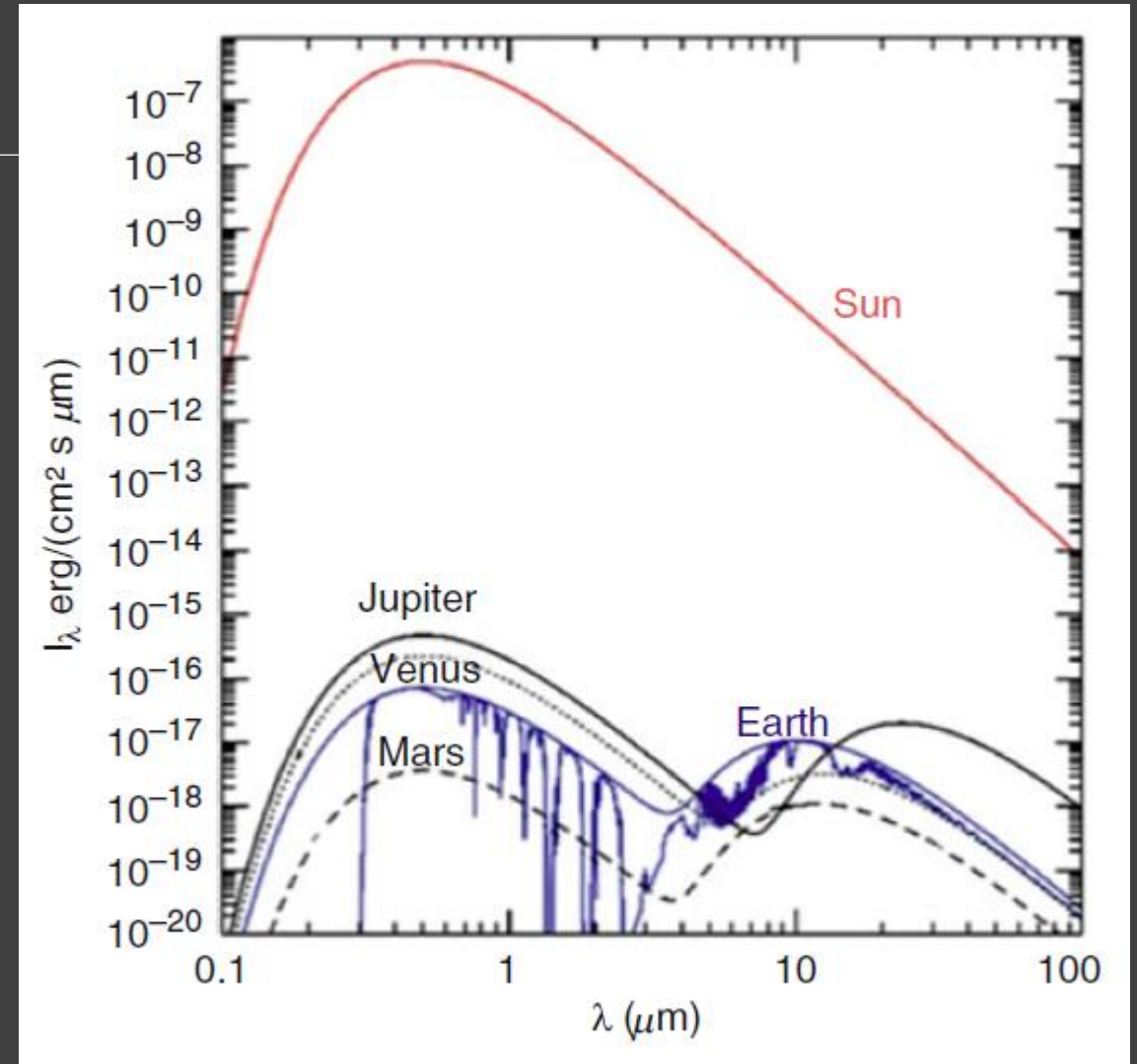
Solar system

Notice, how much better planets are visible in IR.
Especially Jupiter at 20-30 micrometers.

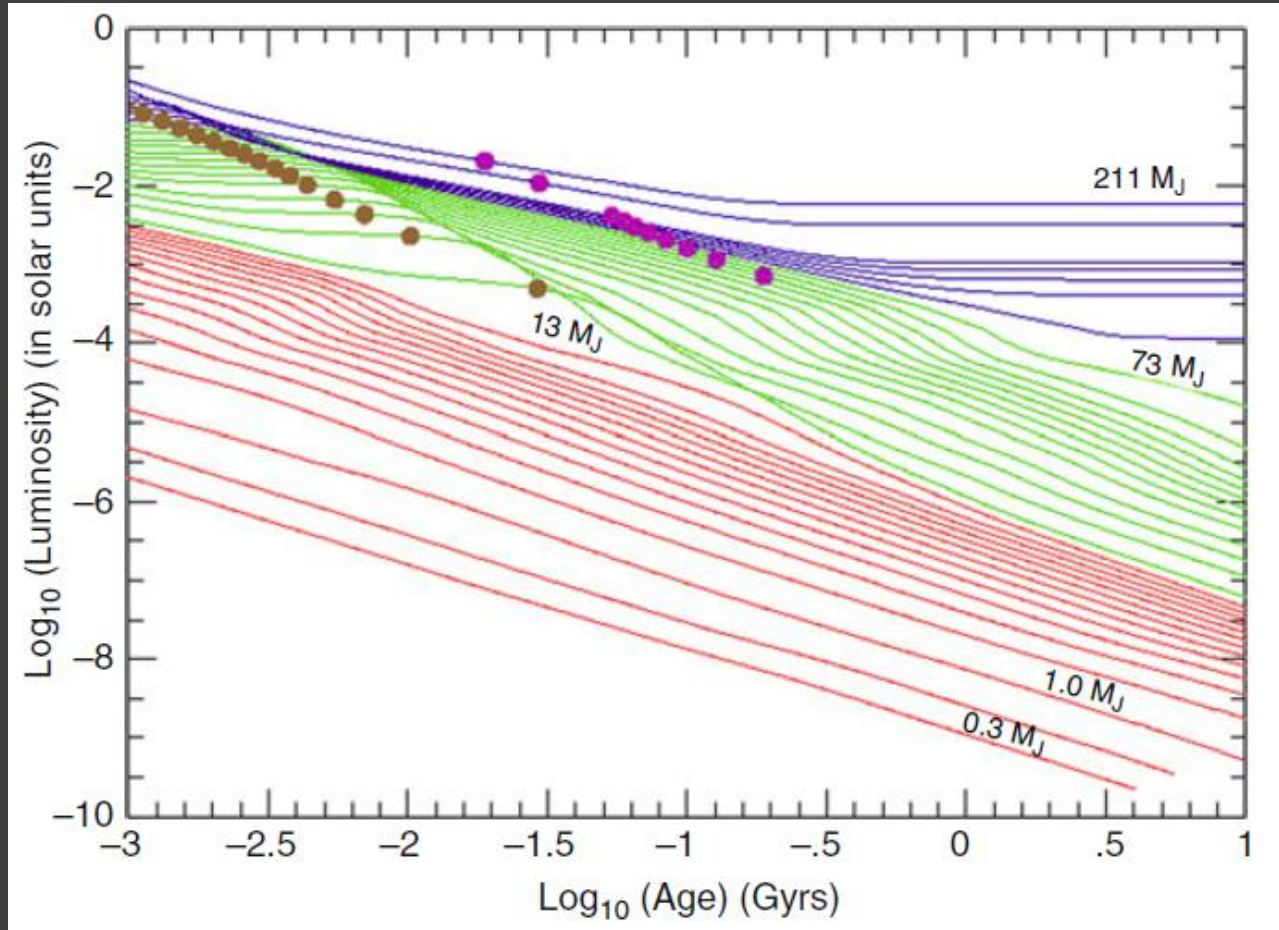
Reflected flux

$$F_{p, \text{vis}} = A(\lambda, t) \phi(t) \frac{R_p^2}{4a^2} B(\lambda, T_{\text{eff}}) R_{\star}^2,$$

(A – albedo, a – semimajor axis, ϕ - phase)

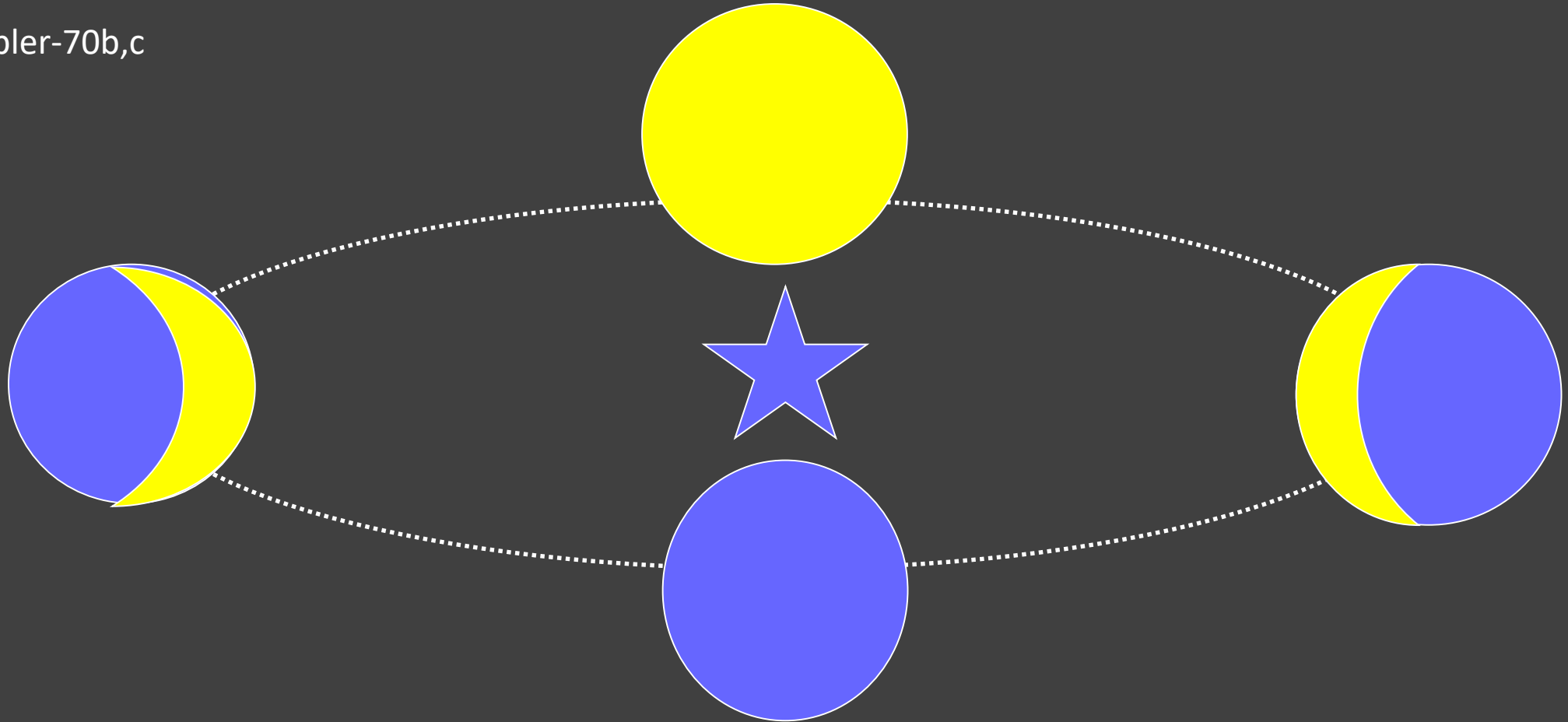


Young planets are hotter

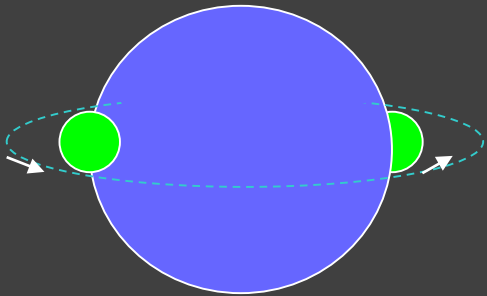


Planet light identification

Kepler-70b,c



IR light



55 Cnc e

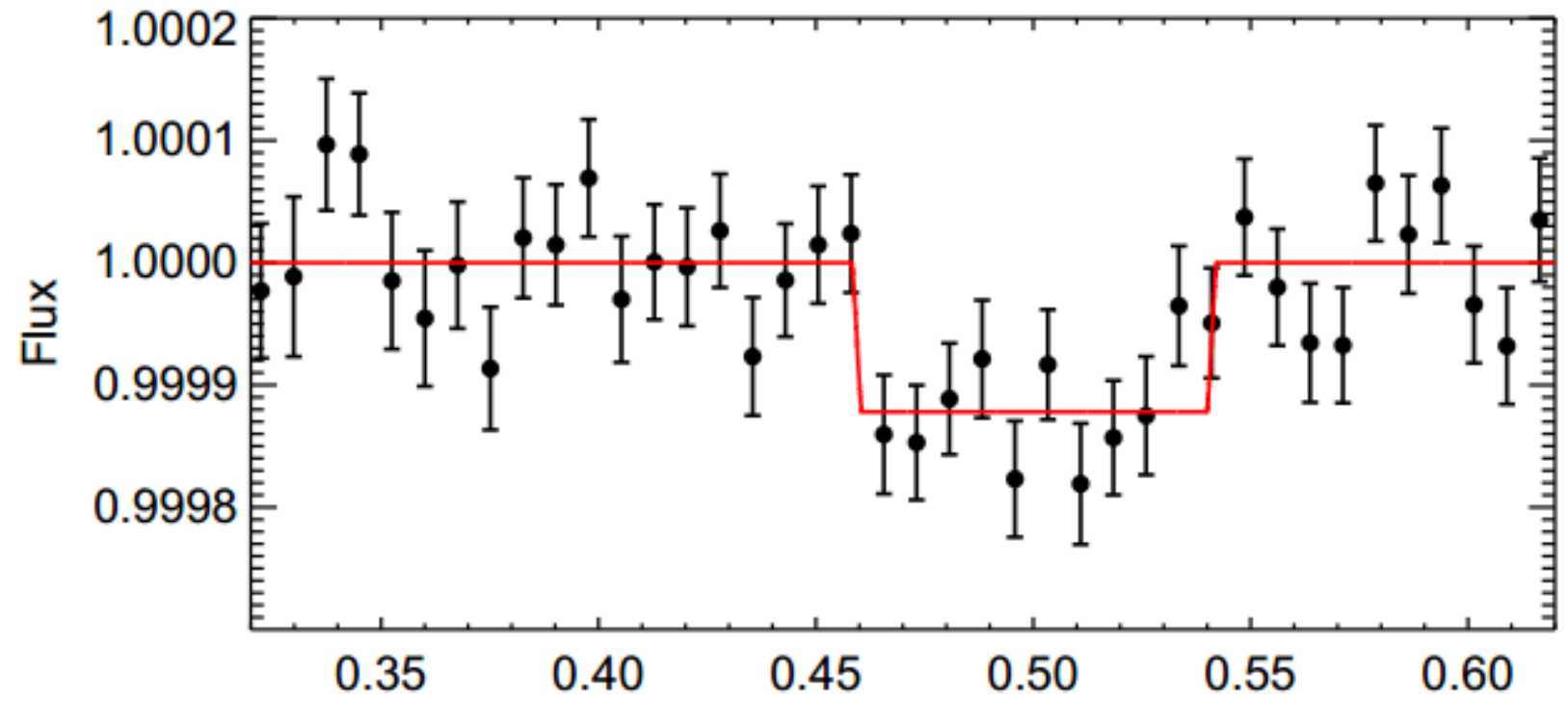
Mass: 7-8 Earth mass

Semi-major axis: 0.016 AU

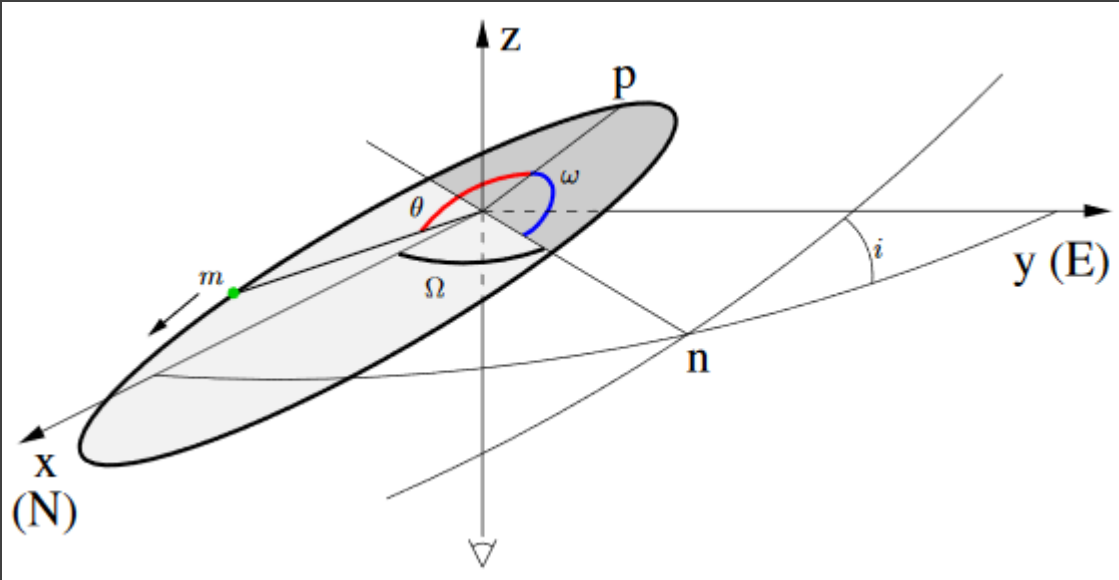
Orbital period: 0.74 days

Temperature 2000-2600K

Occultation light curve



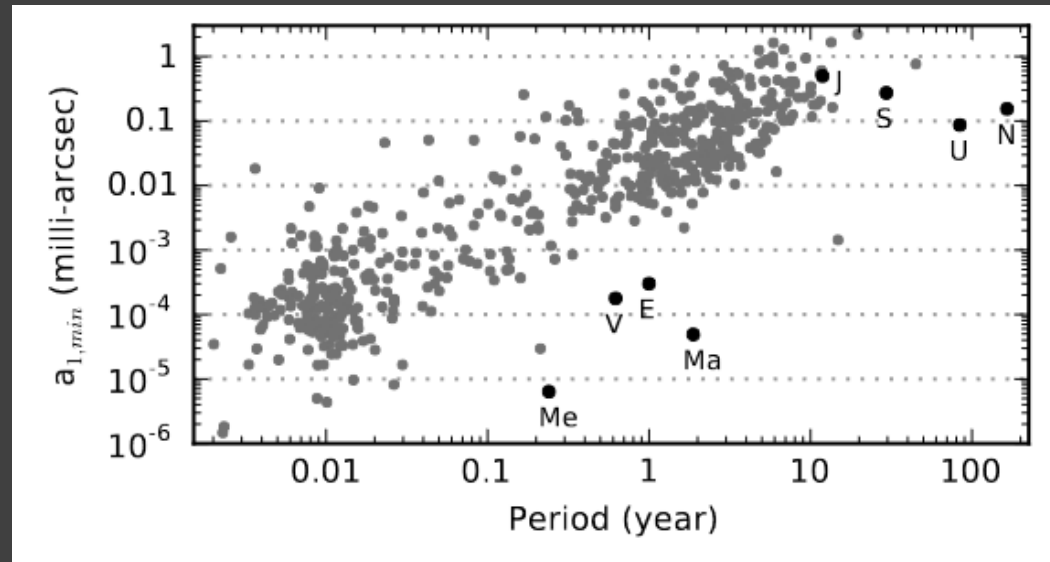
Astrometric detection



$$4\pi^2 \frac{\bar{a}_1^3}{P^2} = G \frac{M_P^3}{(M_* + M_P)^2},$$

It is easier to detect massive long period planets on eccentric orbits.

Astrometry allows to determine $M_{\text{planet}}^3 / (M_{\text{star}} + M_{\text{planet}})^2$



Data on 570 stars with planets are shown.
Solar system data is scaled for a star at 10 pc.

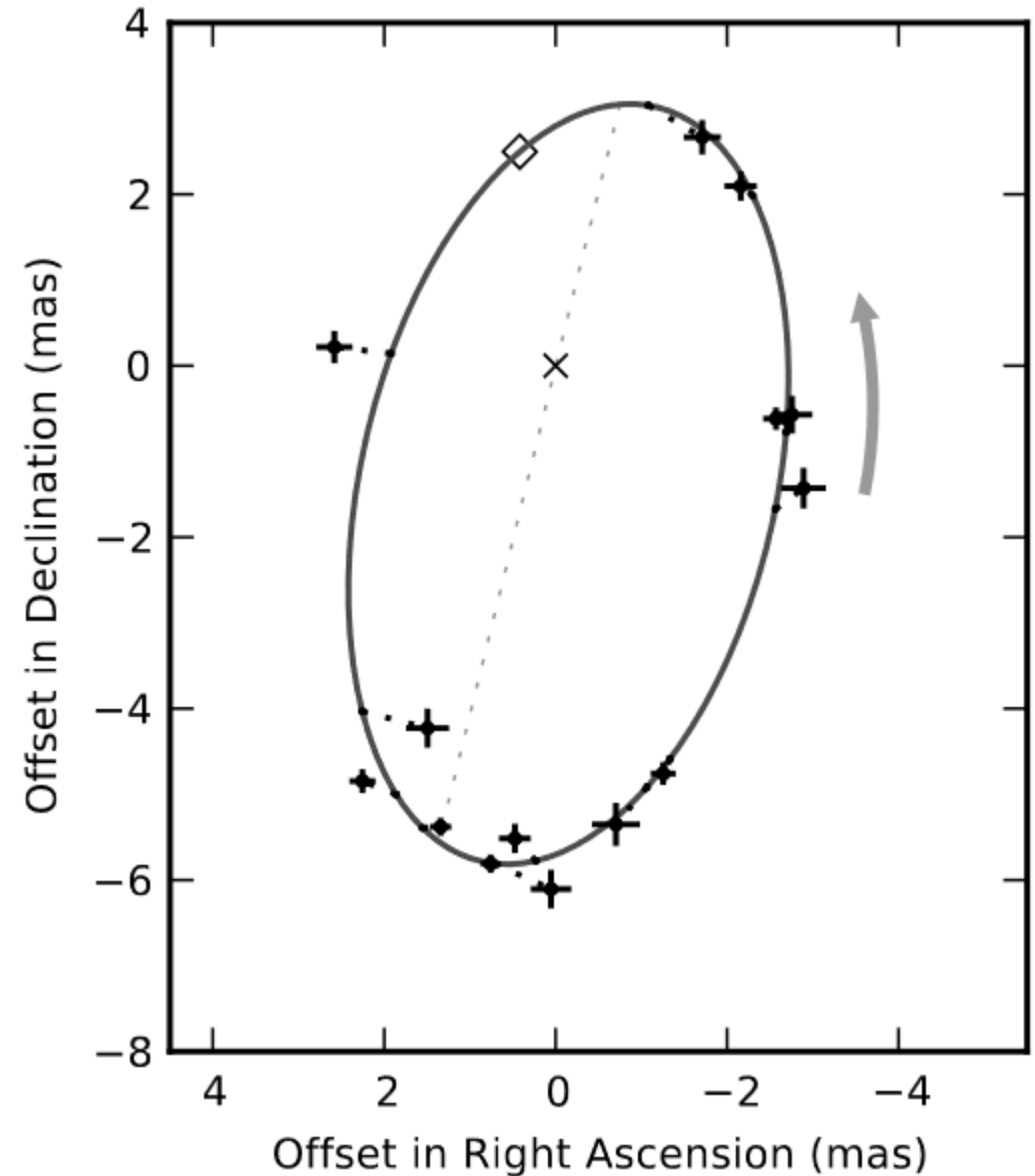
The only candidate

Came out to be a brown dwarf with $28 M_{\text{Jup}}$.

Now waiting for Gaia data.

Fig. 15.— The barycentric orbit of the L1.5 dwarf DENIS-P J082303.1-491201 caused by a 28 Jupiter mass companion in a 246 day orbit discovered through ground-based astrometry with an optical camera on an 8 m telescope ([Sahlmann et al., 2013a](#)).

Few other candidates have been mentioned by Muterspaugh et al. (2010)



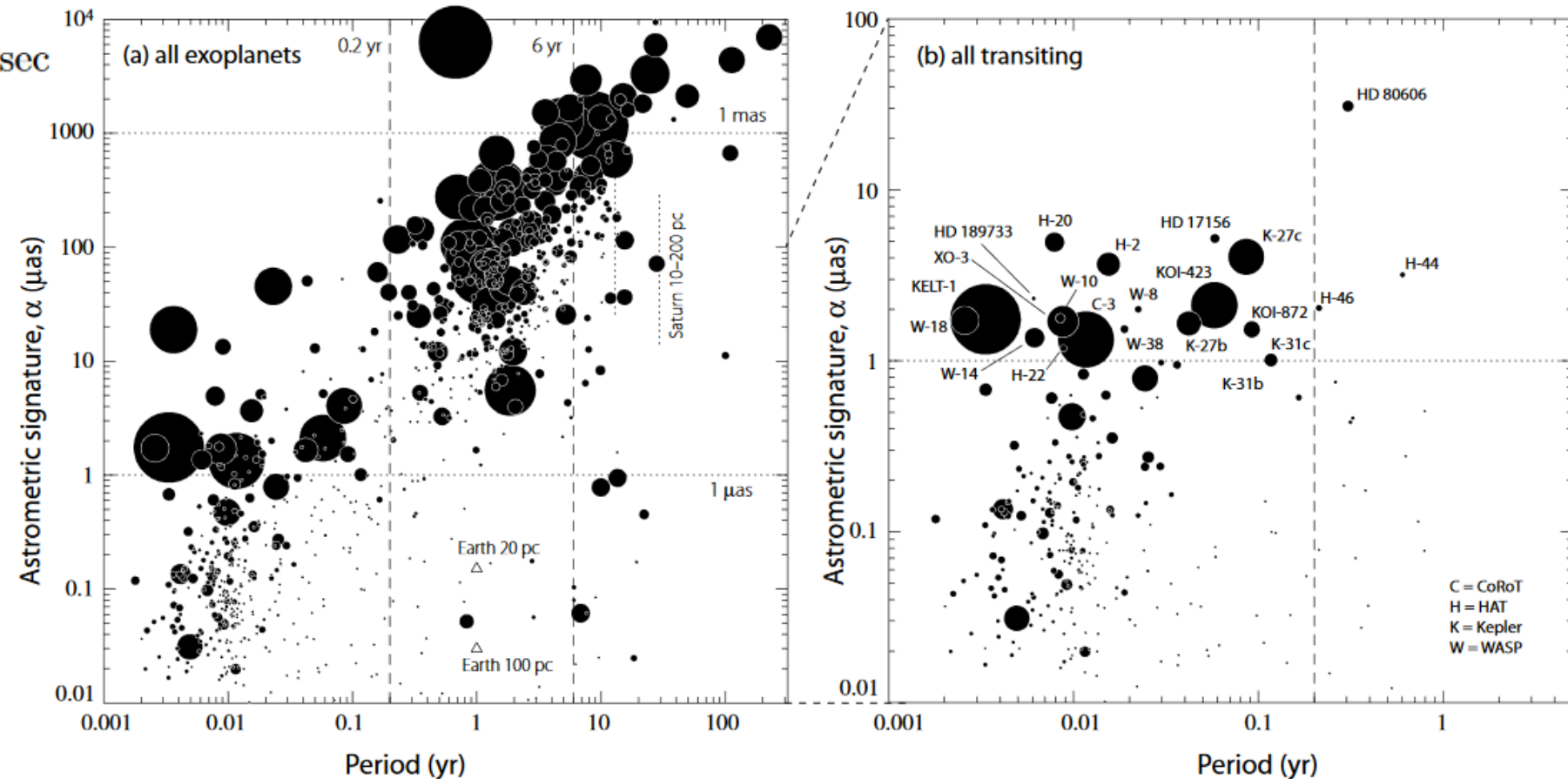
Gaia and astrometric microlensing

$$\alpha = \left(\frac{M_p}{M_\star} \right) \left(\frac{a_p}{1 \text{ AU}} \right) \left(\frac{d}{1 \text{ pc}} \right)^{-1} \text{ arcsec}$$

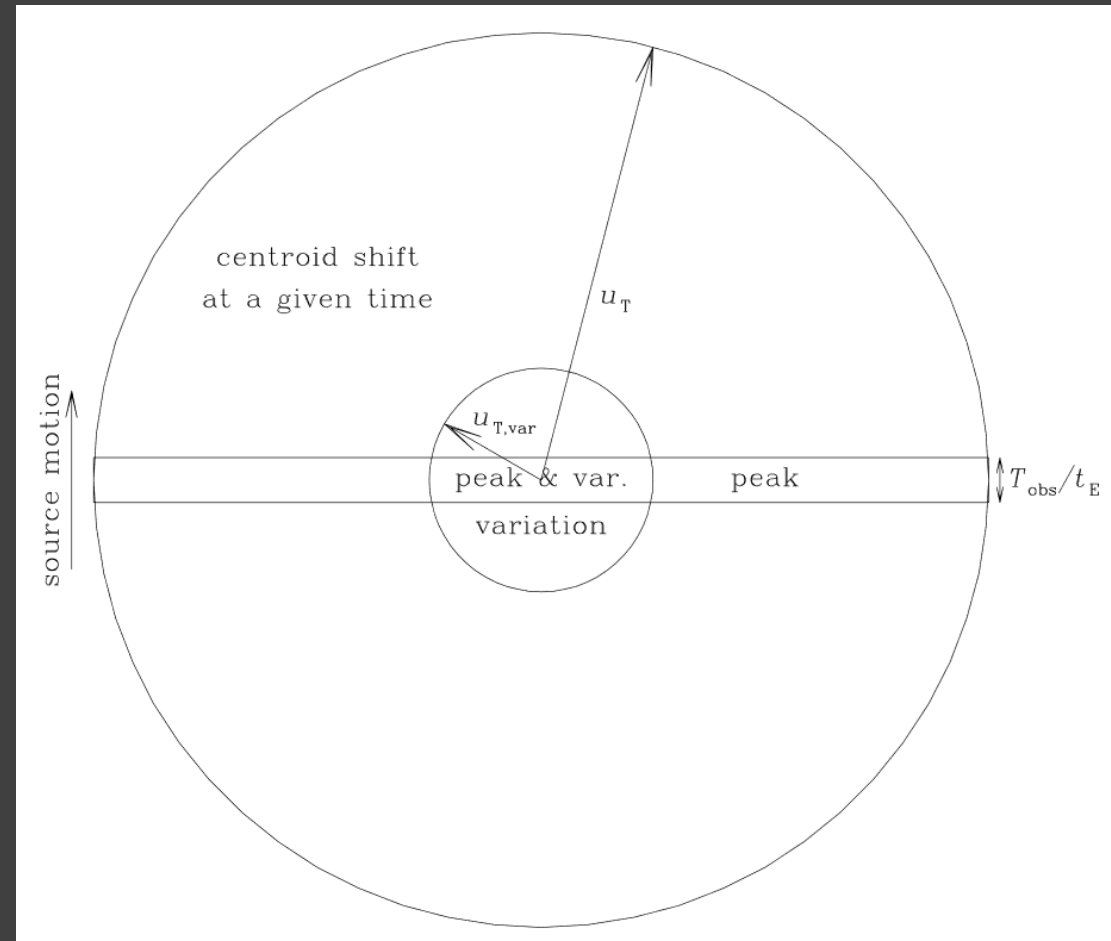
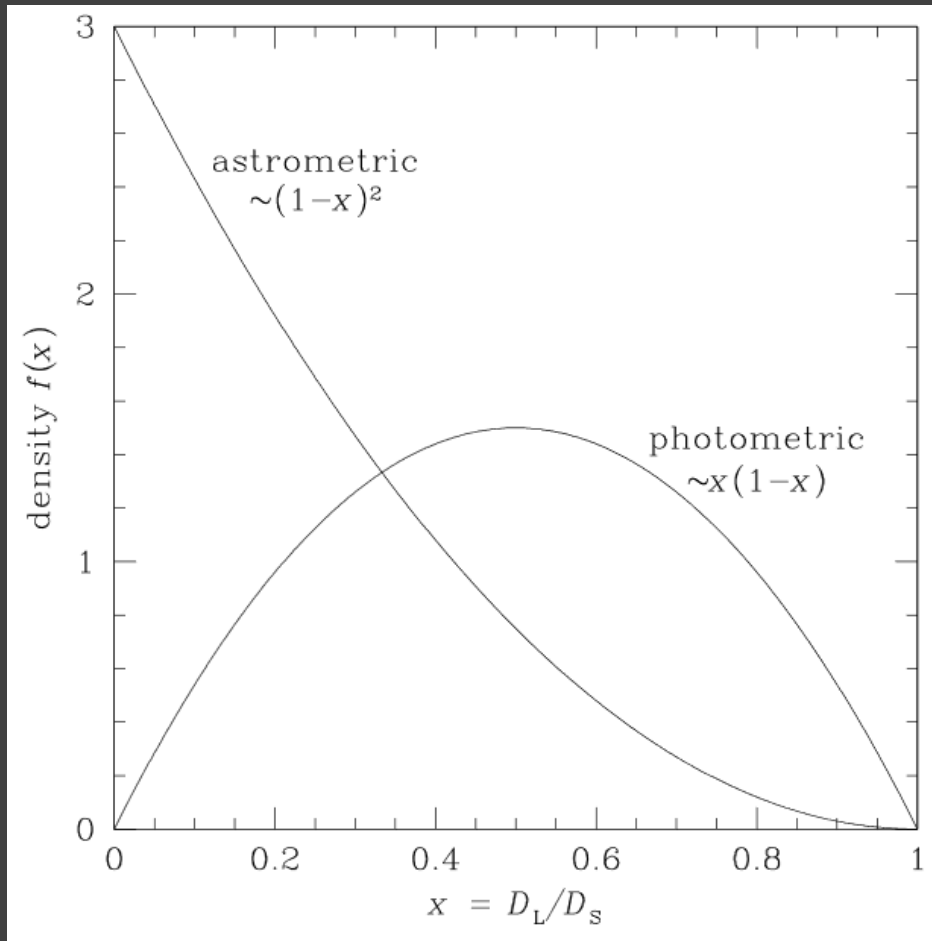
Precision of Gaia
is ~30 microarcsec
(see also 1704.02493).

Optimistic estimates:
tens of thousand planets
(~20000-30000).

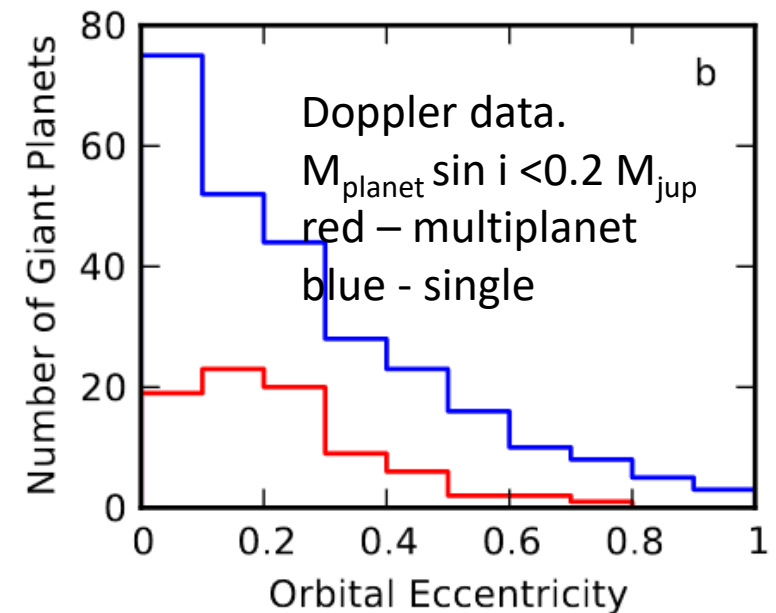
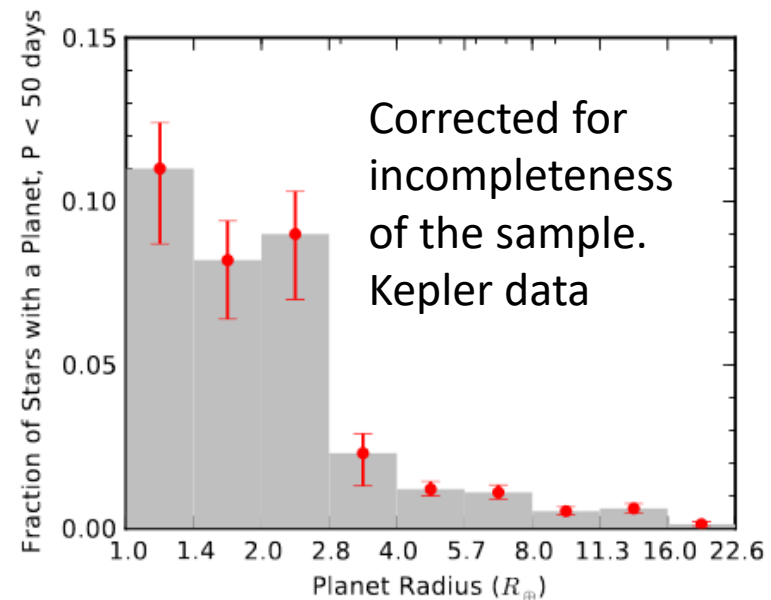
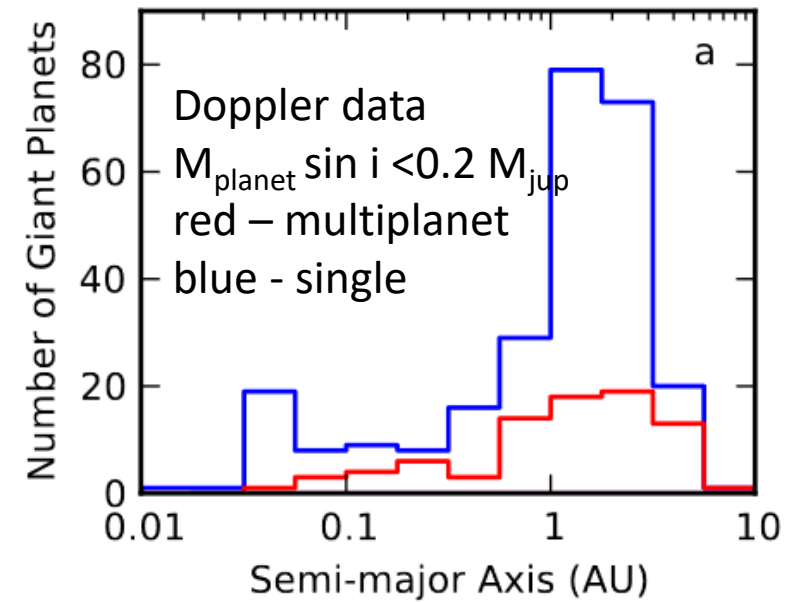
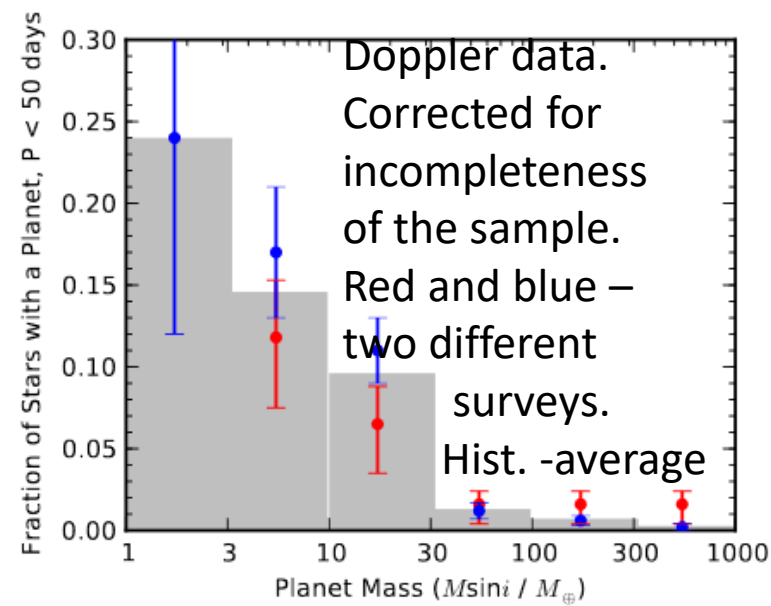
Mostly massive and
with long orbital periods
up to ~500 pc distance.



Astrometric microlensing



Planetary statistics



Literature

arxiv:1505.06869 Exoplanet Detection Techniques

arxiv:1504.04017 The Next Great Exoplanet Hunt

arxiv:1410.4199 The Occurrence and Architecture of Exoplanetary Systems

arXiv:1708.00896 Timing by Stellar Pulsations as an Exoplanet Discovery Method

arxiv:1706.09849 Transit Timing and Duration Variations for the Discovery and Characterization of Exoplanets

arxiv:1705.05791 Exoplanet Biosignatures: A Review of Remotely Detectable Signs of Life

arxiv:1704.07832 Mapping Exoplanets

arxiv:1701.05205 Characterizing Exoplanets for Habitability

arxiv:1411.1173 Astrometric exoplanet detection with Gaia

arxiv:1001.2010 Transits and Occultations

arxiv:0904.0965 Astrometric detection of earthlike planets

arXiv:0904.1100 Exoplanet search with astrometry

arxiv:0902.1761 Detection of extrasolar planets by gravitational microlensing

ApJ (2000) Dominik, Sahu Astrometric microlensing

arXiv:1810.02691 Microlensing searches for exoplanets

